DIPLOMARBEIT

Single-Particle State of an Open Quantum Dynamical System in a Dilaton Environment

zur Erlangung des akademischen Grades

Diplom-Ingenieurin

im Rahmen des Studiums

Technische Physik

eingereicht von

Caroline Voith, BSc

01607478

ausgeführt am Atominstitut
der Fakultät für Physik der Technischen Universität Wien

Betreuung
Betreuer: Univ.Prof. Dipl.-Phys. Dr.rer.nat. Hartmut Abele
Mitwirkung: Christian Käding, PhD & Dipl.-Ing. Dr.techn. Mario Pitschmann

Wien, 10.05.2023 _____ _____

(Unterschrift Verfasserin) (Unterschrift Betreuer)

Die approbierte gedruckte Originalversion dieser Diplomarbeit ist an der TU Wien Bibliothek verfügbar
The approved original version of this thesis is available in print at TU Wien Bibliothek.

Abstract

Einstein's theory of general relativity can be extended or adjusted by modified gravity theories in hopes of answering still open questions like about the nature of dark matter or dark energy. Some theories predict the existence of novel scalar fields causing a gravity-like fifth force. However, such a force, which could exceed gravity in its strength, is tightly constraint within our Solar System due to tests. A popular way to circumvent these constraints is to introduce so-called screening mechanisms which suppress fifth forces in environments of high mass density, like our Solar System, but allowing scalar fields to act with their full strength in vacuum.

In this thesis, the effects of an only little investigated screened scalar field, the dilaton field, on an open quantum system is discussed. For this, an equation for directly calculating the reduced density matrix of a single-particle state of a real scalar field in an environment of another scalar field is derived using techniques from non-equilibrium quantum field theory. Afterwards, this equation is used to approximately calculate the effects of the dilaton environment on a scalar field as a proxy for an atom, motivated by experimental applications like atom interferometry. Some interesting parts of the solution are then renormalized before using them to estimate domains of dilaton parameters where these effects could be measurable.

Die approbierte gedruckte Originalversion dieser Diplomarbeit ist an der TU Wien Bibliothek verfügbar
The approved original version of this thesis is available in print at TU Wien Bibliothek.

Kurzzusammenfassung

Einsteins allgemeine Relativitätstheorie kann durch modifizierte Gravitationstheorien erweitert beziehungweise angepasst werden, in der Hoffnung noch ungelöste Probleme wie dunkle Materie und dunkle Energie zu lösen. Manche dieser Theorien sagen die Existenz von neuen Skalarfeldern, die fünfte Kräfte ähnlich der Gravitation verursachen, vorher. Solche Kräfte, die stärker als Gravitation wirken können, sind allerdings durch Tests innerhalb unseres Sonnensystems stark eingeschränkt. Eine beliebte Methode, um diese Einschränkungen zu umgehen, ist die Einführung von sogenannten Abschirmungsmechanismen, die diese fünfte Kräfte in Umgebungen mit hoher Massendichte, wie unserem Sonnensystem, unterdrücken, aber im Vakuum die gesamte Stärke der Skalarfelder zulassen.

In dieser Diplomarbeit werden die Auswirkungen von einem noch wenig untersuchten abgeschirmten Skalarfeld, dem Dilatonfeld, auf ein offenes Quantensystem untersucht. Dafür wird unter Verwendung von Techniken der Nichtgleichgewichtsquantenfeldtheorie eine Gleichung für die direkte Berechnung der reduzierten Dichtematrix eines Einteilchenzustandes eines reellen Skalarfeldes in Umgebung eines anderen Skalarfeldes hergeleitet. Anschließend wird diese Gleichung verwendet, um näherungsweise die Auswirkung einer Dilatonumgebung auf ein Skalarfeld, das als Näherung für ein Atom herangezogen wird, zu bestimmen. Dies ist motiviert durch experimentelle Anwendungen wie der Atominterferometrie. Interessante Teile des Ergebnisses werden dann renormiert und anschließend verwendet, um Parameterbereiche des Dilatons abzuschätzen, wo diese Auswirkungen messbar wären.

Die approbierte gedruckte Originalversion dieser Diplomarbeit ist an der TU Wien Bibliothek verfügbar
The approved original version of this thesis is available in print at TU Wien Bibliothek.

Contents

Die approbierte gedruckte Originalversion dieser Diplomarbeit ist an der TU Wien Bibliothek verfügbar
The approved original version of this thesis is available in print at TU Wien Bibliothek.

1. Introduction

To this day, there are still some phenomena fundamental to our understanding of the Universe that are not yet explained. Some of these mysteries are the natures of dark energy and dark matter [1–4]. Current estimates suggest that our universe contains about $68 \pm 1\%$ dark energy, $27 \pm 1\%$ dark matter and only about 5% ordinary matter like photons, neutrinos and baryonic matter [4]. Both dark matter - the mass missing in galaxies to explain observations of gravitational lensing and the rotation curves of spiral galaxies [1] - and dark energy - the energy that is assumed to drive the observed accelerated expansion of our universe [5, 6] - are not yet understood but a possible explanation for them could be modifying the theory of general relativity by adding light scalar fields [1, 2, 7]. Modifying general relativity in this way leads to scalar-tensor theories where scalar fields are coupled to the metric tensor of general relativity [8]. References [1, 2, 9] give an overview of such models including comments on which of them have already been disregarded due to cosmological observations and which are still of interest.

Introducing additional scalar fields to modify general relativity may be a rather simple way to explain dark matter and dark energy. However, any added scalar field will generally interact with the fields of Standard Model particles by mediating a so-called fifth force. This fifth force would be an additional fundamental force that has not yet been observed and is tightly constrained by observations of our Solar System [10]. These constraints can easily be circumvented by assuming the coupling of the scalar field to matter to be very weak. More specifically, the fifth force has to be a lot weaker than gravity which is the weakest of all known fundamental forces [11]. Nonetheless, this would result in the problem that it could be impossible to observe the force even when going to astrophysical scales outside of our Solar System.

Therefore, a well-liked alternative to this very weakly coupling is the introduction of screening mechanisms [7, 12]. Scalar fields with such a screening mechanism, so-called screened scalar fields, experience a suppression of themselves and their fifth forces in environments of high mass density. In vacuum, however, they can act with their full strength. Due to this screening mechanism, the scalar field can thus bypass the aforementioned constraints of Solar System observations by being strongly repressed there. So far, several models of screened scalar fields working with different screening mechanisms have been developed. An overview of them as well as some experiments can be found in [2, 13].

In this thesis a new quantum physical test of one particular screened scalar field, the

Die approbierte gedruckte Originalversion dieser Diplomarbeit ist an der TU Wien Bibliothek verfügbar
The approved original version of this thesis is available in print at TU Wien Bibliothek.

dilaton, will be presented. This will be done by calculating the open quantum dynamical system of a Standard Model matter particle, e.g. a cold atom, coupling to the screened scalar system as its environment. Open quantum systems, where the system is influenced and effected by a surrounding environment, can be regarded as some of the most realistic ways of modelling quantum systems [14]. It is therefore possible to calculate occurrences like momentum or energy diffusion [15] leading to phase shifts or decoherence [16] which are caused by the interaction between system and environment. Some of the first applications of open quantum systems include quantum optics [14, 17–19] and physics of cold atoms [20–22].

Open quantum systems, including the one in this thesis, are often described by density operators and matrices since they can also be used when describing mixed states, contrary to wave functions [14]. The quantum Liouville equation can be used to determine the time evolution of the density operator and from there master equations can be obtained. This approach was taken by [23–25]. However, solving such a master equation analytically can become quite difficult if not impossible. Therefore, a different path to directly calculate the reduced density matrix, where the environmental degrees of freedom have been traced out, was developed in [26]. Following the same path but without tracing out the environmental degrees of freedom leads to a formalism able to determine the more general total density matrix elements as shown in [27].

This thesis will follow the calculations of the reduced density matrix outlined in [26] and use this equation to determine the effects a dilaton field can have on a scalar field posing as the system. To do so, first screened scalar fields are introduced in more detail in Section 2 with emphasis on the dilaton field and its coupling to Standard Model matter. Then, in Section 3 the formalism to determine reduced density matrix elements is calculated by following [26]. For this purpose, required theoretical concepts like the Schwinger-Keldysh formalism [28, 29], the Feynman-Vernon influence functional [30] and methods from thermo field dynamics [31, 32] are introduced in Sections 3.2 and 3.3. These concepts are then used to derive the formula in Section 3.4. Afterwards, this formula is used to determine the effects of a dilaton field on the system scalar field in Section 4. In Section 4.1 the physically interesting parts of the result are renormalized. Its experimental implications and predictions are subsequently discussed in Section 4.2. Finally, this thesis is concluded in Section 5.

Die approbierte gedruckte Originalversion dieser Diplomarbeit ist an der TU Wien Bibliothek verfügbar
The approved original version of this thesis is available in print at TU Wien Bibliothek.

2. Screened scalar fields

In classical and quantum field theory, scalar fields are the most simple objects since they are denoted only by a single complex number. Additionally, they are Lorentz invariant[1] and have the dimension of energy in 4-dimensional spacetime. In this thesis, all scalar fields are presumed to be real and they are represented by ϕ and χ. Furthermore, $c_0 = \hbar = 1$ and the $(-,+,+,+)$-metric convention are used.

The equation of motion of a free scalar field,

$$(\Box - m_\phi^2)\phi = 0 \tag{2.1}$$

with the d'Alembert operator $\Box = -\frac{\partial^2}{\partial t^2} + \vec{\nabla}^2$ and the mass of the scalar field m_ϕ, is also known as the Schrödinger-Gordon or Klein-Gordon equation [33]. Its Lagrangian density, also referred to as its Lagrangian, is

$$\mathcal{L}_0 = -\frac{1}{2}(\partial\phi)^2 - \frac{1}{2}m_\phi^2\phi^2, \tag{2.2}$$

while its action results in

$$S_0 = \int_x \mathcal{L}_0 \tag{2.3}$$

with $\int_x = \int d^4x$.

The Lagrangian of an interacting system where ϕ interacts with itself and other fields χ, however, is given by

$$\mathcal{L} = -\frac{1}{2}(\partial\phi)^2 - \frac{1}{2}m_\phi^2\phi^2 - V(\phi,\chi), \tag{2.4}$$

where the interaction potential density $V(\phi,\chi)$ is subtracted from the free Lagrangian in Eq. (2.2). In this case the equation of motion is acquired from the Euler-Lagrange equations [11], resulting in

$$(\Box - m_\phi^2)\phi = \frac{\partial}{\partial\phi}V(\phi,\chi). \tag{2.5}$$

For a scalar field to be used in a quantum field theory, one has to employ either canonical quantisation [34] or Feynman's path integral formalism [35].

When using canonical quantisation, the scalar field ϕ as well as the newly defined

[1] This means that their equations of motion - and consequently their actions - remain unchanged when using an element of the Lorentz group Λ to transform the field like $\phi(x) \to \phi(\Lambda^{-1}x)$.

Die approbierte gedruckte Originalversion dieser Diplomarbeit ist an der TU Wien Bibliothek verfügbar
The approved original version of this thesis is available in print at TU Wien Bibliothek.

conjugate momentum density $\pi(x) \coloneqq \partial\mathcal{L}/\partial\dot{\phi}(x)$ [36] are elevated to operators, $\phi \to \hat{\phi}$ and $\pi \to \hat{\pi}$. This new scalar field operator can be written as a decomposition of plane waves [36],

$$\hat{\phi}(x) = \int d\Pi_{\mathbf{k}} \left(\hat{a} e^{-iE_{\mathbf{k}}t + i\mathbf{k}\cdot\mathbf{x}} + \hat{a}^\dagger e^{iE_{\mathbf{k}}t - i\mathbf{k}\cdot\mathbf{x}} \right), \tag{2.6}$$

where the definitions

$$\int d\Pi_{\mathbf{k}} \coloneqq \int_{\mathbf{k}} \frac{1}{2E_{\mathbf{k}}} \qquad \text{and} \qquad \int_{\mathbf{k}} \coloneqq \int \frac{d^3k}{(2\pi)^3} \tag{2.7}$$

are used, $\hat{a}$ and $\hat{a}^\dagger$ denote the annihilation and creation operators, respectively, and the energy is given by

$$E_{\mathbf{k}} \coloneqq \sqrt{\mathbf{k}^2 + m_\phi^2 + \partial_\phi^2 V(\phi, \chi)|_{\phi_0 \in \{\varphi:\, \partial_\phi \mathcal{L}|_\varphi = 0\}}}. \tag{2.8}$$

The annihilation and creation operators of a certain momentum $\mathbf{p}$, $\hat{a}_{\mathbf{p}}$ and $\hat{a}^\dagger_{\mathbf{p}}$, fulfil the commutation relations [36]

$$\begin{aligned} [\hat{a}_{\mathbf{p}}, \hat{a}^\dagger_{\mathbf{k}}] &= (2\pi)^3 \, 2E_{\mathbf{p}} \delta^{(3)}(\mathbf{p} - \mathbf{k}), \\ [\hat{a}_{\mathbf{p}}, \hat{a}_{\mathbf{k}}] &= [\hat{a}^\dagger_{\mathbf{p}}, \hat{a}^\dagger_{\mathbf{k}}] = 0 \end{aligned} \tag{2.9}$$

and the former can be used to define a vacuum state $|0\rangle$ via

$$\hat{a}_{\mathbf{p}} |0\rangle = 0. \tag{2.10}$$

When calculating the expectation value of two scalar fields, $\hat{\phi}(x)$ and $\hat{\phi}(y)$, in the vacuum state in various ways, the different propagators can be determined. The positive frequency Wightman propagator $\Delta^>_{xy}$, describing the vacuum transition amplitude for a particle when moving from spacetime point x to y, is given by [15, 36]

$$\Delta^>_{xy} \coloneqq \langle 0| \hat{\phi}(x)\hat{\phi}(y) |0\rangle = \int d\Pi_{\mathbf{k}} e^{-iE_{\mathbf{k}}(x^0 - y^0) + i\mathbf{k}\cdot(\mathbf{x}-\mathbf{y})}, \tag{2.11}$$

while the negative frequency Wightman propagator $\Delta^<_{xy}$ is obtained by either complex conjugating the positive frequency Wightman propagator or switching its arguments x and y. Using the time ordering operator $\hat{\mathrm{T}}$ defined by

$$\hat{\mathrm{T}}\hat{\phi}(x)\hat{\phi}(y) \coloneqq \Theta(x^0 - y^0)\hat{\phi}(x)\hat{\phi}(y) + \Theta(y^0 - x^0)\hat{\phi}(y)\hat{\phi}(x), \tag{2.12}$$

the free Feynman propagator is obtained by [15]

$$\Delta^F_{xy} \coloneqq \langle 0| \hat{\mathrm{T}}\hat{\phi}(x)\hat{\phi}(y) |0\rangle = -i \int_k \frac{e^{ik(x-y)}}{k^2 + m_\phi - i\epsilon} \tag{2.13}$$

Die approbierte gedruckte Originalversion dieser Diplomarbeit ist an der TU Wien Bibliothek verfügbar
The approved original version of this thesis is available in print at TU Wien Bibliothek.

with $\int_k := \int \frac{d^4k}{(2\pi)^4}$ and $\epsilon \to 0$. Complex conjugating the Feynman propagator leads to the free Dyson propagator Δ^D_{xy}.

The alternative to canonical quantisation for integrating scalar fields into a quantum field theory is Feynman's path integral formalism. Both ways lead to identical predictions of the physics as they are equivalent theories [37]. However, Feynman's formalism gets the results by integrating over all possible paths in spacetime of a classical particle. As a result, the Feynman propagator in vacuum is given by [36]

$$\Delta^F_{xy} := \langle 0| \hat{\mathrm{T}}\hat{\phi}(x)\hat{\phi}(y) |0\rangle = \frac{\int \mathcal{D}\phi e^{iS_0}\phi(x)\phi(y)}{\int \mathcal{D}\phi e^{iS_0}}, \tag{2.14}$$

where S_0 is the free action of the scalar field ϕ, the denominator is used to normalise the expression and the path integral over all possible paths of ϕ is denoted by

$$\mathcal{D}\phi := \prod_i d\phi(x_i). \tag{2.15}$$

However, to this day, in Nature there has only been found one elementary scalar field experimentally, the Higgs boson of the Standard Model [38–41]. Nevertheless, there is still the possibility to find additional fundamental scalar fields. Additionally, there are actually several theories that speculate on the existence of such fields, like string theory [42, 43], supergravity [44] or $f(R)$-gravity [45], a generalisation of general relativity. Independently of their prediction in such theories, new scalar fields can be used to explain phenomena in various areas of physics. There are different ideas of how such scalar fields can couple to particles of the Standard Model. For example, they could reside in so-called hidden sectors [46], meaning that they do not interact by means of known gauge bosons (photons, gluons, W- or Z-bosons) but by coupling to the Higgs boson which then couples to other Standard Model particles, which is known as the Higgs portal [47]. This could be an explanation for dark matter [48].

Alternatively, novel scalar fields are also used in theories of modified gravity, some of which are so-called scalar-tensor theories where the scalar field is coupled to the metric tensor of gravity $g_{\mu\nu}$ [8] which is for instance motivated by string theory. Two of the first examples of theories of modified gravity include Jordan's theory [49] as well as Brans-Dicke theory [50]. The coupling is usually achieved by a conformal factor $A(\phi)$, for example via $A(\phi)g_{\mu\nu}$. This way of coupling the scalar field to the Standard Model is oftentimes considered in explanations for dark energy or the cosmological constant.

However, scalar-tensor theories predict the existence of a fifth force similar to gravity. Nonetheless, such fifth forces have not yet been found in any observations or experiments and they are therefore tightly constraint by tests within our Solar System [10]. This problem could, for example, be solved by assuming that the force carrying scalar is very heavy or the coupling between scalar and matter is very weak, about 5 orders of magnitude

Die approbierte gedruckte Originalversion dieser Diplomarbeit ist an der TU Wien Bibliothek verfügbar
The approved original version of this thesis is available in print at TU Wien Bibliothek.
TU Bibliothek Your knowledge hub WIEN

weaker than gravity [51]. These explanations, however, follow from fine tuning and they are not very compelling since in this case fifth forces likely only play an insignificant role in interesting physical theories.

Alternatively, the lack of any fifth forces so far could also be described by a so-called screening mechanism which is phenomenologically more interesting. These screening mechanisms contain several methods of repressing a fifth force in dependence of the environment and result from a non-linear scalar field theory. More specifically, the higher the environmental mass or energy density, i.e. the trace of the energy momentum tensor $T^{\mu}{}_{\mu}$ or the curvature, in a specific area is, the higher is the suppression of the fifth force due to the screening mechanism and the coupling between the scalar field and matter is very weak or even vanishing. In contrast, in areas of a small curvature and trace of the energy momentum tensor, respectively, the force is hardly suppressed leading to a significant coupling to matter. For non-relativistic matter it is assumed that $T^{\mu}{}_{\mu} = -\rho$ [2] holds, where ρ is the mass density, leading to the aforementioned dependence on the environmental mass or energy density. Presuming that within the Solar System ρ is large enough, any constraints in this area can be bypassed by a screening mechanism. Scalar fields affected by such a screening mechanism are called screened scalar fields.

So far, several different categories of screening mechanisms have been developed, as well as a variety of different models within each category. These categories differ in the parameters that vary with the environmental mass density and, including the most prominent model within, work as follows [2]:

- The coupling to matter depends on the mass density of the environment leading the coupling to become weaker in areas of higher density. This is also called Damour-Polyakov screening mechanism [52, 53] and an example model is the symmetron [54–57].

- The effective mass of the scalar field depends on the environmental density leading the mass to increase in areas of higher density, resulting in a short-ranged force. The archetypal example is the chameleon [58, 59].

- The kinetic term is modified or new kinetic terms are added leading to kinetic terms depending on the environmental mass density and a repression of the scalar field's kinetics in areas of high mass density resulting in the force becoming short-ranged. This is also called Vainshtein mechanism and one example is the galileon model [60–63].

2.1. Dilaton

The environmentally dependent dilaton field is another example of a screened scalar field [52, 64, 65]. Its screening mechanism works similar to the one of the symmetron field as

Die approbierte gedruckte Originalversion dieser Diplomarbeit ist an der TU Wien Bibliothek verfügbar
The approved original version of this thesis is available in print at TU Wien Bibliothek.
TU Bibliothek Your knowledge hub WIEN

the dilaton is subject to the Damour-Polyakov screening mechanism as well. This means, that the coupling to matter decreases in regions of increasing matter density.

The dilaton's potential $V(\phi)$ decreases exponentially, as required to satisfy the strong coupling limit of string theory, from where it is originating from [52, 66–68]:

$$V(\phi) = V_0\, e^{-\lambda\phi/M_{Pl}}, \tag{2.16}$$

where V_0 is an energy scale related to the dark energy of the Universe, λ is a numerical constant [69] and M_{Pl} is the reduced Planck mass. Furthermore, the dilaton's coupling function $A(\phi)$ results from the least coupling limit [52] which assumes the dilaton's coupling to matter to vanish in areas of very high surrounding densities [70]:

$$A(\phi) = 1 + \frac{A_2}{2M_{Pl}^2}\phi^2, \tag{2.17}$$

where assuming $A_2 \gg 1$ leads to constraints on fifth forces from Solar System tests to be circumvented [53]. A_2 and the coupling constant $\mathcal{M}$, which has the dimension of a mass, are connected via [69]

$$A_2 = \frac{M_{Pl}^2}{\mathcal{M}^2}, \tag{2.18}$$

whereupon $\phi/\mathcal{M} \ll 1$ is required so that terms of higher order in ϕ in the coupling function (2.17) are negligible [70].

Using Eqs. (2.16) and (2.17), the effective potential for the dilaton in an environment of matter density ρ^{ext} reads [2, 69]

$$\begin{aligned} V_{\text{eff}}(\phi;\rho^{\text{ext}}) &= V(\phi) + A(\phi)\rho^{\text{ext}} \\ &= V_0\, e^{-\lambda\phi/M_{Pl}} + \frac{A_2\rho^{\text{ext}}}{2M_{Pl}^2}\phi^2, \end{aligned} \tag{2.19}$$

where the additional term ρ^{ext} was neglected since it does not contribute to the equation of motion.[2] As can be seen in Eq. (2.19), for $\phi \approx 0$ the dilaton's coupling to matter is negligible which is the essence of its screening mechanism [2]. Using the effective potential, the minimum value of the dilaton field in presence of the background density ρ^{ext} can be

[2] A different definition of the effective potential can be found for example in [2, 24] as

$$V_{\text{eff}}(\phi;\rho^{\text{ext}}) = \tilde{V}_0\, e^{-\varphi/M_{Pl}} + \frac{(\varphi-\varphi_*)^2}{2\mathcal{M}^2}\rho^{\text{ext}} \tag{2.20}$$

with φ_* being the critical field value for which the dilaton decouples. This decoupling at $\varphi \approx \varphi_*$ is the gist of the screening mechanism of the dilaton. However, it can be easily shown that these two expressions of the effective potential are equivalent by defining $\phi = \varphi - \varphi_*$ as the deviation from the critical field value, using Eq. (2.18) and redefining the energy scale $\tilde{V}_0 \to V_0$ in such a way that all new terms in the dilaton potential $V(\phi)$ resulting from the transformation $\phi = \varphi - \varphi_*$ are absorbed in V_0 and λ.

Die approbierte gedruckte Originalversion dieser Diplomarbeit ist an der TU Wien Bibliothek verfügbar
The approved original version of this thesis is available in print at TU Wien Bibliothek.
TU Bibliothek Your knowledge hub WIEN

evaluated by using $V_{\text{eff},\phi}(\phi;\rho^{\text{ext}})|_{\phi=\phi_\rho} = 0$ which gives [70]

$$\phi_\rho = \frac{M_{Pl}}{\lambda} W\left(\frac{\lambda^2 V_0}{A_2 \rho^{\text{ext}}}\right), \tag{2.21}$$

where the Lambert W-function

$$W(x) = \sum_{n=1}^{\infty} \frac{(-n)^{n-1}}{n!} x^n = x - x^2 + \frac{3}{2}x^3 - \frac{8}{3}x^4 + \frac{125}{24}x^5 + \dots \tag{2.22}$$

was used. Moreover, the mass of the quantum fluctuation is [70]

$$m_\rho = \sqrt{V_{\text{eff},\phi\phi}(\phi_\rho;\rho^{\text{ext}})} = \frac{1}{M_{Pl}} \sqrt{\lambda^2 V_0\, e^{-\lambda\phi_\rho/M_{Pl}} + A_2\rho^{\text{ext}}}. \tag{2.23}$$

Finally, the fifth force of the dilaton on a point particle is [70]

$$\mathbf{f}_\phi := -m\vec{\nabla}A(\phi) = -m\frac{A_2}{M_{Pl}^2}\phi\vec{\nabla}\phi. \tag{2.24}$$

2.2. Coupling to Standard Model matter

The coupling of scalar-tensor theories, where the additional scalar field ϕ couples to the metric tensor of gravity $g_{\mu\nu}$, is commonly achieved by using a conformal factor $A(\phi)$. Since scalar-tensor theories are only defined up to a conformal transformation, one can change from one conformal frame to another [8]. Each conformal frame leads to a different mathematical formulation, where some computations may be easier to do in some frames than in others. However, all physical predictions of experimental outcomes are the same in all conformal frames, only the theoretical interpretations may vary. As an example of differing interpretations, two of the most common frames, the Einstein and the Jordan frame, are considered. In the Einstein frame, the presence of a new scalar field leads the test particle to experience a fifth force and therefore its trajectory differs from the geodesic. In contrast, in the Jordan frame, the presence of the new scalar field leads to a modification of gravity, namely a change of the geodesics which the test particle still follows. Both frames predict the same trajectories for the test particle but their explanations differ.

The total action used here contains a gravitational action, an action describing the Standard Model matter dynamics with the matter field ϕ[3] as well as the interactions of the matter field with the additional scalar field X. Throughout this thesis, it is assumed

[3]The matter field is modelled as a scalar field for simplicity. However, this approximation has some drawbacks, as scalar fields lack a complex internal structure and, therefore, any stability when it comes to decay and production processes. Matter fields, for example for atoms or molecules, however, are a lot more complex and generally stable. Thus, the production of atom-anti-atom pairs is likely suppressed, justifying a restriction to single particle subspaces as will be done in Section 3.4.

Die approbierte gedruckte Originalversion dieser Diplomarbeit ist an der TU Wien Bibliothek verfügbar
The approved original version of this thesis is available in print at TU Wien Bibliothek.
TU Bibliothek Your knowledge hub WIEN

that the matter field's mass is given by M, while the screened scalar field's mass is given by m. For convenience, the action used is in the Einstein frame, giving [58, 59]

$$\begin{aligned} S = &\int d^4x\sqrt{-g}\left[\frac{1}{2}M_{Pl}^2\mathcal{R} - \frac{1}{2}g^{\mu\nu}\partial_\mu X\partial_\nu X - V(X)\right] \\ &+ \int d^4x\sqrt{-g}A^4(X)\tilde{\mathcal{L}}_M(\tilde{\phi}, A^2(X)g_{\mu\nu}). \end{aligned} \tag{2.25}$$

Here, parameters with a tilde ˜ belong to the Jordan frame while quantities without tilde to the Einstein frame. Furthermore, $\mathcal{R}$ is the associated Ricci scalar, $V(X)$ is the potential for the scalar field X and

$$\tilde{\mathcal{L}}_M = -\frac{1}{2}\tilde{g}^{\mu\nu}\partial_\mu\tilde{\phi}\partial_\nu\tilde{\phi} - \frac{1}{2}\tilde{M}^2\tilde{\phi}^2 \tag{2.26}$$

is the Lagrangian of the matter field in Jordan frame of the single scalar field $\tilde{\phi}$ with mass $\tilde{M}$. The rescaled metric is

$$\tilde{g}_{\mu\nu} = A^2(X)g_{\mu\nu}, \tag{2.27}$$

which also shows the conformal transformation between the two frames. Using the definition of the transformation for the covariant metric, Eq. (2.27), and the requirement $\tilde{g}_{\mu\nu}\tilde{g}^{\mu\nu} = g_{\mu\nu}g^{\mu\nu}$, one finds for the contravariant metric

$$\tilde{g}^{\mu\nu}A^2(X) = g^{\mu\nu}. \tag{2.28}$$

The transformation of the matter Lagrangian in the Jordan frame, Eq. (2.26), to the Einstein frame is given by

$$\begin{aligned} \mathcal{L}_M &\coloneqq A^4(X)\tilde{\mathcal{L}}_M \\ &= -\frac{1}{2}A^2(X)g^{\mu\nu}\partial_\mu\tilde{\phi}\partial_\nu\tilde{\phi} - \frac{1}{2}A^4(X)\tilde{M}^2\tilde{\phi}^2, \end{aligned} \tag{2.29}$$

where Eq. (2.28) was used. Now, the matter field $\tilde{\phi}$ is redefined via

$$\phi \coloneqq A(X)\tilde{\phi}. \tag{2.30}$$

This leads to the matter Lagrangian becoming

$$\begin{aligned} \mathcal{L}_M = &-\frac{1}{2}g^{\mu\nu}\partial_\mu\phi\partial_\nu\phi - \frac{1}{2}\phi^2 g^{\mu\nu}\partial_\mu \ln A(X)\partial_\nu \ln A(X) \\ &+ \phi g^{\mu\nu}\partial_\mu\phi\partial_\nu \ln A(X) - \frac{1}{2}A^2(X)\tilde{M}^2\phi^2. \end{aligned} \tag{2.31}$$

The coupling function $A(X)$ can be expanded under the assumption that the coupling to

Die approbierte gedruckte Originalversion dieser Diplomarbeit ist an der TU Wien Bibliothek verfügbar
The approved original version of this thesis is available in print at TU Wien Bibliothek.

matter is controlled by a mass scale $\mathcal{M}$, where $X/\mathcal{M} \ll 1$ holds, as

$$A^2(X) = a + b\frac{X}{\mathcal{M}} + c\frac{X^2}{\mathcal{M}^2} + \mathcal{O}\left(\frac{X^3}{\mathcal{M}^3}\right), \tag{2.32}$$

where a, b and c are coefficients dictated by the used model. When only keeping operators of dimension 4 or lower, as operators of higher dimensions are suppressed by higher powers of $\mathcal{M}$, the matter Lagrangian becomes

$$\mathcal{L}_M = -\frac{1}{2}g^{\mu\nu}\partial_\mu\phi\partial_\nu\phi - \frac{1}{2}\left(a + b\frac{X}{\mathcal{M}} + c\frac{X^2}{\mathcal{M}^2}\right)\tilde{M}^2\phi^2. \tag{2.33}$$

In case of the dilaton field, the coupling function is given by Eq. (2.17) which becomes

$$A^2(X) = 1 + \frac{A_2}{M_{Pl}^2}X^2 + \mathcal{O}\left(\frac{X^3}{\mathcal{M}^3}\right) \tag{2.34}$$

when using Eq. (2.18). Therefore, for the dilaton, the parameters are $a = c = 1$ and $b = 0$. Furthermore, using the effective potential of the dilaton, Eq. (2.19), and assuming $\lambda X/M_{Pl} \ll 1$ [69][4], the exponent can be expanded to second order:

$$\begin{aligned} V_{\text{eff}}(X) &= V_0\, e^{-\lambda X/M_{Pl}} + \frac{A_2\rho^{\text{ext}}}{2M_{Pl}^2}X^2 \\ &\approx V_0 - V_0\frac{\lambda}{M_{Pl}}X + V_0\frac{\lambda^2}{2M_{Pl}^2}X^2 + \frac{A_2\rho^{\text{ext}}}{2M_{Pl}^2}X^2. \end{aligned} \tag{2.35}$$

Next, the dilaton scalar field X is expanded, $X = \langle X\rangle + \chi$, where $\langle X\rangle \neq 0$ is the background field value or classical expectation value of the field X and χ is the deviation from the background value. When presuming that the background density ρ^{ext} as well as the background field value $\langle X\rangle$ are constant, the classical equation of motion for the background field value is

$$\begin{aligned} \Box\langle X\rangle &= \frac{d}{dX}V_{\text{eff}}(X)|_{X=\langle X\rangle} \\ &= -V_0\frac{\lambda}{M_{Pl}} + V_0\frac{\lambda^2}{M_{Pl}^2}\langle X\rangle + \frac{A_2\rho^{\text{ext}}}{M_{Pl}^2}\langle X\rangle = 0. \end{aligned} \tag{2.36}$$

Putting the dilaton field expansion into the effective potential and using Eq. (2.36) leads to

$$V_{\text{eff}}(\langle X\rangle + \chi) = V_{\text{eff}}(\langle X\rangle) + \frac{1}{2}m^2\chi^2, \tag{2.37}$$

[4]In string theory, where the dilaton originated, this assumption does not hold. On the contrary, it even reads $\lambda X/M_{Pl} \gg 1$. However, for the model itself, there is no reason why the exponent should not be expandable as it is as much a valid model for a screened scalar field as every other model mentioned in Section 2 even when it is no longer compatible with string theory.

Die approbierte gedruckte Originalversion dieser Diplomarbeit ist an der TU Wien Bibliothek verfügbar
The approved original version of this thesis is available in print at TU Wien Bibliothek.
TU Bibliothek Your knowledge hub WIEN

where the squared mass for the χ-field was defined as

$$m^2 \coloneqq \frac{1}{M_{Pl}^2}\left(V_0\lambda^2 + A_2\rho^{\text{ext}}\right). \tag{2.38}$$

This leads to the full Lagrangian of the two scalar system in flat space to be

$$\begin{aligned}\mathcal{L} = &-\frac{1}{2}g^{\mu\nu}\partial_\mu\phi\partial_\nu\phi - \frac{1}{2}M^2\phi^2 - \frac{1}{2}\alpha_1 M\chi\phi^2 - \frac{1}{4}\alpha_2\chi^2\phi^2 \\ &-\frac{1}{2}g^{\mu\nu}\partial_\mu\chi\partial_\nu\chi - \frac{1}{2}m^2\chi^2 - V_{\text{eff}}(\langle X\rangle),\end{aligned} \tag{2.39}$$

where the squared mass of the ϕ-field is defined as

$$M^2 \coloneqq \left(1 + \frac{A_2}{M_{Pl}^2}\langle X\rangle^2\right)\tilde{M}^2 \tag{2.40}$$

and

$$\alpha_1 \coloneqq 2M\frac{A_2}{M_{Pl}^2}\langle X\rangle\left(1 - \frac{A_2}{M_{Pl}^2}\langle X\rangle^2\right), \tag{2.41}$$

$$\alpha_2 \coloneqq 2\frac{A_2}{M_{Pl}^2}M^2\left(1 - \frac{A_2}{M_{Pl}^2}\langle X\rangle^2\right). \tag{2.42}$$

For the calculation later in this thesis, it is useful to separate the full Lagrangian of Eq. (2.39) into the free actions of the massive scalar fields ϕ and χ, respectively, and the action of the interactions between these two fields:

$$S_\phi[\phi] \coloneqq \int_x \left[-\frac{1}{2}g^{\mu\nu}\partial_\mu\phi\partial_\nu\phi - \frac{1}{2}M^2\phi^2\right], \tag{2.43}$$

$$S_\chi[\chi] \coloneqq \int_x \left[-\frac{1}{2}g^{\mu\nu}\partial_\mu\chi\partial_\nu\chi - \frac{1}{2}m^2\chi^2\right], \tag{2.44}$$

$$S_{\text{int}}[\phi,\chi] \coloneqq \int_{x\in\Omega_t} \left[-\frac{1}{2}\alpha_1 M\chi\phi^2 - \frac{1}{4}\alpha_2\chi^2\phi^2\right], \tag{2.45}$$

where the terms in $V_{\text{eff}}(\langle X\rangle)$ were dropped due to the fact that they are constant and do not contribute to the dynamics. Furthermore, in the following calculations it is assumed that the interactions between ϕ and χ take place over a finite amount of time corresponding to the time-span between preparing the initial state and the subsequent measurement of the system. This is why the hypervolume

$$\Omega_t \coloneqq [0,t]\times\mathbb{R} \tag{2.46}$$

was defined.[5] The free actions of ϕ and χ, however, are still supported for all times [71].

[5] Alternatively to restricting the time integration with finite limits, one could also introduce time-dependant coupling constants α_1 and α_2 to simulate the switching on and off of the interaction. Furthermore, the introduction of a switching function would reflect the more general and more realistic switching on and off over a limited period of time instead of switching on and off instantaneously.

Die approbierte gedruckte Originalversion dieser Diplomarbeit ist an der TU Wien Bibliothek verfügbar
The approved original version of this thesis is available in print at TU Wien Bibliothek.
TU Bibliothek Your knowledge hub WIEN

3. Derivation of reduced density matrix elements in open quantum dynamics

Realistic systems, both classical and quantum dynamical ones, can be considered as open. This means that the system is noticeably effected by interactions with its uncontrollable environment [14]. These interactions lead to a variety of phenomena like energy and momentum diffusion [15] which can cause effects like decoherence and phase shifts [16].

The aim of this thesis is to describe how matter fields, like the one of a cold atom, couple to a dilaton field since this can be experimentally investigated in relatively cheap tabletop experiments like atom interferometry. Therefore, the scalar field ϕ, approximating the atom, is regarded as the system which interacts with its environment, the dilaton field χ. The combined system of both the open system ϕ and the environment χ is, in general, considered to be closed and can be described by the density operator $\hat{\rho}_{\phi\chi}(t)$ which fulfils the Liouville-von Neumann equation [14]

$$\frac{\partial}{\partial t}\hat{\rho}_{\phi\chi}(t) = \hat{\mathcal{L}}(t)\hat{\rho}_{\phi\chi}(t). \tag{3.1}$$

This equation describes the time evolution of $\hat{\rho}_{\phi\chi}(t)$ and $\hat{\mathcal{L}}(t)$ is the Liouville superoperator, acting like

$$\hat{\mathcal{L}}(t)\hat{\rho}_{\phi\chi}(t) = -i[\hat{H}(t), \hat{\rho}_{\phi\chi}(t)], \tag{3.2}$$

where $\hat{H}(t)$ is the Hamiltonian of the total system. The density operator can be used to calculate the expectation value of an arbitrary operator $\hat{O}(t)$, which acts on the combined system, via

$$\langle\hat{O}(t)\rangle = \mathrm{Tr}(\hat{\rho}_{\phi\chi}(t)\hat{O}(t)). \tag{3.3}$$

Two common approximations when dealing with an open quantum system are the Born and the Markov approximations. In the Born approximation, the coupling between system and environment is assumed to be weak so that the system is affected by the environment but the environment in return is barely influenced by the system. This leads to the environment to be roughly constant over time so that the combined density matrix can be separated via $\hat{\rho}_{\phi\chi}(t) \approx \hat{\rho}_{\phi}(t) \otimes \hat{\rho}_{\chi}$. Here, $\hat{\rho}_{\phi}(t)$ and $\hat{\rho}_{\chi}$ are the separated density operators for the system and the environment, respectively. In the Markov approximation, on the other hand, all excitations of the environment induced by the system are assumed

Die approbierte gedruckte Originalversion dieser Diplomarbeit ist an der TU Wien Bibliothek verfügbar
The approved original version of this thesis is available in print at TU Wien Bibliothek.
TU Bibliothek Your knowledge hub WIEN

to decay faster than any timescales of interest. This means that on a physical level, memory effects can be ignored - meaning that the open system is unaffected by changes of the environment caused by the system itself and furthermore independent on earlier times - and on a practical level that all time integrals can be integrated to ∞.

As already mentioned, the environment χ is usually difficult to describe theoretically and to control experimentally. Thus, only the open system ϕ and its development under influence of the environment are of interest. Mathematically, the reduced density matrix of only the system ϕ, $\hat{\rho}_\phi(t)$, is extracted by tracing out the environmental degrees of freedom

$$\hat{\rho}_\phi(x_\phi) = \int dx_\chi \hat{\rho}_{\phi\chi}(x_\phi, x_\chi). \tag{3.4}$$

In contrast to the density operator of the closed system $\hat{\rho}_{\phi\chi}(t)$, which is strictly unitary, the evolution of the reduced density operator $\hat{\rho}_\phi(t)$ is usually non-unitary leading to effects like decoherence, typical for open quantum systems. Decoherence might explain the transition of the quantum physical world to the classical world and it works as follows: A quantum system is represented by a superposition of states. However, after the so-called decoherence time, the superposition is destroyed and the quantum system becomes classical and remains in a specific state. Mathematically this means that the density matrix of the open system $\hat{\rho}_\phi(t)$ is not idempotent while the density matrix of the combined system $\hat{\rho}_{\phi\chi}(t)$ is, see for example [24].

In order to directly calculate elements of the reduced density matrix, $\hat{\rho}_\phi(t)$, the path laid out by [26] will be followed. For this, techniques of non-equilibrium quantum field theory are combined, namely the Schwinger-Keldysh formalism [28, 29] and the Feynman-Vernon influence functional based on the path integral formalism [30] in Section 3.2, and an approach based on operators, thermo field dynamics (TFD) [31, 32], in Section 3.3. In combination with the fact that the Liouville equation (3.1) in the Schrödinger picture can be expressed as a Schrödinger-like equation within TFD, a Lehmann-Szymanzik-Zimmermann- or LSZ-like reduction [72] will be used to perturbatively find an explicit formula for determining elements of $\hat{\rho}_\phi(t)$ in momentum space for a single-particle state in Section 3.4. Therefore, the weak coupling of the Born approximation is assumed, but including Markov's approximation is not necessary. The deduced formula will then be used to determine the effect a dilaton field has on a single particle in momentum space for finite temperatures in Section 4. This solution is then renormalized in Section 4.1 before experimental implications are discussed in Section 4.2.

Throughout this thesis, it is assumed that both system ϕ and environment χ have constant mass. Furthermore, it is presumed that the system's mass M is much larger than the environment's mass m, $m/M \ll 1$. When using the scalar field ϕ as a proxy for a heavy atom in atom interferometry, as is done in Section 4.2, this approximation holds true.

Die approbierte gedruckte Originalversion dieser Diplomarbeit ist an der TU Wien Bibliothek verfügbar
The approved original version of this thesis is available in print at TU Wien Bibliothek.

3.1. Density matrices in Fock space

In the following, the density matrix elements are considered in Fock space, which permits the consideration of an arbitrary number of particles. Additionally, the choice to work in a momentum basis is made since atoms in atom interferometers can display momentum superposition. The most universal expression for the density operator in Fock space in momentum basis is given by

$$\hat{\rho}(t) = \sum_{i,j=0}^{\infty} \frac{1}{i!j!} \int \left(\prod_{a=1}^{i} d\Pi_{\mathbf{k}^{(a)}} \right) \left(\prod_{b=1}^{j} d\Pi_{\mathbf{l}^{(b)}} \right) \rho_{i,j}(\mathbf{k}^{(1)}, \ldots, \mathbf{k}^{(i)}, \mathbf{l}^{(1)}, \ldots, \mathbf{l}^{(j)}; t) \times \left| \mathbf{k}^{(1)}, \ldots, \mathbf{k}^{(i)} \right\rangle \left\langle \mathbf{l}^{(1)}, \ldots, \mathbf{l}^{(j)} \right| . \tag{3.5}$$

Here, the cases $i = 0$ and $j = 0$ describe static vacuum states, $|0\rangle$ and $\langle 0|$, respectively. Moreover, each element of the density matrix is determined via

$$\rho_{i,j}(\mathbf{k}^{(1)}, \ldots, \mathbf{k}^{(i)}, \mathbf{l}^{(1)}, \ldots, \mathbf{l}^{(j)}; t) = \left\langle \mathbf{k}^{(1)}, \ldots, \mathbf{k}^{(i)} \right| \hat{\rho}(t) \left| \mathbf{l}^{(1)}, \ldots, \mathbf{l}^{(j)} \right\rangle , \tag{3.6}$$

which for a single-particle state becomes

$$\rho_{1,1}(\mathbf{k}, \mathbf{k}'; t) = \langle \mathbf{k}| \hat{\rho}(t) |\mathbf{k}'\rangle . \tag{3.7}$$

Complex conjugating an arbitrary matrix element leads to the usual relation

$$\rho_{i,j}(\mathbf{k}^{(1)}, \ldots, \mathbf{k}^{(i)}, \mathbf{l}^{(1)}, \ldots, \mathbf{l}^{(j)}; t) = \rho^*_{j,i}(\mathbf{l}^{(1)}, \ldots, \mathbf{l}^{(j)}, \mathbf{k}^{(1)}, \ldots, \mathbf{k}^{(i)}; t). \tag{3.8}$$

Physically, the $\rho_{0,0}$ density matrix element can be interpreted as a 0-particle or vacuum state. Similarly, the $\rho_{i,0}$ and $\rho_{0,j}$ elements can be understood as correlations of the vacuum and the i- and j-particle states, respectively. The $\rho_{i,j}$ elements, meanwhile, can be explained as correlations between the i- and j-particle states.

The time evolution of the density operator is given by the Liouville-von Neumann equation (3.1). It is solved by

$$\hat{\rho}_S(t) = \left(\mathrm{T} e^{-i \int_0^t d\tau \hat{H}_S(\tau)} \right) \hat{\rho}(0) \left(\tilde{\mathrm{T}} e^{i \int_0^t d\tau \hat{H}_S(\tau)} \right) \tag{3.9}$$

with the time ordering and anti-time ordering operators T and $\tilde{\mathrm{T}}$, respectively, and where the time dependency of the Hamiltonian results from an external source. Eq. (3.9) becomes

$$\hat{\rho}_S(t) = e^{-i\hat{H}_S t} \hat{\rho}(0) e^{i\hat{H}_S t} \tag{3.10}$$

if the Hamiltonian is constant over time, as can easily be seen. The index S in equations (3.9) and (3.10) indicates that these operators are given in the Schrödinger picture which

Die approbierte gedruckte Originalversion dieser Diplomarbeit ist an der TU Wien Bibliothek verfügbar
The approved original version of this thesis is available in print at TU Wien Bibliothek.
TU Bibliothek Your knowledge hub WIEN

is the picture of choice for the beginning of the derivation. However, since all pictures coincide at $t = 0$, the subscript S was dropped for $t = 0$.

In the subsequent Sections (3.2, 3.3, 3.4), a projection into a single particle momentum space, $\rho_{1,1}$, is determined by following the derivation laid out in [26].

3.2. The Feynman-Vernon influence functional

When working with an open system in field theory, one oftentimes uses the Feynman-Vernon influence functional [30] based on the Schwinger-Keldysh closed-time-path (CTP) formalism [28, 29], see for example [15]. The CTP formalism works with doubling the degrees of freedom and placing the two copies on branches of a closed time-path labeled with $+$ and $-$. More precisely, the degrees of freedom first evolve on the positive branch from the initial time $t_{\text{initial}} = 0$ to the final time $t_{\text{final}} = t$ and then backwards in time on the negative branch, as can be seen in Figure 3.1. Doubling the degrees of freedom is necessary to write down a path-integral representation of the trace of an operator, as needed for the Feynman-Vernon influence functional. The Feynman-Vernon influence functional, on the other hand, describes the evolution of the open quantum system influenced by the environment but without describing the environmental degrees of freedom themselves. It is an important object in the formula for the reduced density matrix element derived in the next parts. Additionally, it will be shown how it occurs when reducing the total density operator to the reduced density operator of the system.

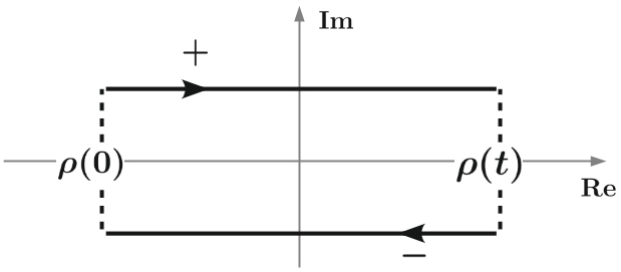

Figure 3.1.: Schematic depiction of the closed time-path for a density matrix ρ evolving from an initial time 0 to a final time t on the $+$-branch and backwards on the $-$-branch. The two time branches $+$ and $-$ are sightly shifted on the imaginary time axis, giving small imaginary contributions, $\pm i\eta$ in the limit $\eta \to 0$, to the time variable. (Taken from Ref. [26])

To do so, it is presumed that the system ϕ and the environment χ are separable at the beginning, when $t = 0$,

$$\hat{\rho}_{\phi\chi}(0) = \hat{\rho}_{\phi}(0) \otimes \hat{\rho}_{\chi}(0). \tag{3.11}$$

Furthermore, the environmental degrees of freedom can be traced out so that the reduced

Die approbierte gedruckte Originalversion dieser Diplomarbeit ist an der TU Wien Bibliothek verfügbar
The approved original version of this thesis is available in print at TU Wien Bibliothek.

density operator for the open system becomes

$$\hat{\rho}_\phi(t) = \mathrm{Tr}_\chi \hat{\rho}_{\phi\chi}(t). \tag{3.12}$$

Next, the reduced density operator is projected into the field basis on the closed time-path leading to

$$\begin{aligned}\rho_\phi[\phi_t^\pm; t] &\coloneqq \left\langle \phi_t^+ \right| \hat{\rho}_\phi(t) \left| \phi_t^- \right\rangle = \left\langle \phi_t^+ \right| \left(\int d\chi_t^+ \left\langle \chi_t^+ \right| \hat{\rho}_{\phi\chi}(t) \left| \chi_t^+ \right\rangle \right) \left| \phi_t^- \right\rangle \\ &= \int d\chi_t^\pm \left\langle \phi_t^+ \right| \left\langle \chi_t^+ \right| \hat{\rho}_{\phi\chi}(t) \left| \chi_t^- \right\rangle \left\langle \chi_t^- \right| \left. \chi_t^+ \right\rangle \left| \phi_t^- \right\rangle \\ &= \int d\chi_t^\pm \delta(\chi_t^+ - \chi_t^-) \rho_{\phi\chi}[\phi_t^\pm, \chi_t^\pm; t],\end{aligned} \tag{3.13}$$

where in the second line a complete set of the eigenstates $\left|\chi_t^-\right\rangle$ at the final time t was inserted, the functional delta function $\int d\chi_t^\pm \left\langle \chi_t^- \right| \left. \chi_t^+ \right\rangle = \int d\chi_t^\pm \delta(\chi_t^+ - \chi_t^-)$ was introduced and

$$\rho_{\phi\chi}[\phi_t^\pm, \chi_t^\pm; t] \coloneqq \left\langle \phi_t^+, \chi_t^+ \right| \hat{\rho}_{\phi\chi}(t) \left| \phi_t^-, \chi_t^- \right\rangle \tag{3.14}$$

was defined. Moreover, $\pm$ shows a dependence of the field eigenstates on $+$- as well as $-$-type operators, $\int d\chi_t^\pm = \int d\chi_t^+ d\chi_t^-$, and the subscript t indicates which time slice has to be taken, $\chi_t = \chi(t)$.

Using the time evolution of $\hat{\rho}_{\phi\chi}(t)$, Eq. (3.13) becomes

$$\rho_\phi[\phi_t^\pm; t] = \int d\chi_t^\pm \delta(\chi_t^+ - \chi_t^-) \left\langle \phi_t^+, \chi_t^+ \right| e^{-it\hat{H}} \hat{\rho}_{\phi\chi}(0) e^{it\hat{H}} \left| \phi_t^-, \chi_t^- \right\rangle, \tag{3.15}$$

where $\hat{H}$ is the Hamiltonian corresponding to the Lagrangian of the two scalar system, Eq. (2.39). Inserting full sets of field and conjugate momentum eigenstates at all times from 0 to t before and after $\hat{\rho}_{\phi\chi}(0)$ and using that for path integrals $\mathcal{D}\phi^\pm = \prod_i d\phi^\pm(x_i)$ holds, leads to

$$\rho_\phi[\phi_t^\pm; t] = \int d\chi_t^\pm \delta(\chi_t^+ - \chi_t^-) \int d\phi_0^\pm \int d\chi_0^\pm \int_{\phi_0^\pm}^{\phi_t^\pm} \mathcal{D}\phi^\pm \int_{\chi_0^\pm}^{\chi_t^\pm} \mathcal{D}\chi^\pm e^{i\widehat{S}[\phi,\chi;t]} \rho_{\phi\chi}[\phi_0^\pm, \chi_0^\pm; 0], \tag{3.16}$$

where $\widehat{S}[\phi, \chi; t] \coloneqq \widehat{S}_\phi[\phi; t] + \widehat{S}_{\phi,\mathrm{int}}[\phi; t] + \widehat{S}_\chi[\chi; t] + \widehat{S}_{\chi,\mathrm{int}}[\chi; t] + \widehat{S}_{\mathrm{int}}[\phi, \chi; t]$ is the total action of the combined system, $\widehat{S}_\phi[\phi; t]$, $\widehat{S}_{\phi,\mathrm{int}}[\phi; t]$, $\widehat{S}_\chi[\chi; t]$ and $\widehat{S}_{\chi,\mathrm{int}}[\chi; t]$ are the free and the self-interacting actions of the system field ϕ and the environment field χ, respectively, $\widehat{S}_{\mathrm{int}}[\phi, \chi; t]$ is the interaction action between ϕ and χ and $\widehat{\ }$ specifies which functionals depend on both $+$- and $-$- type operators. The free action of the system, for example, is given by

$$\widehat{S}_\phi[\phi; t] \coloneqq S_\phi[\phi^+; t] - S_\phi[\phi^-; t]. \tag{3.17}$$

Die approbierte gedruckte Originalversion dieser Diplomarbeit ist an der TU Wien Bibliothek verfügbar
The approved original version of this thesis is available in print at TU Wien Bibliothek.

All of these actions are defined on Ω_t, see Eq. (2.46), because only a finite time interval is considered, so that the actions are structured as

$$S[t] = \int_{x\in\Omega_t} \mathcal{L}[x]. \tag{3.18}$$

Additionally, in this calculation two different types of functional integrals are used. The one indicated by d regards fields over $\mathbb{R}$ at one distinct time slice, whereas the one represented by $\mathcal{D}$ includes fields at all points in Ω_t.

In a last step, the separability of the system and environment at $t = 0$ from Eq. (3.11), which leads to

$$\rho_{\phi\chi}[\phi_0^\pm, \chi_0^\pm; 0] = \rho_\phi[\phi_0^\pm; 0]\rho_\chi[\chi_0^\pm; 0], \tag{3.19}$$

is used to find the final expression for the reduced density functional at time t:

$$\rho_\phi[\phi_t^\pm; t] = \int d\phi_0^\pm \mathcal{I}[\phi_t^\pm, \phi_0^\pm; t, 0]\rho_\phi[\phi_0^\pm; 0] \tag{3.20}$$

with

$$\mathcal{I}[\phi_t^\pm, \phi_0^\pm; t, 0] = \int_{\phi_0^\pm}^{\phi_t^\pm} \mathcal{D}\phi^\pm e^{i\widehat{S}_{\text{eff}}[\phi;t]} \tag{3.21}$$

being the so-called influence functional propagator (see for example [15]). The effective action is given by

$$\widehat{S}_{\text{eff}}[\phi; t] = \widehat{S}_\phi[\phi; t] + \widehat{S}_{\phi,\text{int}}[\phi; t] + \widehat{S}_{\text{IF}}[\phi; t], \tag{3.22}$$

where the influence action $\widehat{S}_{\text{IF}}[\phi; t]$ is defined via the Feynman-Vernon influence functional

$$\begin{aligned}\widehat{\mathcal{F}}[\phi; t] &= e^{i\widehat{S}_{\text{IF}}[\phi;t]} \\ &= \int d\chi_t^\pm d\chi_0^\pm \delta(\chi_t^+ - \chi_t^-)\rho_\chi[\chi_0^\pm; 0] \int_{\chi_0^\pm}^{\chi_t^\pm} \mathcal{D}\chi^\pm e^{i\left(\widehat{S}_\chi[\chi;t]+\widehat{S}_{\chi,\text{int}}[\chi;t]+\widehat{S}_{\text{int}}[\phi,\chi;t]\right)}.\end{aligned} \tag{3.23}$$

It is also possible to define the influence functional as an expectation value with respect to χ as

$$\widehat{\mathcal{F}}[\phi; t] = \langle e^{i\left(\widehat{S}_{\chi,\text{int}}[\chi;t]+\widehat{S}_{\text{int}}[\phi,\chi;t]\right)}\rangle_\chi \tag{3.24}$$

when defining the expectation value via

$$\langle A[\chi^a]\rangle_\chi \coloneqq \int d\chi_t^\pm d\chi_0^\pm \delta(\chi_t^+ - \chi_t^-)\rho_\chi[\chi_0^\pm; 0] \int_{\chi_0^\pm}^{\chi_t^\pm} \mathcal{D}\chi^\pm A[\chi^a] e^{i\widehat{S}_\chi[\chi;t]}. \tag{3.25}$$

3.3. Thermo field dynamics

Using the operator-based approach of thermo field dynamics (TFD) [31, 32, 73] leads to the desired formula for calculating reduced density matrix elements. Similarly to the

Die approbierte gedruckte Originalversion dieser Diplomarbeit ist an der TU Wien Bibliothek verfügbar
The approved original version of this thesis is available in print at TU Wien Bibliothek.

Schwinger-Keldysh closed-time-path formalism described in the previous section, TFD works with doubled degrees of freedom on a positive (+) and negative (−) time branch. Therefore, TFD can be understood as an algebraic version of the CTP formalism, to some degree. However, TFD works by doubling the number of Hilbert spaces, so that each Hilbert space corresponds to one of the ±-branches of the time-path, $\mathcal{H}^{\pm}$:

$$\widehat{\mathcal{H}} \coloneqq \mathcal{H}^{+} \otimes \mathcal{H}^{-}. \tag{3.26}$$

Again, $\widehat{\ }$ is used to mark objects living on both the +- and −-time branch. A general +- or −-type field operator in TFD is defined via

$$\hat{\mathcal{O}}^{+} = \hat{\mathcal{O}} \otimes \hat{\mathbb{1}}, \tag{3.27}$$
$$\hat{\mathcal{O}}^{-} = \hat{\mathbb{1}} \otimes \hat{\mathcal{O}}^{\mathcal{T}} \tag{3.28}$$

with $\hat{\mathbb{1}}$ being the unit operator and $\mathcal{T}$ indicating time reversal.

Furthermore, the doubled vacuum state of TFD in momentum basis is defined as

$$|0\rangle\rangle \coloneqq |0\rangle \otimes |0\rangle\,. \tag{3.29}$$

Every other state can be reached by acting with creation operators on this vacuum state like

$$\hat{a}_{\mathbf{k}}^{+\dagger}\,|0\rangle\rangle = |\mathbf{k}\rangle \otimes |0\rangle =: |\mathbf{k}_{+}\rangle\rangle, \tag{3.30}$$
$$\hat{a}_{\mathbf{k}}^{-\dagger}\,|0\rangle\rangle = |0\rangle \otimes |\mathbf{k}\rangle =: |\mathbf{k}_{-}\rangle\rangle. \tag{3.31}$$

The annihilation operators are

$$\hat{a}_{\mathbf{k}}^{+}\,|\mathbf{p}_{+},\mathbf{p}_{-}\rangle\rangle = (2\pi)^2 2E_{\mathbf{k}}^{\phi}\delta^{(3)}(\mathbf{p}-\mathbf{k})\,|\mathbf{p}_{-}\rangle\rangle, \tag{3.32}$$
$$\hat{a}_{\mathbf{k}}^{-}\,|\mathbf{p}_{+},\mathbf{p}_{-}\rangle\rangle = (2\pi)^2 2E_{\mathbf{k}}^{\phi}\delta^{(3)}(\mathbf{p}-\mathbf{k})\,|\mathbf{p}_{+}\rangle\rangle \tag{3.33}$$

with $|\mathbf{p}_{+},\mathbf{p}_{-}\rangle\rangle \coloneqq |\mathbf{p}\rangle \otimes |\mathbf{p}\rangle$. Additionally, a special state which corresponds to the unit operator can be created. It is defined in [31, 32, 73] by

$$|1\rangle\rangle \coloneqq \sum_{n} |n_{+},n_{-}\rangle\rangle = e^{\hat{a}^{+\dagger}\hat{a}^{-\dagger}}\,|0\rangle\rangle. \tag{3.34}$$

In momentum basis this state becomes

$$|1\rangle\rangle = |0\rangle\rangle + \int d\Pi_{\mathbf{k}}\,|\mathbf{k}_{+},\mathbf{k}_{-}\rangle\rangle + \frac{1}{2!}\int d\Pi_{\mathbf{k}} d\Pi_{\mathbf{k}'}\,|\mathbf{k}_{+},\mathbf{k}'_{+},\mathbf{k}_{-},\mathbf{k}'_{-}\rangle\rangle + \dots \tag{3.35}$$

Die approbierte gedruckte Originalversion dieser Diplomarbeit ist an der TU Wien Bibliothek verfügbar
The approved original version of this thesis is available in print at TU Wien Bibliothek.

and thus allows to write the expectation value of an arbitrary operator as

$$\langle \hat{\mathcal{O}}(t) \rangle = \mathrm{Tr}\, \hat{\mathcal{O}}(t)\hat{\rho}(t) = \langle\langle 1| \hat{\mathcal{O}}^{+}(t)\hat{\rho}^{+}(t) |1\rangle\rangle. \tag{3.36}$$

Using all this, one can now see that in the Schrödinger picture the Liouville-von Neumann equation (3.1) can be rewritten into an form similar to the Schrödinger equation[1]

$$\frac{\partial}{\partial t}\hat{\rho}_S^{+}(t) |1\rangle\rangle_S = -i\widehat{H}_S(t)\hat{\rho}_S^{+}(t) |1\rangle\rangle_S \tag{3.37}$$

with $\widehat{H}_S(t) \coloneqq \hat{H}_S(t) \otimes \mathbb{1} - \mathbb{1} \otimes \hat{H}_S(t)$ which, in general, is solved by

$$\hat{\rho}_S^{+}(t) |1\rangle\rangle_S = \mathrm{T} e^{-i\int_0^t \widehat{H}_S(\tau)d\tau} \hat{\rho}^{+}(0) |1\rangle\rangle_S \,. \tag{3.38}$$

Since all pictures coincide at $t = 0$, the subscript S was dropped on the right-hand side.

Similarly to Eq. (3.37), one can write down the Schrödinger-like equation for the reduced density operator of the open system ϕ

$$\frac{\partial}{\partial t}\hat{\rho}_{\phi,S}^{+}(t) |1\rangle\rangle_S = -i\widehat{H}_{\mathrm{eff},S}(t)\hat{\rho}_{\phi,S}^{+}(t) |1\rangle\rangle_S. \tag{3.39}$$

The effective Hamiltonian is given by

$$\widehat{H}_{\mathrm{eff},S}(t) = [\hat{H}_{0,S}(t) + \hat{H}_{\mathrm{int},S}(t)] \otimes \mathbb{1} - \mathbb{1} \otimes [\hat{H}_{0,S}(t) + \hat{H}_{\mathrm{int},S}(t)] + \widehat{H}_{\mathrm{IF},S}(t), \tag{3.40}$$

where $\widehat{H}_{\mathrm{IF},S}(t)$ is non-unitary, in contrast to $\hat{H}_{0,S}(t)$ and $\hat{H}_{\mathrm{int},S}(t)$. Since the general relation $H(t) = -\frac{\partial}{\partial t}S(t)$ holds true, one can find correlations between the effective action in Eq. (3.22), which represents the open system's evolution in ρ_ϕ, and the Hamiltonian of

[1] After multiplying Eq. (3.1) from the right-hand side with $\otimes\mathbb{1} |1\rangle\rangle_S$ one can easily see that the relation $[\hat{H}_S(t), \hat{\rho}_S(t)] \otimes \mathbb{1} |1\rangle\rangle_S = -i\widehat{H}_S(t)\hat{\rho}_S^{+} |1\rangle\rangle_S$ has to be shown. Using the expansion of $\widehat{H}_S(t)$, the first term of the commutator on the left-hand side and the first term of $\widehat{H}_S(t)$ on the right-hand side cancel each other, leaving $\hat{\rho}_S(t)\hat{H}_S(t) \otimes \mathbb{1} |1\rangle\rangle_S = \hat{\rho}_S(t) \otimes \hat{H}_S(t) |1\rangle\rangle_S$ to be proven. This relation will be shown for single-particle states only, for simplicity. In this case, $|1\rangle\rangle_S = \int d\Pi_{\mathbf{p}} |\mathbf{p}\rangle \otimes |\mathbf{p}\rangle$ and $\hat{\rho}_S(t) = \int d\Pi_{\mathbf{k}} d\Pi_{\mathbf{k}'} \rho_{1,1}(\mathbf{k}, \mathbf{k}'; t) |\mathbf{k}\rangle \langle\mathbf{k}'|$. Therefore, the left-hand side is

$$\begin{aligned}\hat{\rho}_S(t)\hat{H}_S(t) \otimes \mathbb{1} |1\rangle\rangle_S &= \int d\Pi_{\mathbf{k}} d\Pi_{\mathbf{k}'} d\Pi_{\mathbf{p}} \rho_{1,1}(\mathbf{k}, \mathbf{k}'; t) |\mathbf{k}\rangle \langle\mathbf{k}'| \hat{H}_S(t) |\mathbf{p}\rangle \otimes |\mathbf{p}\rangle \\ &= \int d\Pi_{\mathbf{k}} d\Pi'_{\mathbf{k}} h_{\mathbf{k}'} \rho_{1,1}(\mathbf{k}, \mathbf{k}'; t) |\mathbf{k}\rangle \otimes |\mathbf{k}'\rangle \,,\end{aligned}$$

where $h_{\mathbf{k}'}$ is the eigenvalue of $\hat{H}_S(t)$ for momentum $\mathbf{k}'$ in momentum space. Meanwhile the right-hand side is

$$\begin{aligned}\hat{\rho}_S(t) \otimes \hat{H}_S(t) |1\rangle\rangle_S &= \int d\Pi_{\mathbf{k}} d\Pi_{\mathbf{k}'} d\Pi_{\mathbf{p}} \rho_{1,1}(\mathbf{k}, \mathbf{k}'; t) |\mathbf{k}\rangle \langle\mathbf{k}'|\mathbf{p}\rangle \otimes \hat{H}_S(t) |\mathbf{p}\rangle \\ &= \int d\Pi_{\mathbf{k}} d\Pi'_{\mathbf{k}} h_{\mathbf{k}'} \rho_{1,1}(\mathbf{k}, \mathbf{k}'; t) |\mathbf{k}\rangle \otimes |\mathbf{k}'\rangle \,,\end{aligned}$$

identically to the left-hand side.

Die approbierte gedruckte Originalversion dieser Diplomarbeit ist an der TU Wien Bibliothek verfügbar
The approved original version of this thesis is available in print at TU Wien Bibliothek.
TU Bibliothek Your knowledge hub WIEN

the ϕ-field in the interaction picture $\widehat{H}_{\mathrm{IF},I}(t)$. More precisely, $\hat{H}_{0,S}(t) + \hat{H}_{\mathrm{int},S}(t)$ correlate to $S_\phi(t) + S_{\phi,\mathrm{int}}(t)$ and $\widehat{H}_{\mathrm{IF},S}(t)$ to the influence action in Eq. (3.23), which will be of more importance later on when the path integral expression for the reduced density matrix elements is determined. Furthermore, it should be noted that the free Hamiltonian is picture-independent and the subscript can, thus, be dropped, $\hat{H}_{0,S} = \hat{H}_{0,I} = \hat{H}_0$.

Going forward, the interaction picture will be more useful than the Schrödinger picture, so that Eq. (3.39) will now be transformed. To do so, a unitary evolution operator

$$\widehat{U} \coloneqq e^{-i\hat{H}_0 t} \otimes e^{i\hat{H}_0 t} \tag{3.41}$$

is defined to transform operators on the doubled Hilbert space of TFD via[2]

$$\mathcal{O}_S \coloneqq \widehat{U}\mathcal{O}_I(t)\widehat{U}^\dagger. \tag{3.42}$$

The state corresponding to the unit operator $|1\rangle\rangle$ introduced in Eq. (3.35) transforms like a base vector

$$\widehat{U}^\dagger |1\rangle\rangle_S = |1(t)\rangle\rangle_I. \tag{3.43}$$

Similarly to the free Hamiltonian, it is picture-independent since the evolution operators $\widehat{U}$ and $\widehat{U}^\dagger$ act like unit operators on $|1\rangle\rangle_S$[3], which also implies time-independence. Therefore, the subscripts can, again, be dropped $|1\rangle\rangle_S = |1(t)\rangle\rangle_I = |1\rangle\rangle$.

With this at hand, Eq. (3.39) becomes

$$\frac{\partial}{\partial t}\left(\widehat{U}\hat{\rho}^+_{\phi,I}(t)\widehat{U}^\dagger\right)|1\rangle\rangle = -i\widehat{U}\widehat{H}_{\mathrm{eff},I}(t)\hat{\rho}^+_{\phi,I}(t)\,|1\rangle\rangle \tag{3.44}$$

in the interaction picture. Calculating the partial derivative gives

$$\frac{\partial}{\partial t}\left(\widehat{U}\hat{\rho}^+_{\phi,I}(t)\widehat{U}^\dagger\right)|1\rangle\rangle = \widehat{U}\left[-i\widehat{H}_0\hat{\rho}^+_{\phi,I}(t) + \partial_t\hat{\rho}^+_{\phi,I}(t) + i\hat{\rho}^+_{\phi,I}(t)\widehat{H}_0\right]|1\rangle\rangle\,, \tag{3.45}$$

where $\partial_t\widehat{U} = -i\widehat{H}_0\widehat{U}$, $\partial_t\widehat{U}^\dagger = i\widehat{H}_0\widehat{U}^\dagger$, Eq. (3.43) and $\widehat{H}_0 = \hat{H}_0 \otimes \mathbb{1} - \mathbb{1} \otimes \hat{H}_0$ was used.

[2] It should be remembered that operators acting on a general single Hilbert space transform like $\hat{\mathcal{O}}_S = e^{-i\hat{H}_0 t}\hat{\mathcal{O}}_I(t)e^{i\hat{H}_0 t}$

[3]
$$\begin{aligned}\widehat{U}^\dagger|1\rangle\rangle_S &= |0\rangle\otimes|0\rangle + \int d\Pi_{\mathbf{k}} e^{iE_{\mathbf{k}}t}|\mathbf{k}\rangle\otimes e^{-iE_{\mathbf{k}}t}|\mathbf{k}\rangle \\ &\quad + \frac{1}{2!}\int d\Pi_{\mathbf{k}} d\Pi_{\mathbf{k}'} e^{i(E_{\mathbf{k}}+E_{\mathbf{k}'})t}|\mathbf{k},\mathbf{k}'\rangle\otimes e^{-i(E_{\mathbf{k}}+E_{\mathbf{k}'})t}|\mathbf{k},\mathbf{k}'\rangle + \dots \\ &= |1\rangle\rangle_S\end{aligned}$$

Die approbierte gedruckte Originalversion dieser Diplomarbeit ist an der TU Wien Bibliothek verfügbar
The approved original version of this thesis is available in print at TU Wien Bibliothek.
TU Bibliothek Your knowledge hub WIEN

Next, $\widehat{H}_0 |1\rangle\rangle = 0$ is applied[4], so that Eq. (3.44) becomes

$$\left[-i\widehat{H}_0\hat{\rho}^+_{\phi,I}(t) + \partial_t\hat{\rho}^+_{\phi,I}(t)\right] |1\rangle\rangle = -i\widehat{H}_{\text{eff},I}(t)\hat{\rho}^+_{\phi,I}(t) |1\rangle\rangle \,. \tag{3.46}$$

Using $\widehat{H}_{\text{eff},I}(t) = \widehat{H}_0 + \widehat{H}_{\text{int},I}(t) + \widehat{H}_{\text{IF},I}(t)$ with $\widehat{H}_{\text{int},I}(t) = \hat{H}_{\text{int},I}(t) \otimes \mathbb{1} - \mathbb{1} \otimes \hat{H}_{\text{int},I}(t)$ finally leads to

$$\partial_t\hat{\rho}^+_{\phi,I}(t) |1\rangle\rangle = -i \left[\widehat{H}_{\text{int},I}(t) + \widehat{H}_{\text{IF},I}(t)\right] \hat{\rho}^+_{\phi,I}(t) |1\rangle\rangle \,, \tag{3.47}$$

which can be solved by

$$\hat{\rho}^+_{\phi,I}(t) |1\rangle\rangle = \mathrm{T} e^{-i\int_0^t \left[\widehat{H}_{\text{int},I}(\tau) + \widehat{H}_{\text{IF},I}(\tau)\right] d\tau} \hat{\rho}^+_{\phi,I}(0) |1\rangle\rangle \,. \tag{3.48}$$

3.4. Reduced density matrix elements

Using what was presented in Sections 3.1, 3.2 and 3.3, the formula for directly determining the reduced density matrix element of a single-particle state in momentum basis can be derived now. This restriction to a single-particle subspace is justified since the production of atom-anti-atom pairs is probably highly suppressed due to the complex structure of atoms and their large masses. Since only the interaction picture will be used from now on and only the reduced density matrix of the open system will be considered, both subscripts, I and ϕ, will be dropped for easier readability.

The reduced density matrix element of a single particle is given by

$$\rho_{1,1}(\mathbf{p}, \mathbf{p}'; t) = \langle \mathbf{p}; t| \, \hat{\rho}(t) \, |\mathbf{p}'; t\rangle \,. \tag{3.49}$$

This matrix element is picture-independent since all basis states and operators are independently evaluated from each other at the same time t [71, 74]. Additionally, in TFD it can be represented as

$$\mathrm{Tr} \, |\mathbf{p}'; t\rangle \langle \mathbf{p}; t| \, \hat{\rho}(t) = \langle\langle 1| \, (|\mathbf{p}'; t\rangle \langle \mathbf{p}; t| \otimes \mathbb{1}) \hat{\rho}^+(t) \, |1\rangle\rangle. \tag{3.50}$$

Inserting Eq. (3.48) leads to

$$\rho_{1,1}(\mathbf{p}, \mathbf{p}'; t) = \langle\langle 1| \, (|\mathbf{p}'; t\rangle \langle \mathbf{p}; t| \otimes \mathbb{1}) \mathrm{T} e^{-i\int_0^t \left[\widehat{H}_{\text{int}}(\tau) + \widehat{H}_{\text{IF}}(\tau)\right] d\tau} \hat{\rho}^+(0) \, |1\rangle\rangle. \tag{3.51}$$

The fact that only a single-particle state is considered, $|1\rangle\rangle = \int d\Pi_{\mathbf{k}} \, |\mathbf{k}\rangle \otimes |\mathbf{k}\rangle$, can be used to write $\langle\langle 1| \, (|\mathbf{p}'; t\rangle \langle \mathbf{p}; t| \otimes \mathbb{1}) = \langle\langle \mathbf{p}_+, \mathbf{p}'_-; t|$. Furthermore, it is assumed that at $t = 0$ the exact number of particles and their correlations are known and a single-particle state

[4] $$\widehat{H}_0 |1\rangle\rangle = (\hat{H}_0 \otimes \mathbb{1} - \mathbb{1} \otimes \hat{H}_0) \sum_n |n\rangle \otimes |n\rangle = \sum_n (E_n |n\rangle \otimes |n\rangle - |n\rangle \otimes E_n |n\rangle) = 0$$

Die approbierte gedruckte Originalversion dieser Diplomarbeit ist an der TU Wien Bibliothek verfügbar
The approved original version of this thesis is available in print at TU Wien Bibliothek.

at the initial time is chosen. Thus, only $\rho_{1,1}(0) \neq 0$ whereas $\rho_{i,j} = 0$ for all $i \neq 1$ and $j \neq 1$. With this assumption, the density operator from Eq. (3.51) can be expanded using Eq. (3.5), so that

$$\begin{aligned}\hat{\rho}^{+}(0)\,|1\rangle\rangle &= \left(\int d\Pi_{\mathbf{k}} d\Pi_{\mathbf{k}'} \rho_{1,1}(\mathbf{k},\mathbf{k}';0)\,|\mathbf{k}\rangle\,\langle\mathbf{k}'|\otimes\mathbb{1}\right)|1\rangle\rangle \\ &= \int d\Pi_{\mathbf{k}} d\Pi_{\mathbf{k}'} \rho_{1,1}(\mathbf{k},\mathbf{k}';0)\,\left|\mathbf{k}_{+},\mathbf{k}'_{-}\right\rangle\rangle.\end{aligned} \tag{3.52}$$

So, Eq. (3.51) can be written as

$$\rho_{1,1}(\mathbf{p},\mathbf{p}';t) = \langle\langle \mathbf{p}_{+},\mathbf{p}'_{-};t|\,\mathrm{T}e^{-i\int_0^t\left[\widehat{H}_{\mathrm{int}}(\tau)+\widehat{H}_{\mathrm{IF}}(\tau)\right]d\tau}\int d\Pi_{\mathbf{k}} d\Pi_{\mathbf{k}'}\rho_{1,1}(\mathbf{k},\mathbf{k}';0)\,\left|\mathbf{k}_{+},\mathbf{k}'_{-}\right\rangle\rangle, \tag{3.53}$$

which by using the creation and annihilation operators from Eqs. (3.30)-(3.33) turns into

$$\begin{aligned}\rho_{1,1}(\mathbf{p},\mathbf{p}';t) = &\int d\Pi_{\mathbf{k}} d\Pi_{\mathbf{k}'}\rho_{1,1}(\mathbf{k},\mathbf{k}';0) \\ &\times\langle\langle 0|\,\mathrm{T}\hat{a}^{+}_{\mathbf{p}}(t)\hat{a}^{-}_{\mathbf{p}'}(t)e^{-i\int_0^t\left[\widehat{H}_{\mathrm{int}}(\tau)+\widehat{H}_{\mathrm{IF}}(\tau)\right]d\tau}\hat{a}^{+\dagger}_{\mathbf{k}}(0)\hat{a}^{-\dagger}_{\mathbf{k}'}(0)\,|0\rangle\rangle\,.\end{aligned} \tag{3.54}$$

Moreover, the creation and annihilation operators can be written in terms of field operators:

$$\begin{aligned}\hat{a}^{+}_{\mathbf{p}}(t) &= i\int_{\mathbf{x}} e^{-i\mathbf{p}\cdot\mathbf{x}}\partial_{t,E^{\phi}_{\mathbf{p}}}\hat{\phi}^{+}(t,\mathbf{x}), \qquad \hat{a}^{+\dagger}_{\mathbf{p}}(t) = -i\int_{\mathbf{x}} e^{i\mathbf{p}\cdot\mathbf{x}}\partial^{*}_{t,E^{\phi}_{\mathbf{p}}}\hat{\phi}^{+}(t,\mathbf{x}), \\ \hat{a}^{-}_{\mathbf{p}}(t) &= -i\int_{\mathbf{x}} e^{i\mathbf{p}\cdot\mathbf{x}}\partial^{*}_{t,E^{\phi}_{\mathbf{p}}}\hat{\phi}^{-}(t,\mathbf{x}), \qquad \hat{a}^{-\dagger}_{\mathbf{p}}(t) = i\int_{\mathbf{x}} e^{-i\mathbf{p}\cdot\mathbf{x}}\partial_{t,E^{\phi}_{\mathbf{p}}}\hat{\phi}^{-}(t,\mathbf{x})\end{aligned} \tag{3.55}$$

with $\int_{\mathbf{x}} \coloneqq \int d^3x$ and $\partial_{t,E^{\phi}_{\mathbf{p}}} \coloneqq \vec{\partial}_t - iE^{\phi}_{\mathbf{p}}$, where $E^{\phi}_{\mathbf{p}} = \sqrt{\mathbf{p}^2+M^2}$ for the scalar field ϕ. Inserting (3.55) yields

$$\begin{aligned}\rho_{1,1}(\mathbf{p},\mathbf{p}';t) = &\lim_{\substack{x^{0(\prime)}\to t^{+}\\ y^{0(\prime)}\to 0^{-}}}\int d\Pi_{\mathbf{k}} d\Pi_{\mathbf{k}'}\rho_{1,1}(\mathbf{k},\mathbf{k}';0) \\ &\times\int_{\mathbf{x}\mathbf{x}'\mathbf{y}\mathbf{y}'} e^{-i(\mathbf{p}\cdot\mathbf{x}-\mathbf{p}'\cdot\mathbf{x}')+i(\mathbf{k}\cdot\mathbf{y}-\mathbf{k}'\cdot\mathbf{y}')}\partial_{x^0,E^{\phi}_{\mathbf{p}}}\partial^{*}_{x^{0\prime},E^{\phi}_{\mathbf{p}'}}\partial^{*}_{y^0,E^{\phi}_{\mathbf{k}}}\partial_{y^{0\prime},E^{\phi}_{\mathbf{k}'}} \\ &\times\langle\langle 0|\,\mathrm{T}\left[\hat{\phi}^{+}_{x}\hat{\phi}^{-}_{x'}e^{-i\int_0^t\left[\widehat{H}_{\mathrm{int}}(\tau)+\widehat{H}_{\mathrm{IF}}(\tau)\right]d\tau}\hat{\phi}^{+}_{y}\hat{\phi}^{-}_{y'}\right]|0\rangle\rangle,\end{aligned} \tag{3.56}$$

where limits were introduced to ensure the right time ordering. x^0 and $x^{0\prime}$ approach t from above while y^0 and $y^{0\prime}$ approach 0 from below. Furthermore, the notation $\phi_x \coloneqq \phi(x)$ was introduced.

Die approbierte gedruckte Originalversion dieser Diplomarbeit ist an der TU Wien Bibliothek verfügbar
The approved original version of this thesis is available in print at TU Wien Bibliothek.
TU Bibliothek Your knowledge hub WIEN

Writing this expression in the path integral formalism, leads to

$$\begin{aligned}\rho_{1,1}(\mathbf{p},\mathbf{p}';t) = &\lim_{\substack{x^{0(\prime)}\to t^+\\ y^{0(\prime)}\to 0^-}} \int d\Pi_{\mathbf{k}} d\Pi_{\mathbf{k}'} \rho_{1,1}(\mathbf{k},\mathbf{k}';0) \\ &\times \int_{\mathbf{x}\mathbf{x}'\mathbf{y}\mathbf{y}'} e^{-i(\mathbf{p}\cdot\mathbf{x}-\mathbf{p}'\cdot\mathbf{x}')+i(\mathbf{k}\cdot\mathbf{y}-\mathbf{k}'\cdot\mathbf{y}')} \partial_{x^0,E^\phi_{\mathbf{p}}} \partial^*_{x^{0\prime},E^\phi_{\mathbf{p}'}} \partial^*_{y^0,E^\phi_{\mathbf{k}}} \partial_{y^{0\prime},E^\phi_{\mathbf{k}'}} \\ &\times \int \mathcal{D}\phi^{\pm} e^{i\widehat{S}_\phi[\phi]} \phi^+_x \phi^-_{x'} e^{i\int_0^t \frac{d}{d\tau}\left[\widehat{S}_{\phi,\mathrm{int}}[\phi;\tau]+\widehat{S}_{\mathrm{IF}}[\phi;\tau]\right]d\tau} \phi^+_y \phi^-_{y'},\end{aligned} \tag{3.57}$$

where $\widehat{H}_{\mathrm{int}}(\tau)+\widehat{H}_{\mathrm{IF}}(\tau) = -\frac{d}{d\tau}\left[\widehat{S}_{\phi,\mathrm{int}}(\tau)+\widehat{S}_{\mathrm{IF}}(\tau)\right]$ was used[5]. Next, the integral in the exponent has to be evaluated. Using that for $t=0$: $\widehat{S}_{\phi,\mathrm{int}}[\phi;0] = \widehat{S}_{\mathrm{IF}}[\phi;0] = 0$, this becomes $\int_0^t \frac{d}{d\tau}\left[\widehat{S}_{\phi,\mathrm{int}}[\phi;\tau]+\widehat{S}_{\mathrm{IF}}[\phi;\tau]\right]d\tau = \widehat{S}_{\phi,\mathrm{int}}[\phi;t]+\widehat{S}_{\mathrm{IF}}[\phi;t]$. Finally, inserting the definition of the Feynman-Vernon influence functional (3.23), gives the formula for calculating the reduced density matrix element of a single-particle state in momentum basis which was sought after:

$$\begin{aligned}\rho_{1,1}(\mathbf{p},\mathbf{p}';t) = &\lim_{\substack{x^{0(\prime)}\to t^+\\ y^{0(\prime)}\to 0^-}} \int d\Pi_{\mathbf{k}} d\Pi_{\mathbf{k}'} \rho_{1,1}(\mathbf{k},\mathbf{k}';0) \\ &\times \int_{\mathbf{x}\mathbf{x}'\mathbf{y}\mathbf{y}'} e^{-i(\mathbf{p}\cdot\mathbf{x}-\mathbf{p}'\cdot\mathbf{x}')+i(\mathbf{k}\cdot\mathbf{y}-\mathbf{k}'\cdot\mathbf{y}')} \partial_{x^0,E^\phi_{\mathbf{p}}} \partial^*_{x^{0\prime},E^\phi_{\mathbf{p}'}} \partial^*_{y^0,E^\phi_{\mathbf{k}}} \partial_{y^{0\prime},E^\phi_{\mathbf{k}'}} \\ &\times \int \mathcal{D}\phi^{\pm} e^{i\widehat{S}_\phi[\phi]} \phi^+_x \phi^-_{x'} e^{i\widehat{S}_{\phi,\mathrm{int}}[\phi;t]} \widehat{\mathcal{F}}[\phi;t] \phi^+_y \phi^-_{y'}.\end{aligned} \tag{3.58}$$

Going forward, this equation will be used to calculate the influence of a dilaton environment on the open system ϕ in the subsequent sections.

In [26] and [27] the authors also extrapolated this formula for the universal case of determining a general density matrix element $\rho_{g,h}(\mathbf{k}^{(1)},\ldots,\mathbf{k}^{(g)},\mathbf{l}^{(1)},\ldots,\mathbf{l}^{(h)};t)$ with the initial non-vanishing density matrix elements being chosen arbitrarily. However, since this thesis only focuses on the single-particle case, this more general equation will not be elaborated on further here.

[5] This relation can be easily seen when using that $\widehat{H}_{\mathrm{eff}}(t) = \widehat{H}_0 + \widehat{H}_{\mathrm{int}}(t) + \widehat{H}_{\mathrm{IF}}(t)$, the relations between $H(t)$ and $S(t)$ discussed below Eq. (3.40) and Eq. (3.22):

$$\begin{aligned}\widehat{H}_{\mathrm{int}}(\tau)+\widehat{H}_{\mathrm{IF}}(\tau) &= \widehat{H}_{\mathrm{eff}}(\tau) - \widehat{H}_0(\tau) = \frac{\partial}{\partial\tau}\widehat{S}_\phi(\tau) - \frac{\partial}{\partial\tau}\widehat{S}_{\mathrm{eff}}(\tau) \\ &= \frac{\partial}{\partial\tau}\widehat{S}_\phi(\tau) + \sum_{a=\pm} a(\dot{\phi}^a\pi^a_\phi + \dot{\varphi}^a\pi^a_\varphi) - \left[\frac{\partial}{\partial\tau}\widehat{S}_{\mathrm{eff}}(\tau) + \sum_{a=\pm} a(\dot{\phi}^a\pi^a_\phi + \dot{\varphi}^a\pi^a_\varphi)\right] \\ &= \frac{d}{d\tau}\widehat{S}_\phi(\tau) - \frac{d}{d\tau}\widehat{S}_{\mathrm{eff}}(\tau) = -\frac{d}{d\tau}\left[\widehat{S}_{\phi,\mathrm{int}}(\tau)+\widehat{S}_{\mathrm{IF}}(\tau)\right].\end{aligned}$$

Die approbierte gedruckte Originalversion dieser Diplomarbeit ist an der TU Wien Bibliothek verfügbar
The approved original version of this thesis is available in print at TU Wien Bibliothek.
TU Bibliothek Your knowledge hub WIEN

4. Single-particle state in dilaton environment

In order to evaluate Eq. (3.58) for a dilaton environment, contractions of the system field ϕ, leading to propagators denoted by D, have to be calculated. In the case of a single-particle subspace, only contractions between plus- and minus-type operators ($++$ and $--$) are permitted. Mixed contractions, however, ($+-$ or $-+$) are not possible due to the way the vacuum state is defined in TFD:

$$\langle\langle 0|\, \hat{\phi}_x^{+(-)} \hat{\phi}_y^{-(+)}\, |0\rangle\rangle = 0, \tag{4.1}$$

as shown in [23]. The Feynman and Dyson propagators, however, are allowed and read

$$\langle\langle 0|\, \mathrm{T}[\hat{\phi}_x^{+} \hat{\phi}_y^{+}]\, |0\rangle\rangle = D_{xy}^{++} = D_{xy}^{F} = -i \int_k \frac{e^{ik\cdot(x-y)}}{k^2 + M^2 - i\epsilon}, \tag{4.2}$$

$$\langle\langle 0|\, \mathrm{T}[\hat{\phi}_x^{-} \hat{\phi}_y^{-}]\, |0\rangle\rangle = D_{xy}^{--} = D_{xy}^{D} = i \int_k \frac{e^{ik\cdot(x-y)}}{k^2 + M^2 + i\epsilon}. \tag{4.3}$$

Restricting to a single-particle subspace also implies the system field ϕ to remain at zero temperature. Contrary to the ϕ field, when contracting the χ-field in the course of evaluating the Feynman-Vernon influence functional (3.24), all contractions are allowed. Additionally, the environment χ can be taken at finite temperatures, in which case the system ϕ and the environment χ are out of equilibrium. This is so, because the dilaton fluctuations can be assumed to be in thermal exchange with the walls from the vacuum chamber. The Feynman, Dyson, negative and positive frequency Wightman propagators

Die approbierte gedruckte Originalversion dieser Diplomarbeit ist an der TU Wien Bibliothek verfügbar
The approved original version of this thesis is available in print at TU Wien Bibliothek.

for the χ field, denoted by Δ, are therefore [75]

$$\begin{aligned}
\overbracket{\chi_x^+\chi_y^+} &= \langle \mathrm{T}\chi_x\chi_y\rangle = \Delta_{xy}^{++} = \Delta_{xy}^F \\
&= -i\int_k e^{ik\cdot(x-y)}\left[\frac{1}{k^2+m^2-i\epsilon} + 2\pi i f(|k^0|)\delta(k^2+m^2)\right], \qquad (4.4)\\
\overbracket{\chi_x^-\chi_y^-} &= \langle \tilde{\mathrm{T}}\chi_x\chi_y\rangle = \Delta_{xy}^{--} = \Delta_{xy}^D \\
&= i\int_k e^{ik\cdot(x-y)}\left[\frac{1}{k^2+m^2+i\epsilon} - 2\pi i f(|k^0|)\delta(k^2+m^2)\right], \qquad (4.5)\\
\overbracket{\chi_x^+\chi_y^-} &= \langle \chi_y\chi_x\rangle = \Delta_{xy}^{+-} = \Delta_{xy}^< = \int_k e^{ik\cdot(x-y)} 2\pi \mathrm{sgn}(k^0) f(k^0)\delta(k^2+m^2), \qquad (4.6)\\
\overbracket{\chi_x^-\chi_y^+} &= \langle \chi_x\chi_y\rangle = \Delta_{xy}^{-+} = \Delta_{xy}^> = \Delta_{yx}^< = (\Delta^<)_{xy}^*, \qquad (4.7)
\end{aligned}$$

where the thermal contributions are included via the Bose-Einstein distribution function

$$f(k^0) := \frac{1}{e^{\beta k^0}-1} \qquad (4.8)$$

with β being the inverse temperature. The Bose-Einstein distribution also follows the identity

$$f(-k^0) = -[1+f(k^0)], \qquad (4.9)$$

which can easily be shown[1]. Lastly, the signum function in both the negative and positive frequency Wightman propagators is given by $\mathrm{sgn}(k^0) = \Theta(k^0) - \Theta(-k^0)$.

Additional information on the propagators of scalar fields can be found in Appendix A.

Furthermore, for evaluating Eq. (3.58), the Feynman-Vernon influence functional $\widehat{\mathcal{F}}[\phi;t]$ has to be determined. Assuming a weak coupling between the system ϕ and the environment χ, Eq. (3.24) can be expanded up to second order in α_1 and α_2:

$$\begin{aligned}
\widehat{\mathcal{F}}[\phi;t] &= \langle e^{i\widehat{S}_{\mathrm{int}}[\phi,\chi;t]}\rangle_\chi \\
&\approx 1 + i\sum_{a=\pm} a\langle S_{\mathrm{int}}[\phi^a,\chi^a;t]\rangle_\chi - \frac{1}{2}\sum_{a,b=\pm} ab\langle S_{\mathrm{int}}[\phi^a,\chi^a;t]S_{\mathrm{int}}[\phi^b,\chi^b;t]\rangle_\chi + \mathcal{O}(\alpha_{1,2}^3)
\end{aligned} \qquad (4.10)$$

when considering that for the dilaton field $S_{\chi,\mathrm{int}}[\chi;t] = 0$. Inserting Eq. (2.45), using Eqs. (4.4)-(4.7) and the coincidence limit at equal times, Eq. (A.5), as described in Ap-

[1]
$$\begin{aligned}
f(-k^0) &= \frac{1}{e^{-\beta k^0}-1} = \frac{e^{\beta k^0}}{1-e^{\beta k^0}} = \frac{e^{\beta k^0}-1+1}{1-e^{\beta k^0}} = \frac{1-e^{-\beta k^0}}{e^{-\beta k^0}-1} + \frac{1}{1-e^{\beta k^0}} \\
&= -[1+f(k^0)]
\end{aligned}$$

Die approbierte gedruckte Originalversion dieser Diplomarbeit ist an der TU Wien Bibliothek verfügbar
The approved original version of this thesis is available in print at TU Wien Bibliothek.

pendix A, the expectation values are

$$\langle S_{\text{int}}[\phi^a,\chi^a;t]\rangle_\chi = -\frac{\alpha_2}{4}\int_x (\phi_x^a)^2\Delta_{xx}^F, \tag{4.11}$$

$$\begin{aligned}\langle S_{\text{int}}[\phi^a,\chi^a;t]S_{\text{int}}[\phi^b,\chi^b;t]\rangle_\chi = {}& \frac{\alpha_1^2M^2}{4}\int_{xy}(\phi_x^a)^2(\phi_y^b)^2\Delta_{xy}^{ab} \\ &+ \frac{\alpha_2^2}{16}\int_{xy}(\phi_x^a)^2(\phi_y^b)^2\left[\Delta_{xx}^F\Delta_{yy}^F + 2(\Delta_{xy}^{ab})^2\right].\end{aligned} \tag{4.12}$$

For an easier readability the subscript Ω_t (Eq. (2.46)) for the integral was dropped, but time integrations still run over the interval $[0;t]$. Putting this back into the influence functional leads to

$$\begin{aligned}\widehat{\mathcal{F}}[\phi;t] = 1 - i\frac{\alpha_2}{4}\sum_{a=\pm} a\int_x(\phi_x^a)^2\Delta_{xx}^F - \frac{1}{2}\sum_{a,b=\pm}ab\int_{xy}\Bigg[&\frac{\alpha_1^2M^2}{4}(\phi_x^a)^2(\phi_y^b)^2\Delta_{xy}^{ab} \\ &+ \frac{\alpha_2^2}{16}(\phi_x^a)^2(\phi_y^b)^2\left(\Delta_{xx}^F\Delta_{yy}^F + 2(\Delta_{xy}^{ab})^2\right)\Bigg] + \mathcal{O}(\alpha_{1,2}^3).\end{aligned} \tag{4.13}$$

Inserting Eq. (4.13) into the formula for the reduced density matrix element of a single-particle state in momentum basis, Eq. (3.58), gives

$$\begin{aligned}\rho_{1,1}(\mathbf{p},\mathbf{p}';t) = \lim_{\substack{x^{0(\prime)}\to t^+\\ y^{0(\prime)}\to 0^-}}&\int d\Pi_{\mathbf{k}}d\Pi_{\mathbf{k}'}\rho_{1,1}(\mathbf{k},\mathbf{k}';0) \\ &\times\int_{\mathbf{xx}'\mathbf{yy}'} e^{-i(\mathbf{p}\cdot\mathbf{x}-\mathbf{p}'\cdot\mathbf{x}')+i(\mathbf{k}\cdot\mathbf{y}-\mathbf{k}'\cdot\mathbf{y}')}\partial_{x^0,E_{\mathbf{p}}^\phi}\partial^*_{x^{0\prime},E_{\mathbf{p}'}^\phi}\partial^*_{y^0,E_{\mathbf{k}}^\phi}\partial_{y^{0\prime},E_{\mathbf{k}'}^\phi} \\ &\times\int\mathcal{D}\phi^\pm e^{i\widehat{S}_\phi[\phi]}\phi_x^+\phi_{x'}^-\Bigg\{1 - i\frac{\alpha_2}{4}\sum_{a=\pm}a\int_z(\phi_z^a)^2\Delta_{zz}^F \\ &\quad - \frac{1}{2}\sum_{a,b=\pm}ab\int_{zz'}\Bigg[\frac{\alpha_1^2M^2}{4}(\phi_z^a)^2(\phi_{z'}^b)^2\Delta_{zz'}^{ab} \\ &\quad + \frac{\alpha_2^2}{16}(\phi_z^a)^2(\phi_{z'}^b)^2\left(\Delta_{zz}^F\Delta_{z'z'}^F + 2(\Delta_{zz'}^{ab})^2\right)\Bigg]\Bigg\}\phi_y^+\phi_{y'}^-\end{aligned} \tag{4.14}$$

when using that for this system $S_{\phi,\text{int}}[\phi;t] = 0$.

Die approbierte gedruckte Originalversion dieser Diplomarbeit ist an der TU Wien Bibliothek verfügbar
The approved original version of this thesis is available in print at TU Wien Bibliothek.

Next, contracting the system fields according to Eqs. (4.2)-(4.3) leads to

$$
\begin{aligned}
\rho_{1,1}(\mathbf{p},\mathbf{p}';t) = \lim_{\substack{x^{0(\prime)}\to t^+\\ y^{0(\prime)}\to 0^-}} \int d\Pi_{\mathbf{k}} d\Pi_{\mathbf{k}'} \rho_{1,1}(\mathbf{k},\mathbf{k}';0)
&\times \int_{\mathbf{x}\mathbf{x}'\mathbf{y}\mathbf{y}'} e^{-i(\mathbf{p}\cdot\mathbf{x}-\mathbf{p}'\cdot\mathbf{x}')+i(\mathbf{k}\cdot\mathbf{y}-\mathbf{k}'\cdot\mathbf{y}')} \partial_{x^0,E^\phi_{\mathbf{p}}} \partial^*_{x^{0\prime},E^\phi_{\mathbf{p}'}} \partial^*_{y^0,E^\phi_{\mathbf{k}}} \partial_{y^{0\prime},E^\phi_{\mathbf{k}'}} \\
&\times \Bigg\{ D^F_{xy} D^D_{x'y'} - i\frac{\alpha_2}{2} \int_z \left[D^F_{xz} D^F_{zy} D^D_{x'y'} - D^F_{xy} D^D_{x'z} D^D_{zy'} \right] \Delta^F_{zz} \\
&- \frac{\alpha_1^2 M^2}{8} \int_{zz'} \Big[D^D_{x'y'} \Big(8 D^F_{xz} D^F_{zz'} D^F_{z'y} + 2 D^F_{xy} D^F_{zz'} D^F_{zz'} + 4 D^F_{xz} D^F_{zy} D^F_{z'z'} \\
&\qquad + D^F_{xy} D^F_{zz} D^F_{z'z'} \Big) \Delta^F_{zz'} \\
&\quad - \Big(8 D^F_{xz} D^F_{zy} D^D_{x'z'} D^D_{z'y'} + 4 D^F_{xy} D^F_{zz} D^D_{x'z'} D^D_{z'y'} + 4 D^F_{xz} D^F_{zy} D^D_{x'y'} D^D_{z'z'} \\
&\qquad + 2 D^F_{xy} D^F_{zz} D^D_{x'y'} D^D_{z'z'} \Big) \Delta^{+-}_{zz'} \\
&\quad + D^F_{xy} \Big(8 D^D_{x'z} D^D_{zz'} D^D_{z'y'} + 2 D^D_{x'y'} D^D_{zz'} D^D_{zz'} + 4 D^D_{x'z} D^D_{zy'} D^D_{z'z'} \\
&\qquad + D^D_{x'y'} D^D_{zz} D^D_{z'z'} \Big) \Delta^D_{zz'} \Big] \\
&- \frac{\alpha_2^2}{32} \int_{zz'} \Big[D^D_{x'y'} \Big(8 D^F_{xz} D^F_{zz'} D^F_{z'y} + 2 D^F_{xy} D^F_{zz'} D^F_{zz'} + 4 D^F_{xz} D^F_{zy} D^F_{z'z'} \\
&\qquad + D^F_{xy} D^F_{zz} D^F_{z'z'} \Big) \Big(\Delta^F_{zz} \Delta^F_{z'z'} + 2 (\Delta^F_{zz'})^2 \Big) \\
&\quad - \Big(8 D^F_{xz} D^F_{zy} D^D_{x'z'} D^D_{z'y'} + 4 D^F_{xy} D^F_{zz} D^D_{x'z'} D^D_{z'y'} + 4 D^F_{xz} D^F_{zy} D^D_{x'y'} D^D_{z'z'} \\
&\qquad + 2 D^F_{xy} D^F_{zz} D^D_{x'y'} D^D_{z'z'} \Big) \Big(\Delta^F_{zz} \Delta^F_{z'z'} + 2 (\Delta^{+-}_{zz'})^2 \Big) \\
&\quad + D^F_{xy} \Big(8 D^D_{x'z} D^D_{zz'} D^D_{z'y'} + 2 D^D_{x'y'} D^D_{zz'} D^D_{zz'} + 4 D^D_{x'z} D^D_{zy'} D^D_{z'z'} \\
&\qquad + D^D_{x'y'} D^D_{zz} D^D_{z'z'} \Big) \Big(\Delta^F_{zz} \Delta^F_{z'z'} + 2 (\Delta^D_{zz'})^2 \Big) \Big] \Bigg\}.
\end{aligned}
\tag{4.15}
$$

How to evaluate this equation is demonstrated in Appendix B for the example of the first term in the fourth line of Eq. (4.15). After evaluating all terms, one finds for the

Die approbierte gedruckte Originalversion dieser Diplomarbeit ist an der TU Wien Bibliothek verfügbar
The approved original version of this thesis is available in print at TU Wien Bibliothek.

single-particle in a dilaton environment:

$$
\begin{aligned}
\rho_{1;1}(\mathbf{p},\mathbf{p}';t) = \rho_{1;1}(\mathbf{p},\mathbf{p}';0)e^{-i(E^{\phi}_{\mathbf{p}}-E^{\phi}_{\mathbf{p}'})t}\Bigg\{1-(2\pi)^3\delta^{(3)}(\mathbf{0})\Bigg[\frac{\alpha_2^2}{8}\int_{\mathbf{q}}\frac{\sin^2(E^{\phi}_{\mathbf{q}}t)}{4(E^{\phi}_{\mathbf{q}})^4}\Delta^F_{zz}\Delta^F_{z'z'} \\
+\frac{\alpha_1^2M^2}{2}\int_{\mathbf{kq}}\frac{1}{2E^{\phi}_{\mathbf{k}}E^{\phi}_{\mathbf{q}}E^{\chi}_{\mathbf{q-k}}}\left(\frac{\sin^2\left(\frac{(E^{\phi}_{\mathbf{k}}+E^{\phi}_{\mathbf{q}}+E^{\chi}_{\mathbf{q-k}})t}{2}\right)}{(E^{\phi}_{\mathbf{k}}+E^{\phi}_{\mathbf{q}}+E^{\chi}_{\mathbf{q-k}})^2}+\sum_{s=\pm}\frac{\sin^2\left(\frac{(E^{\phi}_{\mathbf{k}}+E^{\phi}_{\mathbf{q}}+sE^{\chi}_{\mathbf{q-k}})t}{2}\right)}{(E^{\phi}_{\mathbf{k}}+E^{\phi}_{\mathbf{q}}+sE^{\chi}_{\mathbf{q-k}})^2}f(E^{\chi}_{\mathbf{q-k}})\right) \\
+\frac{\alpha_2^2}{4}\int_{\mathbf{kql}}\frac{1}{2E^{\phi}_{\mathbf{k}}E^{\phi}_{\mathbf{k+q+l}}E^{\chi}_{\mathbf{q}}E^{\chi}_{\mathbf{l}}}\Bigg(\sum_{r,s=\pm}\frac{\sin^2\left(\frac{(E^{\phi}_{\mathbf{k}}+E^{\phi}_{\mathbf{k+q+l}}+sE^{\chi}_{\mathbf{q}}+rE^{\chi}_{\mathbf{l}})t}{2}\right)}{2(E^{\phi}_{\mathbf{k}}+E^{\phi}_{\mathbf{k+q+l}}+sE^{\chi}_{\mathbf{q}}+rE^{\chi}_{\mathbf{l}})^2}f(E^{\chi}_{\mathbf{q}})f(E^{\chi}_{\mathbf{l}}) \\
+\frac{\sin^2\left(\frac{(E^{\phi}_{\mathbf{k}}+E^{\phi}_{\mathbf{k+q+l}}+E^{\chi}_{\mathbf{q}}+E^{\chi}_{\mathbf{l}})t}{2}\right)}{2(E^{\phi}_{\mathbf{k}}+E^{\phi}_{\mathbf{k+q+l}}+E^{\chi}_{\mathbf{q}}+E^{\chi}_{\mathbf{l}})^2}+\sum_{s=\pm}\frac{\sin^2\left(\frac{(E^{\phi}_{\mathbf{k}}+E^{\phi}_{\mathbf{k+q+l}}+E^{\chi}_{\mathbf{q}}+sE^{\chi}_{\mathbf{l}})t}{2}\right)}{(E^{\phi}_{\mathbf{k}}+E^{\phi}_{\mathbf{k+q+l}}+E^{\chi}_{\mathbf{q}}+sE^{\chi}_{\mathbf{l}})^2}f(E^{\chi}_{\mathbf{l}})\Bigg)\Bigg] \\
-\frac{i\alpha_2}{4}\left(\frac{1}{E^{\phi}_{\mathbf{p}}}-\frac{1}{E^{\phi}_{\mathbf{p}'}}\right)t\Delta^F_{zz}-\frac{\alpha_2^2}{16}\Bigg[\frac{1}{2}\left(\frac{1}{(E^{\phi}_{\mathbf{p}})^2}-\frac{2}{E^{\phi}_{\mathbf{p}}E^{\phi}_{\mathbf{p}'}}+\frac{1}{(E^{\phi}_{\mathbf{p}'})^2}\right)t^2 \\
+\left(\left(\frac{-i}{2(E^{\phi}_{\mathbf{p}})^3}t+\frac{1-e^{-2iE^{\phi}_{\mathbf{p}}t}}{4(E^{\phi}_{\mathbf{p}})^4}\right)+(\mathbf{p}\longleftrightarrow\mathbf{p}')^*\right)\Bigg]\Delta^F_{zz}\Delta^F_{z'z'} \\
+i\alpha_1^2M^2\int_{\mathbf{q}}\Bigg[\frac{1}{8E^{\phi}_{\mathbf{p}}E^{\phi}_{\mathbf{q}}E^{\chi}_{\mathbf{p-q}}}\Bigg(\sum_{s=\pm}\frac{\frac{i}{sE^{\phi}_{\mathbf{p}}+E^{\phi}_{\mathbf{q}}+E^{\chi}_{\mathbf{p-q}}}\left(1-e^{-i(sE^{\phi}_{\mathbf{p}}+E^{\phi}_{\mathbf{q}}+E^{\chi}_{\mathbf{p-q}})t}\right)+t}{sE^{\phi}_{\mathbf{p}}+E^{\phi}_{\mathbf{q}}+E^{\chi}_{\mathbf{p-q}}} \qquad (4.16)\\
+\sum_{r,s=\pm}\frac{\frac{i}{rE^{\phi}_{\mathbf{p}}+E^{\phi}_{\mathbf{q}}+sE^{\chi}_{\mathbf{p-q}}}\left(1-e^{-i(rE^{\phi}_{\mathbf{p}}+E^{\phi}_{\mathbf{q}}+sE^{\chi}_{\mathbf{p-q}})t}\right)+t}{rE^{\phi}_{\mathbf{p}}+E^{\phi}_{\mathbf{q}}+sE^{\chi}_{\mathbf{p-q}}}f(E^{\chi}_{\mathbf{p-q}})\Bigg)+(\mathbf{p}\longleftrightarrow\mathbf{p}')^*\Bigg] \\
+i\frac{\alpha_2^2}{2}\int_{\mathbf{kq}}\Bigg[\frac{1}{8E^{\phi}_{\mathbf{p}}E^{\phi}_{\mathbf{p-k-q}}E^{\chi}_{\mathbf{k}}E^{\chi}_{\mathbf{q}}}\Bigg(\sum_{s=\pm}\frac{\frac{i}{sE^{\phi}_{\mathbf{p}}+E^{\phi}_{\mathbf{p-k-q}}+E^{\chi}_{\mathbf{k}}+E^{\chi}_{\mathbf{q}}}\left(1-e^{-i(sE^{\phi}_{\mathbf{p}}+E^{\phi}_{\mathbf{p-k-q}}+E^{\chi}_{\mathbf{k}}+E^{\chi}_{\mathbf{q}})t}\right)+t}{2(sE^{\phi}_{\mathbf{p}}+E^{\phi}_{\mathbf{p-k-q}}+E^{\chi}_{\mathbf{k}}+E^{\chi}_{\mathbf{q}})} \\
+\sum_{r,s,v=\pm}\frac{\frac{i}{rE^{\phi}_{\mathbf{p}}+E^{\phi}_{\mathbf{p-k-q}}+sE^{\chi}_{\mathbf{k}}+vE^{\chi}_{\mathbf{q}}}\left(1-e^{-i(rE^{\phi}_{\mathbf{p}}+E^{\phi}_{\mathbf{p-k-q}}+sE^{\chi}_{\mathbf{k}}+vE^{\chi}_{\mathbf{q}})t}\right)+t}{2(rE^{\phi}_{\mathbf{p}}+E^{\phi}_{\mathbf{p-k-q}}+sE^{\chi}_{\mathbf{k}}+vE^{\chi}_{\mathbf{q}})}f(E^{\chi}_{\mathbf{k}})f(E^{\chi}_{\mathbf{q}}) \\
+\sum_{r,s=\pm}\frac{\frac{i}{rE^{\phi}_{\mathbf{p}}+E^{\phi}_{\mathbf{p-k-q}}+E^{\chi}_{\mathbf{k}}+sE^{\chi}_{\mathbf{q}}}\left(1-e^{-i(rE^{\phi}_{\mathbf{p}}+E^{\phi}_{\mathbf{p-k-q}}+E^{\chi}_{\mathbf{k}}+sE^{\chi}_{\mathbf{q}})t}\right)+t}{rE^{\phi}_{\mathbf{p}}+E^{\phi}_{\mathbf{p-k-q}}+E^{\chi}_{\mathbf{k}}+sE^{\chi}_{\mathbf{q}}}f(E^{\chi}_{\mathbf{q}})\Bigg)-(\mathbf{p}\longleftrightarrow\mathbf{p}')^*\Bigg] \\
-i\frac{\alpha_1^2M^2}{2}\frac{1}{2m^3}\left(\frac{1}{E^{\phi}_{\mathbf{p}}}-\frac{1}{E^{\phi}_{\mathbf{p}'}}\right)\left[\sin(mt)-mt\right]D^F_{zz} \\
-i\frac{\alpha_2^2}{4}\int_{\mathbf{q}}\frac{1}{8(E^{\chi}_{\mathbf{q}})^4}\left(\frac{1}{E^{\phi}_{\mathbf{p}}}-\frac{1}{E^{\phi}_{\mathbf{p}'}}\right)\left[\left(\frac{1}{2}\sin\left(2E^{\chi}_{\mathbf{q}}t\right)-E^{\chi}_{\mathbf{q}}t\right)\left(1+2f(E^{\chi}_{\mathbf{q}})\right)\right]D^F_{zz}\Bigg\} \\
+\alpha_1^2M^2\int_{\mathbf{q}}\rho_{1;1}(\mathbf{p}-\mathbf{q},\mathbf{p}'-\mathbf{q};0)e^{-i(E^{\phi}_{\mathbf{p}}-E^{\phi}_{\mathbf{p}'})t}\sum_{s=\pm}\left(e^{i(E^{\phi}_{\mathbf{p}}-E^{\phi}_{\mathbf{p-q}}-sE^{\chi}_{\mathbf{q}})t}-1\right) \\
\times\left(e^{-i(E^{\phi}_{\mathbf{p}'}-E^{\phi}_{\mathbf{p}'-\mathbf{q}}-sE^{\chi}_{\mathbf{q}})t}-1\right)\frac{sf(sE^{\chi}_{\mathbf{q}})}{8E^{\phi}_{\mathbf{p-q}}E^{\phi}_{\mathbf{p}'-\mathbf{q}}E^{\chi}_{\mathbf{q}}(E^{\phi}_{\mathbf{p}}-E^{\phi}_{\mathbf{p-q}}-sE^{\chi}_{\mathbf{q}})(E^{\phi}_{\mathbf{p}'}-E^{\phi}_{\mathbf{p}'-\mathbf{q}}-sE^{\chi}_{\mathbf{q}})}
\end{aligned}
$$

Die approbierte gedruckte Originalversion dieser Diplomarbeit ist an der TU Wien Bibliothek verfügbar
The approved original version of this thesis is available in print at TU Wien Bibliothek.

$$+\frac{\alpha_2^2}{2}\int_{\mathbf{kq}}\rho_{1;1}(\mathbf{p}-\mathbf{k}-\mathbf{q},\mathbf{p}'-\mathbf{k}-\mathbf{q};0)e^{-i(E^\phi_{\mathbf{p}}-E^\phi_{\mathbf{p}'})t}$$
$$\times\sum_{r,s=\pm}\left(e^{i(E^\phi_{\mathbf{p}}-E^\phi_{\mathbf{p}-\mathbf{k}-\mathbf{q}}-sE^\chi_{\mathbf{k}}-rE^\chi_{\mathbf{q}})t}-1\right)\left(e^{-i(E^\phi_{\mathbf{p}'}-E^\phi_{\mathbf{p}'-\mathbf{k}-\mathbf{q}}-sE^\chi_{\mathbf{k}}-rE^\chi_{\mathbf{q}})t}-1\right)$$
$$\times\frac{rsf(sE^\chi_{\mathbf{k}})f(rE^\chi_{\mathbf{q}})}{16E^\phi_{\mathbf{p}-\mathbf{k}-\mathbf{q}}E^\phi_{\mathbf{p}'-\mathbf{k}-\mathbf{q}}E^\chi_{\mathbf{k}}E^\chi_{\mathbf{q}}(E^\phi_{\mathbf{p}}-E^\phi_{\mathbf{p}-\mathbf{k}-\mathbf{q}}-sE^\chi_{\mathbf{k}}-rE^\chi_{\mathbf{q}})(E^\phi_{\mathbf{p}'}-E^\phi_{\mathbf{p}'-\mathbf{k}-\mathbf{q}}-sE^\chi_{\mathbf{k}}-rE^\chi_{\mathbf{q}})}$$

where the dummy parameters $r, s, v = \pm$ were introduced to simplify the sum over two different energy flows.

One finds this to be the unitary evolution and corrections thereof resulting in decoherence and phase shifts. The diagrammatic representation of these correction term can be found in Figures 4.1 and 4.2, where the former one depicts all diagrams containing χ tadpoles and χ-ϕ bubble diagrams while the latter one shows the ones with ϕ tadpoles. Figures 4.1 (a)-(c) show the disconnected vacuum diagrams corresponding to the additional terms in the first four lines of Eq. (4.16). Lines five and six of Eq. (4.16) can be seen in the χ tadpoles of Figures 4.1 (d)-(h) whereas the first term of the fifth line in Eq. (4.16) describes the diagrams with only one χ tadpole and the other ones those with two χ tadpoles. The χ-ϕ bubble diagrams in Figure 4.1 (i) and (j) are described by the seventh and eighth line of Eq. (4.16), while the bubble diagrams of Figures 4.1 (k) and (l) appear in lines nine to eleven of Eq. (4.16). Lines twelve and thirteen of Eq. (4.16) contain ϕ tadpoles and are represented by Figures 4.2 (d)-(g) with line twelve corresponding to Figures 4.2 (d) and (e) and line thirteen to the other two diagrams. The last five lines of Eq. (4.16) are depicted by the last two diagrams in Figure 4.1, namely (m) and (n).

Eq. (4.15) also contains additional terms with ϕ tadpoles which cancel each other as can easily be seen when considering the coincidence in the equal time limit (see Eq. (A.5)) and the greatest time equation (see Eq. (A.11)). Therefore, they do not show up in Eq. (4.16). The diagrammatic representation of these ϕ tadpole terms can also be seen in Figure 4.2. Again, they include vacuum diagrams (4.2(a)-(c)). Additionally, two diagrams of a mixture of vacuum and tadpole diagrams can be found (4.2(h)-(i)). However, in reality all terms containing a ϕ tadpole are expected to not exist, even the ones in the twelfth and thirteenth line of Eq. (4.16). This is so because realistic atoms are complex and stable and contain many elementary particles. Therefore, our proxy of describing them by a single scalar field is a major simplification and any decay ($\chi \to \phi\phi$) and production processes ($\phi\phi \to \chi$) as well as loops resulting from this simplification are not permitted for real atoms.

Inspecting (4.16) more closely, one can easily see that in the limit $t \to 0$ all terms except the very first one vanish identically, as expected, i.e. $\rho_{1,1}(\mathbf{p},\mathbf{p}';t\to 0) = \rho_{1,1}(\mathbf{p},\mathbf{p}';0)$. Additionally, it is consistent with the property for complex conjugating the density matrix element given in Eq. (3.8): $\rho_{1,1}(\mathbf{p},\mathbf{p}';t) = \rho^*_{1,1}(\mathbf{p}',\mathbf{p};t)$. Furthermore, only looking at the very first term in the first line and the terms in the fifth line (corresponding to Figures

Die approbierte gedruckte Originalversion dieser Diplomarbeit ist an der TU Wien Bibliothek verfügbar
The approved original version of this thesis is available in print at TU Wien Bibliothek.
TU Bibliothek Your knowledge hub WIEN

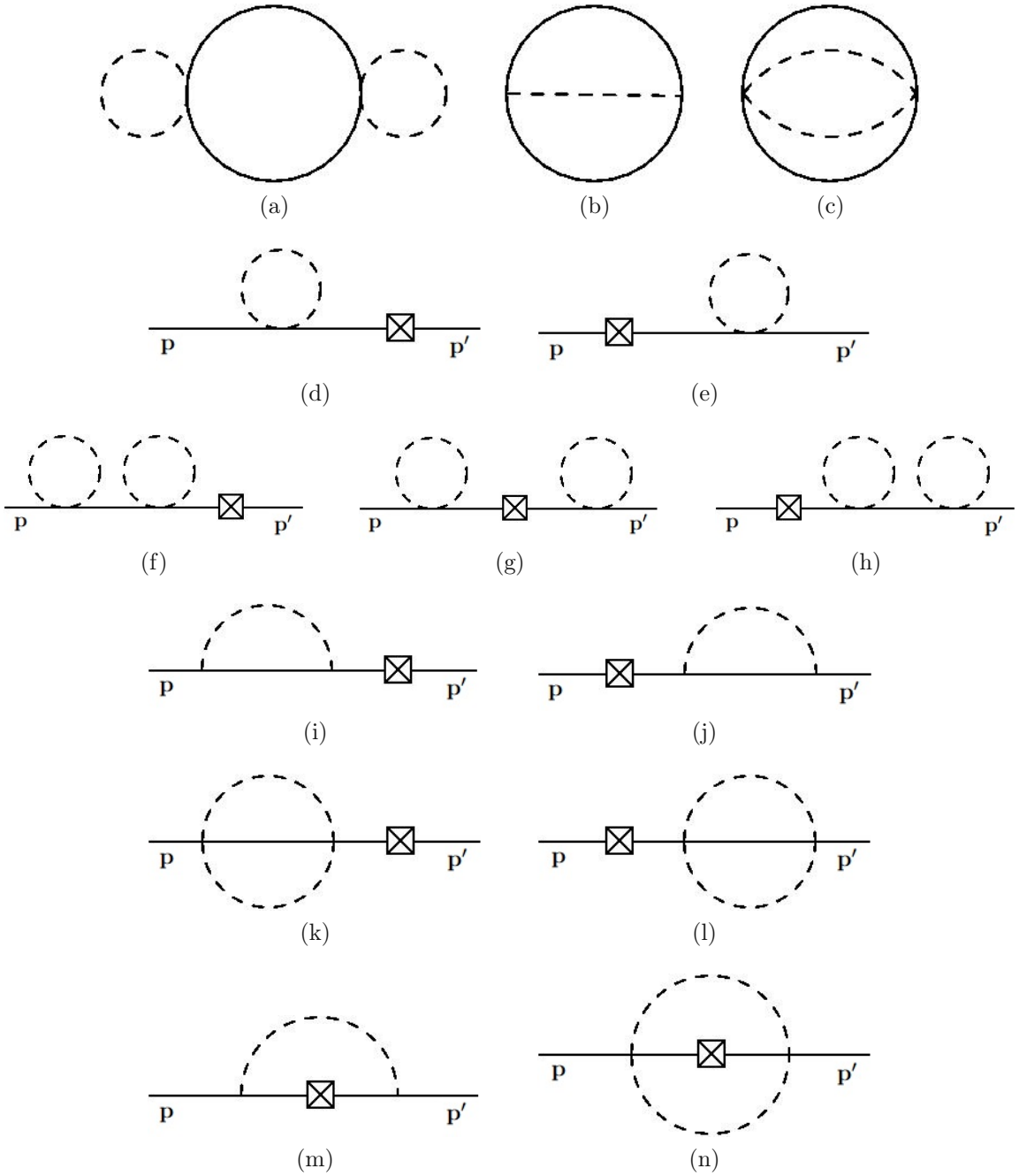

Figure 4.1.: Diagrammatic representation of terms in reduced density matrix (4.16); solid lines represent atoms, dashed lines represent dilatons and crossed boxes represent the reduced density operator.

Die approbierte gedruckte Originalversion dieser Diplomarbeit ist an der TU Wien Bibliothek verfügbar
The approved original version of this thesis is available in print at TU Wien Bibliothek.

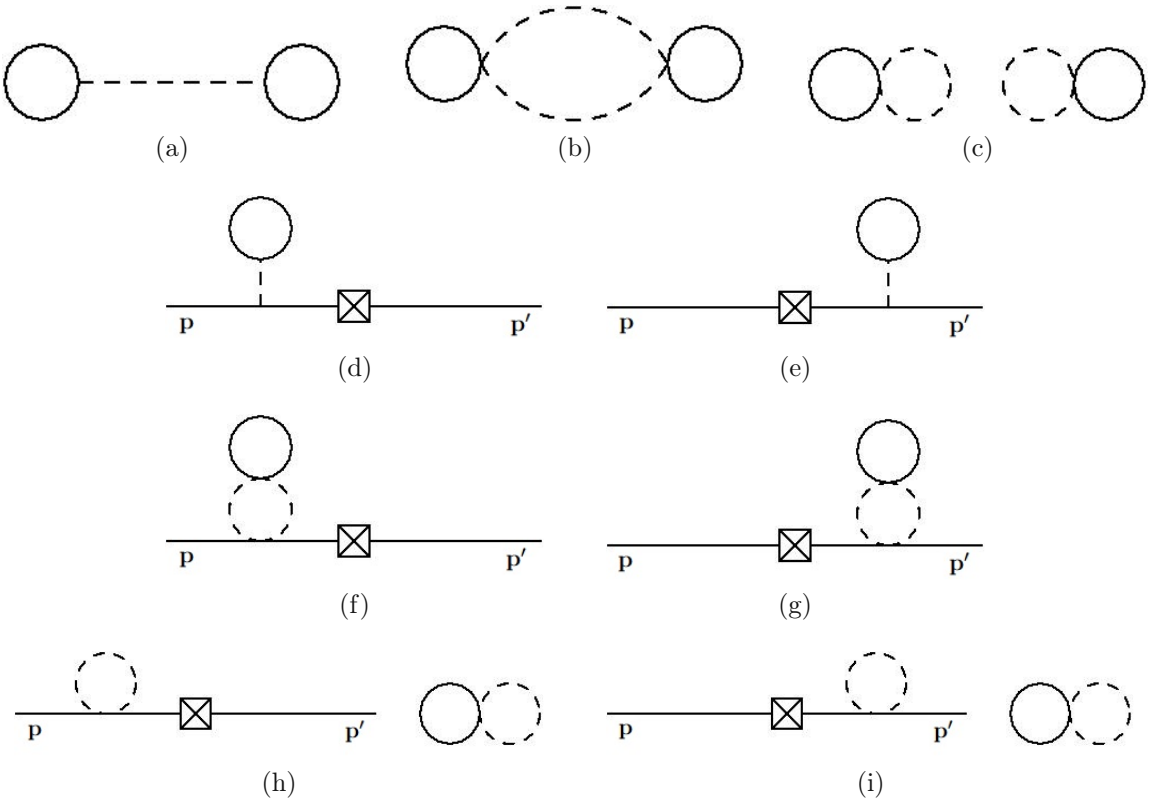

Figure 4.2.: Diagrammatic representation of terms with atomic loops in reduced density matrix (4.15); solid lines represent atoms, dashed lines represent dilatons and crossed boxes represent the reduced density operator.

Die approbierte gedruckte Originalversion dieser Diplomarbeit ist an der TU Wien Bibliothek verfügbar
The approved original version of this thesis is available in print at TU Wien Bibliothek.

4.1 (d)-(h)), one finds an expansion of an exponential function up to second order:

$$\begin{aligned}\rho_{1;1}(\mathbf{p},\mathbf{p}';0)e^{-i(E^{\phi}_{\mathbf{p}}-E^{\phi}_{\mathbf{p}'})t}\Bigg\{1-\frac{i\alpha_2}{4}\left(\frac{1}{E^{\phi}_{\mathbf{p}}}-\frac{1}{E^{\phi}_{\mathbf{p}'}}\right)t\;\Delta^F_{zz}\\ -\frac{\alpha_2^2}{16}\frac{1}{2}\left(\frac{1}{(E^{\phi}_{\mathbf{p}})^2}-\frac{2}{E^{\phi}_{\mathbf{p}}E^{\phi}_{\mathbf{p}'}}+\frac{1}{(E^{\phi}_{\mathbf{p}'})^2}\right)t^2\;\Delta^F_{zz}\Delta^F_{z'z'}\Bigg\} \qquad (4.17)\\ \approx \rho_{1;1}(\mathbf{p},\mathbf{p}';0)e^{-i(E^{\phi}_{\mathbf{p}}-E^{\phi}_{\mathbf{p}'})t}\cdot\left\{e^{-\frac{i\alpha_2}{4}\left(\frac{1}{E^{\phi}_{\mathbf{p}}}-\frac{1}{E^{\phi}_{\mathbf{p}'}}\right)t\;\Delta^F_{zz}}+\mathcal{O}(\alpha_2^3)\right\}.\end{aligned}$$

These terms, therefore, result in a first order correction to the unitary evolution, i.e. a phase shift. Some of the higher order imaginary terms may also describe phase shifts. All other terms that do not contribute to phase shifts result in decoherence. However, the phase shift in Eq. (4.17) can be measured more easily since it is of first order while all others only occur in second order and this phase shift is, therefore, the leading effect. Thus, all further calculations and discussions in the subsequent Sections 4.1 and 4.2 focus on the terms contributing to the phase shift in Eq. (4.17).

4.1. Renormalization

Looking at the terms in the fifth line of (4.16), which contribute to the phase shift in (4.17), one finds them to be quadratically and quartically divergent. Therefore, these terms will be renormalized now.

Since the relevant terms only contain tadpole divergences, they can be renormalized by counterterms. The relevant ones for this case are the mass counterterm for the ϕ- and χ-field and the tadpole counterterm for the χ-field.[2] Additionally, the thermal corrections ($T \neq 0$) can be ignored due to the fact that they are ultraviolet finite and thus do not have to be renormalized. For that reason, relevant counterterms have to contain only the parts where $T = 0$.

With this in mind, an ansatz for the counterterm action for the terms contributing to the phase shift can be made as

$$\delta\widehat{S}_{\mathrm{IF}} = -\sum_{a=\pm} a\left[\int_x \delta\alpha_2\chi^a_x + \frac{1}{2}\int_{xy}\delta M^2_{xy}\phi^a_x\phi^a_y + \frac{1}{2}\int_{xy}\delta m^2_{xy}\chi^a_x\chi^a_y\right] \qquad (4.18)$$

[2] When renormalizing the other terms of Eq. (4.16) one has to consider that these interactions take place over a finite time due to the fact that they are not local tadpole diagrams. Therefore, relevant counterterms must have equivalent time dependencies to ensure right behaviours in the limits $t \to 0$ and $t \to \infty$. A more detailed discussion can be found in [23].

Die approbierte gedruckte Originalversion dieser Diplomarbeit ist an der TU Wien Bibliothek verfügbar
The approved original version of this thesis is available in print at TU Wien Bibliothek.
TU Bibliothek Your knowledge hub WIEN

with

$$\delta\alpha_2 = -dD_{xx}^{F(T=0)}, \tag{4.19}$$
$$\delta M_{xy}^2 = -e\Delta_{xx}^{F(T=0)}\delta_{xy}^{(4)}, \tag{4.20}$$
$$\delta m_{xy}^2 = -fD_{xx}^{F(T=0)}\delta_{xy}^{(4)}, \tag{4.21}$$

where d, e and f are coefficients to still be determined so that the divergences completely cancel. Inserting (4.18) into the Feynman-Vernon influence functional (3.24), calculating it and inserting it into the reduced density matrix element of a single-particle state in momentum basis (3.58) leads the coefficients to be

$$d = \frac{\alpha_1 M}{2}, \qquad e = \frac{\alpha_2}{2}, \qquad f = \frac{\alpha_2}{2} \tag{4.22}$$

and therefore

$$\delta\alpha_2 = -\frac{\alpha_1 M}{2}D_{xx}^{F(T=0)}, \tag{4.23}$$
$$\delta M_{xy}^2 = -\frac{\alpha_2}{2}\Delta_{xx}^{F(T=0)}\delta_{xy}^{(4)}, \tag{4.24}$$
$$\delta m_{xy}^2 = -\frac{\alpha_2}{2}D_{xx}^{F(T=0)}\delta_{xy}^{(4)}. \tag{4.25}$$

After renormalization, all parts of the tadpole diagrams at zero temperature are nullified and only the thermal parts of the χ-field remain which are given by the integral [23]

$$\begin{aligned}\Delta_{xx}^{F(T\neq 0)} &= \int_k 2\pi f(|k^0|)\delta(k^2+m^2) = 2\int \frac{d^3k}{(2\pi)^3}\frac{1}{2E_{\mathbf{k}}^\chi}\frac{1}{e^{\beta E_{\mathbf{k}}^\chi}-1} \\ &= 2\int d\Pi_{\mathbf{k}} f(E_{\mathbf{k}}^\chi) = \frac{T^2}{2\pi^2}\int_{m/T}^\infty d\xi \frac{\sqrt{\xi^2-(\frac{m}{T})^2}}{e^\xi - 1}.\end{aligned} \tag{4.26}$$

However, since the ϕ-field was defined to not contain thermal parts (see Eqs. (4.2)-(4.3)), all diagrams with ϕ-tadpoles cancel when renormalizing. All other terms of Eq. (4.16) were not renormalized and, thus, remain unchanged.

Consequently, the reduced density matrix element can be rewritten as

$$\begin{aligned}\rho_{1;1}(\mathbf{p},\mathbf{p}';t) = \rho_{1;1}(\mathbf{p},\mathbf{p}';0)e^{-i(E_{\mathbf{p}}^\phi - E_{\mathbf{p}'}^\phi)t}\big\{1+\kappa(\mathbf{p},\mathbf{p}';t)+u(\mathbf{p},\mathbf{p}';t) \\ +\Gamma(\mathbf{p},\mathbf{p}';t)+\gamma(\mathbf{p},\mathbf{p}';t)\big\}\end{aligned} \tag{4.27}$$

with $\kappa(\mathbf{p},\mathbf{p}';t)$ representing the vacuum diagrams in the first four lines of Eq. (4.16), $\Gamma(\mathbf{p},\mathbf{p}';t)$ representing the terms in the seventh to eleventh lines of Eq. (4.16) corresponding to decays and $\gamma(\mathbf{p},\mathbf{p}';t)$ representing the last five lines of Eq. (4.16) and leading to momentum diffusion due to coupling between different momentum states. Γ and γ both are responsible for decoherence. Lastly, $u(\mathbf{p},\mathbf{p}';t)$ contains the terms from the fifth and

Die approbierte gedruckte Originalversion dieser Diplomarbeit ist an der TU Wien Bibliothek verfügbar
The approved original version of this thesis is available in print at TU Wien Bibliothek.
TU Bibliothek Your knowledge hub WIEN

sixth line of Eq. (4.16) describing mass shifts which result in a phase shift. After renormalization they are given by

$$u(\mathbf{p},\mathbf{p}';t) = -\frac{i\alpha_2}{2}\left(\frac{1}{E^\phi_{\mathbf{p}}}-\frac{1}{E^\phi_{\mathbf{p}'}}\right)t\int d\Pi_{\mathbf{k}} f(E^\chi_{\mathbf{k}}) - \frac{\alpha_2^2}{4}\left[\frac{1}{2}\left(\frac{1}{(E^\phi_{\mathbf{p}})^2}-\frac{2}{E^\phi_{\mathbf{p}}E^\phi_{\mathbf{p}'}}+\frac{1}{(E^\phi_{\mathbf{p}'})^2}\right)t^2 + \left(\left(\frac{-i}{2(E^\phi_{\mathbf{p}})^3}t+\frac{1-\exp\{(-2iE^\phi_{\mathbf{p}}t)\}}{4(E^\phi_{\mathbf{p}})^4}\right)+(\mathbf{p}\longleftrightarrow\mathbf{p}')^*\right)\right] \times\int d\Pi_{\mathbf{k}}d\Pi_{\mathbf{k}'}f(E^\chi_{\mathbf{k}})f(E^\chi_{\mathbf{k}'}). \tag{4.28}$$

4.2. Experimental implications

Before discussing the effect of a dilaton field on a single-particle state like the one discussed earlier, the general functionality of atom interferometry shall be explained since atom interferometry has already been used to constrain other screened scalar fields like the symmetron or chameleon fields [76–82]. With this overview it can then be understood what effects a conformally coupled dilaton can have. Atom interferometry experiments have the advantage of allowing a broad choice of atomic properties, like mass, polarization and magnetic moments, a large cross section for scattering light, high precision, and low costs [83]. Further information on atom interferometry can, for example, be found in [83, 84].

The theory behind atom interferometry is similar to the one behind optical interferometry. In the latter one, light is split into two paths, travels along these paths for a certain distance and is then recombined giving a characteristic interference pattern. Any differences in the path lengths lead to modifications of this interference pattern. With such a setup, LIGO was, for instance, able to detect gravitational waves [85]. Similarly, atom interferometry uses the wave-like behaviour of quantum mechanical atoms to achieve interference between different atoms or superposed states of the same atom. For this, the atomic wave is split into two or more parts which travel along different paths until being recombined later to give the interference pattern.

There are various ways to split an atom into two momentum states, the most common one is to use laser light [84]. For this method, a laser pulse with the correct energy to excite the atom from the ground state $|g\rangle$ to a higher energy state $|e\rangle$ is used. However, the atom only has a certain probability $P(g\to e)<1$ to absorb the photon and get excited. Without measuring whether the photon was absorbed, the atom is therefore in a superposed state

$$|\Psi\rangle = \sqrt{1-P(g\to e)}\,|g\rangle + \sqrt{P(g\to e)}\,|e\rangle\,.$$

Die approbierte gedruckte Originalversion dieser Diplomarbeit ist an der TU Wien Bibliothek verfügbar
The approved original version of this thesis is available in print at TU Wien Bibliothek.
TU Bibliothek Your knowledge hub WIEN

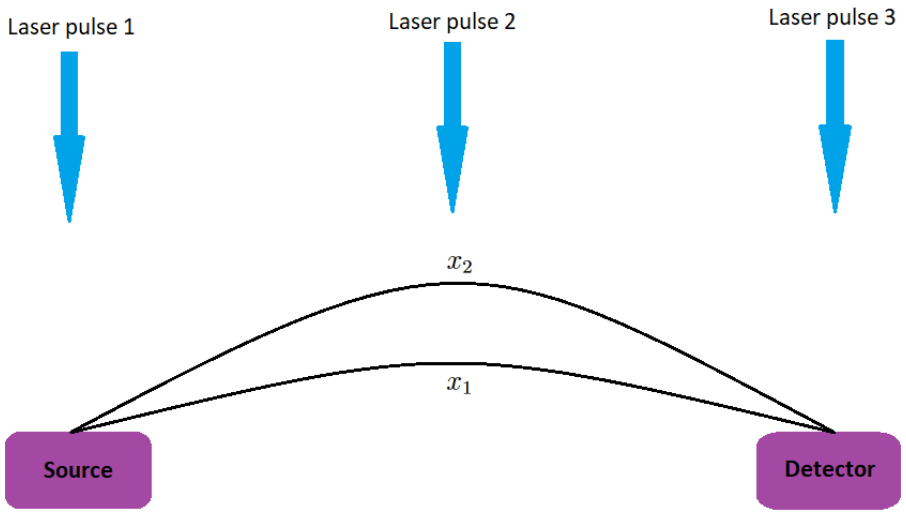

Figure 4.3.: Schematic depiction of the paths in atom interferometry; an atom is produced in a source, a first laser pulse splits the atom into two superposed states which travel along the paths x_1 and x_2, a second laser pulse redirects the two paths back towards each other, a third laser pulse recombines the states before the detector measures the resulting interference pattern.

Furthermore, absorbing the photon also means absorbing the photon's momentum resulting in a larger atom momentum for the excited state $|e\rangle$. When assuming that the photon's momentum is parallel to the atom's direction of motion, this larger momentum would lead to the excited state to reach the detector earlier than the ground state which is not preferable since this would not lead to interference. Therefore, the laser's momentum should not be aligned with the atom's direction of motion so that the two states have to travel along different paths [84], x_1 for the ground state and x_2 for the excited state, and arrive at the same time at the detector to interfere. Using another laser, the different path lengths and shapes can be controlled via absorption or induced emission [86] to redirect the two paths towards each other again. Lastly, a third laser pulse is used to recombine the states before reaching the detector where the interference pattern is measured. A schematic depiction of the different paths x_1 and x_2 is shown in Figure 4.3.

The difference between the path lengths $\Delta x = |x_1 - x_2|$ (or between the momenta $\Delta x = |(p_1 - p_2)|t/m$ with p_1 and p_2 being the momenta for the ground state and excited state, respectively [83]) gives the intensity I measured at the detector. This intensity can lie between 0 and $2I_{\mathrm{cl}}$, when the intensity a classical atom would exhibit is I_{cl}. If the measured intensity is bigger than the one expected for a classical particle $I > I_{\mathrm{cl}}$, the beams interfere constructively, while a smaller intensity $I < I_{\mathrm{cl}}$ correlates to destructive

Die approbierte gedruckte Originalversion dieser Diplomarbeit ist an der TU Wien Bibliothek verfügbar
The approved original version of this thesis is available in print at TU Wien Bibliothek.

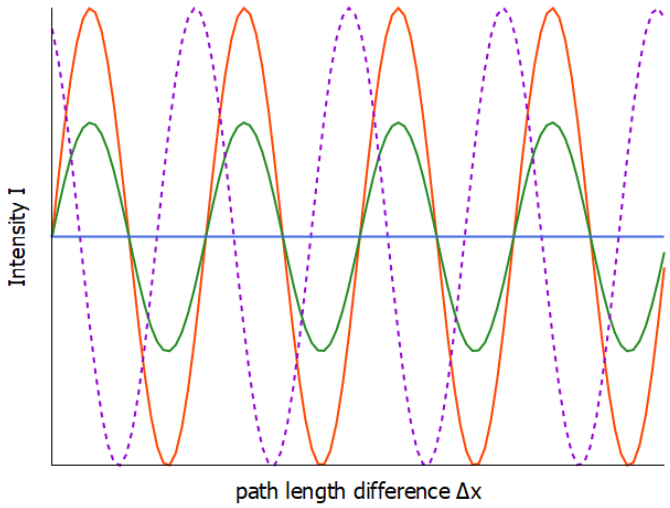

Figure 4.4.: Schematic depiction of interference pattern in atom interferometry given by the intensity I over the difference in path lengths Δx; the blue line corresponds to the intensity I_{cl} expected for a classical atom, which would be seen if every atom in the interferometer has decohered. In contrast, the orange line depicts the case in which no particle experiences decoherence with a peak-to-peak amplitude of $2I_{\mathrm{cl}}$. Meanwhile, the green line illustrates the case in between: when reaching the detector, some atoms have already decohered while others are still in superposition. Therefore, the peak-to-peak amplitude is larger than 0 but smaller than $2I_{\mathrm{cl}}$. Lastly, the dashed purple line shows the interference pattern of an atom experiencing a phase shift but no decoherence.

interference. The dependence of the intensity on the path length difference Δx is shown in Figure 4.4, where the blue line corresponds to I_{cl} and the orange and green line show the interference pattern.

One can use an interference pattern as depicted in Figure 4.4 to observe decoherence. For this, one should remember that decoherence might be an explanation for the transition from the quantum physical to the classical world as after the decoherence time all superpositions collapse and the quantum system becomes classical. Further, decoherence seems like a statistical effect as an atomic superposition only decoheres with a certain probability before reaching the detector while others remain in superposition. Therefore, the interference pattern does not disappear completely but the peak-to-peak intensities lessen for only a reduced amount of atoms interfere (see the green line in Figure 4.4). So, if a detected pattern exhibits a peak-to-peak intensity amplitude which is smaller than $2I_{\mathrm{cl}}$ it is an indication for decoherence and thus for the presence of an environment. Additionally, an interference pattern can be used to identify phase shifts which are assumed to be the dominant effect of the system discussed in this thesis. Due to a phase shift the peaks of the intensity are shifted, as can be seen in the dashed purple line in Figure 4.4 for the case of an atom without experiencing decoherence.

Die approbierte gedruckte Originalversion dieser Diplomarbeit ist an der TU Wien Bibliothek verfügbar
The approved original version of this thesis is available in print at TU Wien Bibliothek.

Having understood this, the effects of a dilaton field on atom interferometry can now be discussed[3]. However, contrary to other screened scalar fields like the chameleon and symmetron (see for example [76–82]), the dilaton field has not yet been investigated experimentally to a great extent. Therefore, the dilaton's parameters, λ, V_0 and A_2, can be chosen rather freely. The subsequent discussion is thus used to set boundaries to the orders of magnitude of these parameters and to determine with which parameter spaces the dilaton would be expected to show measurable effects in atom interferometry. For this discussion, only the terms relevant for phase shifts (see Eq. (4.17)) will be considered.

It should be remembered that most of the calculations until now were performed using a rescaled mass for the ϕ-field as defined in Eq. (2.40) which depends on the background value of the dilaton field, $\langle X\rangle$. Thus, to determine the leading term of the phase shift, all quantities in the phase shift of Eq. (4.17) depending on the matter field mass have to be expressed in terms of the absolute mass value $\tilde{M}$, since this is the mass the experiment is sensitive to. Recalling that $E^\phi_{\mathbf{p}} = \sqrt{\mathbf{p}^2 + M^2}$, one can expand the energies to first order to find

$$\begin{aligned} E^\phi_{\mathbf{p}} - E^\phi_{\mathbf{p}'} &= \sqrt{\mathbf{p}^2 + M^2} - \sqrt{\mathbf{p}'^2 + M^2} \\ &= \sqrt{\mathbf{p}^2 + \left(1 + \frac{A_2}{M_{Pl}^2}\langle X\rangle^2\right)\tilde{M}^2} - \sqrt{\mathbf{p}'^2 + \left(1 + \frac{A_2}{M_{Pl}^2}\langle X\rangle^2\right)\tilde{M}^2} \\ &\approx \tilde{E}^\phi_{\mathbf{p}}\left(1 + \frac{1}{2(\tilde{E}^\phi_{\mathbf{p}})^2}\tilde{M}^2\frac{A_2}{M_{Pl}^2}\langle X\rangle^2\right) - \tilde{E}^\phi_{\mathbf{p}'}\left(1 + \frac{1}{2(\tilde{E}^\phi_{\mathbf{p}'})^2}\tilde{M}^2\frac{A_2}{M_{Pl}^2}\langle X\rangle^2\right) \\ &= \tilde{E}^\phi_{\mathbf{p}} - \tilde{E}^\phi_{\mathbf{p}'} + \tilde{M}^2\frac{A_2}{2M_{Pl}^2}\langle X\rangle^2\left(\frac{1}{\tilde{E}^\phi_{\mathbf{p}}} - \frac{1}{\tilde{E}^\phi_{\mathbf{p}'}}\right) \end{aligned} \tag{4.29}$$

and

$$\begin{aligned} \frac{1}{E^\phi_{\mathbf{p}}} - \frac{1}{E^\phi_{\mathbf{p}'}} &= \frac{1}{\sqrt{\mathbf{p}^2 + M^2}} - \frac{1}{\sqrt{\mathbf{p}'^2 + M^2}} \\ &= \frac{1}{\sqrt{\mathbf{p}^2 + \tilde{M}^2 + \frac{A_2}{M_{Pl}^2}\langle X\rangle^2\tilde{M}^2}} - \frac{1}{\sqrt{\mathbf{p}'^2 + \tilde{M}^2 + \frac{A_2}{M_{Pl}^2}\langle X\rangle^2\tilde{M}^2}} \\ &\approx \frac{1}{\tilde{E}^\phi_{\mathbf{p}}}\left(1 - \frac{\tilde{M}^2}{2(\tilde{E}^\phi_{\mathbf{p}})^2}\frac{A_2}{M_{Pl}^2}\langle X\rangle^2\right) - \frac{1}{\tilde{E}^\phi_{\mathbf{p}'}}\left(1 - \frac{\tilde{M}^2}{2(\tilde{E}^\phi_{\mathbf{p}'})^2}\frac{A_2}{M_{Pl}^2}\langle X\rangle^2\right) \\ &\approx \frac{1}{\tilde{E}^\phi_{\mathbf{p}}} - \frac{1}{\tilde{E}^\phi_{\mathbf{p}'}}, \end{aligned} \tag{4.30}$$

where $\tilde{E}^\phi_{\mathbf{p}} = \sqrt{\mathbf{p}^2 + \tilde{M}^2}$ was defined. Therefore, the leading term of the phase shift,

[3] This part is based on [23]

Die approbierte gedruckte Originalversion dieser Diplomarbeit ist an der TU Wien Bibliothek verfügbar
The approved original version of this thesis is available in print at TU Wien Bibliothek.
TU Bibliothek Your knowledge hub WIEN

without the unitary evolution in Eq. (4.29), is given by

$$|\Delta u| = \left| \tilde{M}^2 \frac{A_2}{2M_{Pl}^2} \langle X \rangle^2 \left(\frac{1}{\tilde{E}^{\phi}_{\mathbf{p}}} - \frac{1}{\tilde{E}^{\phi}_{\mathbf{p}'}} \right) + \frac{\alpha_2}{4} \left(\frac{1}{\tilde{E}^{\phi}_{\mathbf{p}}} - \frac{1}{\tilde{E}^{\phi}_{\mathbf{p}'}} \right) \Delta_{zz}^{F(T\neq 0)} \right|, \tag{4.31}$$

with the Feynman propagator at finite temperatures being given by Eq. (4.26). Additionally, by taking Eq. (2.42), α_2 can be written in terms of the absolute mass value $\tilde{M}$ as

$$\alpha_2 = 2\frac{A_2}{M_{Pl}^2}\tilde{M}^2. \tag{4.32}$$

Next, these energies can be expanded under the non-relativistic assumption $\tilde{M}^2 \gg \mathbf{p}^2$:

$$\frac{1}{\tilde{E}^{\phi}_{\mathbf{p}}} = \frac{1}{\tilde{M}\sqrt{1+\frac{\mathbf{p}^2}{\tilde{M}^2}}} \approx \frac{1}{\tilde{M}} \left(1 - \frac{\mathbf{p}^2}{2\tilde{M}^2} \right). \tag{4.33}$$

This leads to

$$\frac{1}{\tilde{E}^{\phi}_{\mathbf{p}}} - \frac{1}{\tilde{E}^{\phi}_{\mathbf{p}'}} = \frac{v^2}{2\tilde{M}} \tag{4.34}$$

where $v \coloneqq \frac{||\mathbf{p}|-|\mathbf{p}'||}{\tilde{M}}$ was defined as the difference in speeds between the two atomic states. Thus, the absolute value of Eq. (4.31) can be expressed as

$$|\Delta u| = \left| \tilde{M} \frac{A_2}{2M_{Pl}^2} \left[\langle X \rangle^2 + \Delta_{zz}^{F(T\neq 0)} \right] \frac{v^2}{2} \right|. \tag{4.35}$$

In order to estimate relevant parameter domains using Eq. (4.35), common values for atom interferometry experiments are chosen. The vacuum chamber is assumed to be spherical with a radius of $L = 10$ cm [78, 81] and made of steel with a density of $\rho^{\text{ext}}_{\text{steel}} = 7860\ \text{kg m}^{-3}$ [87]. Furthermore, the density of the residual gas inside the vacuum chamber is supposed to be $\rho^{\text{ext}} = 3 \times 10^{-14}\ \text{kg m}^{-3}$ [82]. Additionally, it is assumed that the quantum test mass is a Rubidium-87 atom with a mass of $\tilde{M} = 87\, m_u$ [82] with m_u being the atomic mass unit. The speed difference between the two atomic states is given by $v = 50\ \text{mm s}^{-1}$ [88]. Furthermore, the reduced Planck mass is given by $M_{Pl} = \sqrt{\frac{\hbar c_0}{8\pi G}} \approx 2.435 \times 10^{27}$ eV. In current atom interferometry tests, phase shifts of up to $\Delta u_{\text{min}} \approx 10^{-8}$ Hz are measurable (inferred from [88, 89]). Additionally, three different temperatures are chosen, namely 0.5 mK, 300 K and 1000 K. The lowest value was chosen to be one of the lowest values which still made it possible to numerically evaluate the integral in Eq. (4.26), the other values were selected to be roughly room temperature and a temperature even higher than that, respectively.

As already mentioned, due to a lack of experiments, the dilaton's parameters λ, A_2 and V_0 can be chosen rather freely. However, in the course of the evaluation process in this thesis, some approximations have been made which set some conditions on these param-

Die approbierte gedruckte Originalversion dieser Diplomarbeit ist an der TU Wien Bibliothek verfügbar
The approved original version of this thesis is available in print at TU Wien Bibliothek.
TU Bibliothek Your knowledge hub WIEN

eters. Firstly, as discussed below Eq. (2.17), $A_2 \gg 1$ is required so that constraints from Solar System based tests can be circumvented. Secondly, as mentioned below Eq. (2.18), $\langle X\rangle/\mathcal{M} = \sqrt{A_2}\langle X\rangle/M_{Pl} \ll 1$ has to be true in order for the coupling function to contain no higher order terms. Thirdly, in Eq. (2.35) the exponent of the effective potential was expanded, giving the condition $\lambda\langle X\rangle/M_{Pl} \ll 1$. Next, the argument of the Lambert W-function (see Eq. (2.22)) is assumed to be small so that its expansion can be assumed to only contain terms up to second order, making the evaluation of the dilaton's field (see Eq. (2.21)) and thus also its mass (see Eq. (2.23)) more straightforward. This assumption leads to $\lambda^2 V_0/(A_2\rho^{\text{ext}}) \ll 1$. Lastly, for the effects to be noticeable, the phase shift due to the dilaton has to be at least of order of the minimal phase shift measurable today, $|\Delta u| \gtrsim \Delta u_{\text{min}}$.

Additionally, in [23, 24, 77] it was discussed that a chameleon field could not reach the minimum of its potential since its Compton wavelength was larger than the radius of the vacuum chamber. Therefore, it adjusts its Compton wavelength to become equal to the chamber radius. A similar situation is assumed for some parameter spaces for the dilaton, while for other parameter domains the dilaton field can reach its minimum. The dilaton's Compton wavelength is given by $\lambda_C = \frac{q}{m}$, where the fudge factor q is assumed to be roughly 1 based on similar situations for the chameleon field, see [23, 77, 81, 90]. For parameter spaces where the Compton wavelength is smaller than the chamber's radius, i.e. $\lambda_C \leq L$, the dilaton field can reach its minimum. In this case, the dilaton's field value and mass are given by Eqs. (2.21) and (2.23) as

$$\begin{aligned} \langle X\rangle &= \frac{M_{Pl}}{\lambda}\left[\frac{\lambda^2 V_0}{A_2\rho^{\text{ext}}} - \left(\frac{\lambda^2 V_0}{A_2\rho^{\text{ext}}}\right)^2\right], \\ m &= \frac{1}{M_{Pl}}\sqrt{\lambda^2 V_0\, e^{-\frac{\lambda^2 V_0}{A_2\rho^{\text{ext}}} + \left(\frac{\lambda^2 V_0}{A_2\rho^{\text{ext}}}\right)^2} + A_2\rho^{\text{ext}}}. \end{aligned} \tag{4.36}$$

In contrast, when the Compton wavelength is larger than the chamber's radius, i.e. $\lambda_C > L$, the minimum cannot be reached and the dilaton adapts its Compton wavelength to the size of the vacuum chamber. If so, the dilaton's field value and mass are assumed to be

$$\begin{aligned} \langle X\rangle &= \langle X\rangle_{\text{wall}} + (\langle X\rangle_{\text{vacuum}} - \langle X\rangle_{\text{wall}})\,\frac{L}{\lambda_C}, \\ m &= \frac{1}{L}. \end{aligned} \tag{4.37}$$

Here, $\langle X\rangle_{\text{wall}}$ and $\langle X\rangle_{\text{vacuum}}$ correspond to the field value given by Eq. (2.21) the dilaton would have inside of the chamber's walls (made of steel with density $\rho^{\text{ext}}_{\text{steel}}$) and in the vacuum of the vacuum chamber (with density ρ^{ext}), respectively. Furthermore, to obtain the field value for the case $\lambda_C > L$ as given by Eq. (4.37), a linear increase from the value

Die approbierte gedruckte Originalversion dieser Diplomarbeit ist an der TU Wien Bibliothek verfügbar
The approved original version of this thesis is available in print at TU Wien Bibliothek.

inside of the wall to the value in vacuum in assumed, for lack of a more precise estimation.

Domains where all these discussed conditions hold can be seen for each of the chosen temperature values in Figures 4.5, 4.6 and 4.7. In each image the blue area represents the parameter domain for which a phase shift could be noticeable under the assumption that $\lambda_C > L$ whereas for the orange region $\lambda_C < L$ holds. For each of the temperatures, V_0 was chosen to stay fixed at different values, while λ and A_2 are varied. For T=0.5 mK (see Figure 4.5) it can be seen that the minimal value of λ decreases for increasing values of V_0. In contrast, both for T=300 K (see Figure 4.6) and T=1000 K (see Figure 4.7) no minimum value of λ was found for any value of V_0 for the case of $\lambda_C < L$. However, the possible minimum values of A_2 seem to decrease for increasing values of V_0 until reaching the boundary of the first condition discussed ($A_2 \gg 1$) for all temperatures in the same way. Additionally, all areas for which $\lambda_C > L$ have smaller values of A_2 than areas for which $\lambda_C < L$. Interestingly, for T=300 K (see Figure 4.6) and T=1000 K (see Figure 4.7) the values for λ and A_2 for which dilaton-induced changes in the interference pattern would be measurable are quite similar. Furthermore, while the areas where $\lambda_C > L$ (blue areas in Figures 4.5, 4.6 and 4.7) change shape and position when modifying V_0, they seem to hardly alter when varying the temperature as can for example be seen for $V_0 = 10^{20}\,\mathrm{eV}^4$ when comparing Figures 4.5 (b), 4.6 (c) and 4.7 (c).

The reason for this apparent temperature independence in areas with $\lambda_C > L$ is that in these parameter domains the field value $\langle X \rangle$ contributes in a higher degree to the phase shift $|\Delta u|$ in Eq. (4.35) than the thermal part does. However, in other areas the thermal contribution dominates. By comparing Figures 4.5, 4.6 and 4.7 one easily finds this to be the case for $\lambda_C < L$ when λ is smaller than the minimal value of λ in the $\lambda_C > L$ domain. The temperature dependent development of the phase shift caused by the dilaton for a fixed set of parameters in an area where the thermal contribution prevails can be seen in Figure 4.8. Here, the values $\lambda = 10^{-8}$, $V_0 = 10^7\,\mathrm{eV}^4$ and $A_2 = 10^{48}$ were chosen and the temperature was varied from 0.5 mK to 1000 K. The resulting progress of $|\Delta u|$ is shown in the blue line, while the green line depicts the boundary of detection $\Delta u_{\min}$. For these values of λ, V_0 and A_2, $|\Delta u| \gtrsim \Delta u_{\min}$ only holds for temperatures higher than roughly 25 K.

However, it should be kept in mind that for a phase shift to be detectable, an experiment has to be conducted at least twice in different conditions. This is so, because without comparing two interference patterns, a phase shift is not noticeable. Therefore, the conditions of the two experimental runs have to differ in such a way as to allow the interference patterns to show distinguished phase shifts. This may be achieved by altering any parameter value appearing in the dilaton-induced phase shift in Eq. (4.35), for example the temperature or the density of the residual gas inside the vacuum chamber.

It would be interesting to conduct atom interferometry experiments at these temperatures to discover whether these domains for the parameters λ, V_0 and A_2 should be

Die approbierte gedruckte Originalversion dieser Diplomarbeit ist an der TU Wien Bibliothek verfügbar
The approved original version of this thesis is available in print at TU Wien Bibliothek.

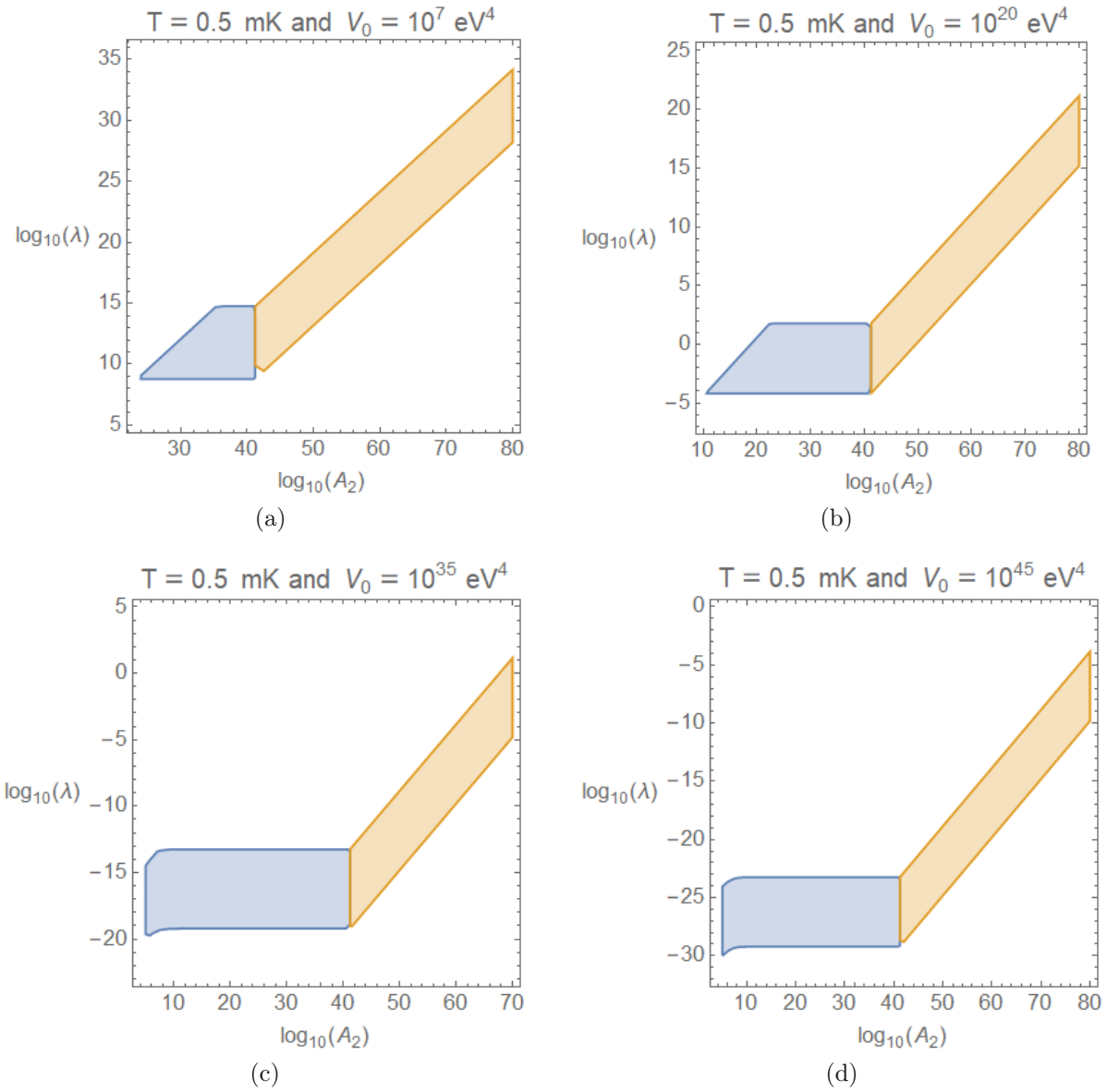

Figure 4.5.: Diagrammatic depiction of allowed parameter spaces for fixed T=0.5 mK and several values for V_0; the depicted domains show for which combination of λ and A_2 the dilaton-induced phase shift would be measurable. Blue areas correspond to the case $\lambda_C > L$ while orange areas correspond to $\lambda_C < L$.

Die approbierte gedruckte Originalversion dieser Diplomarbeit ist an der TU Wien Bibliothek verfügbar
The approved original version of this thesis is available in print at TU Wien Bibliothek.

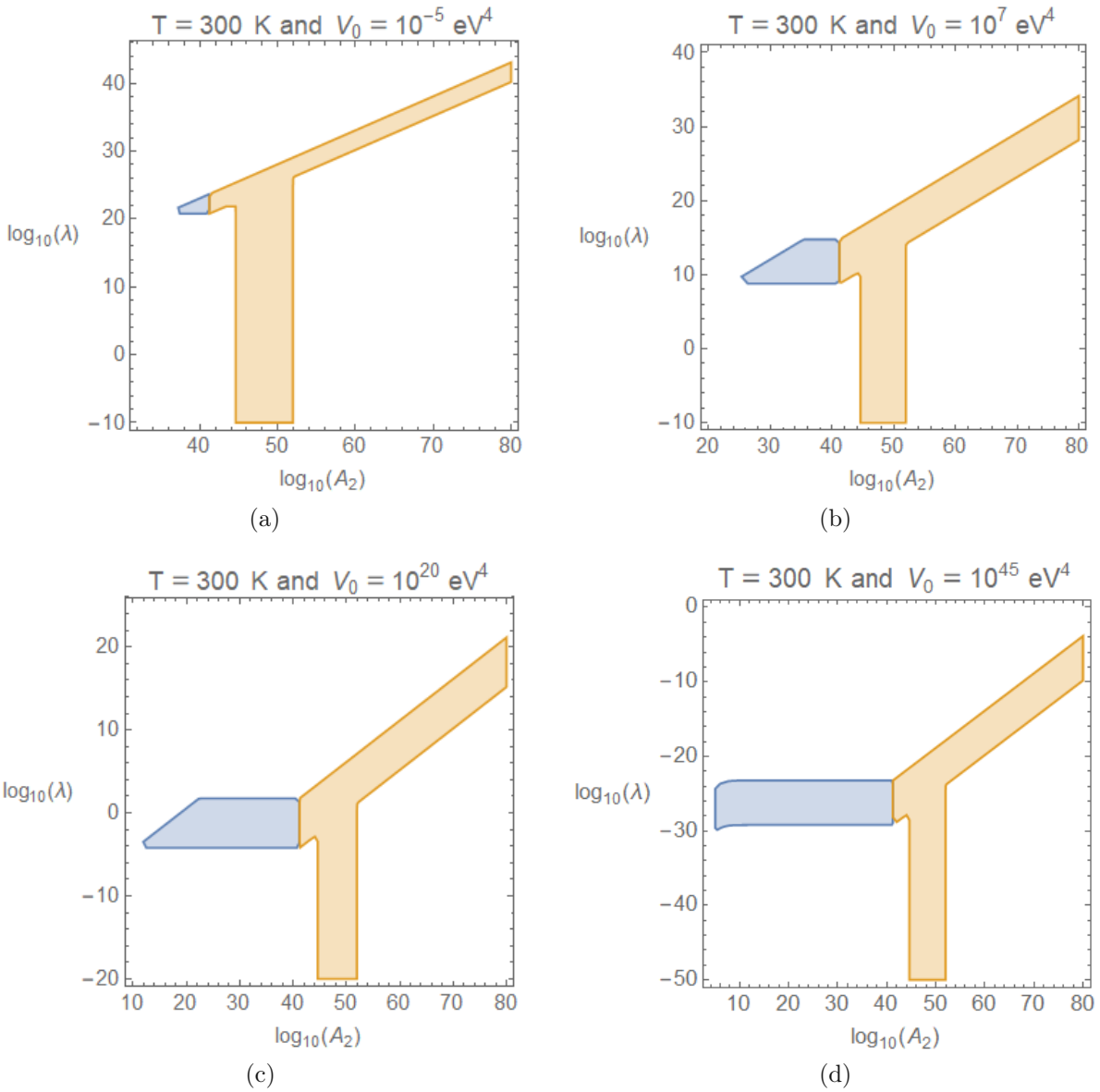

Figure 4.6.: Diagrammatic depiction of allowed parameter spaces for fixed T=300 K and several values for V_0; the depicted domains show for which combination of λ and A_2 the dilaton-induced phase shift would be measurable. Blue areas correspond to the case $\lambda_C > L$ while orange areas correspond to $\lambda_C < L$.

Die approbierte gedruckte Originalversion dieser Diplomarbeit ist an der TU Wien Bibliothek verfügbar
The approved original version of this thesis is available in print at TU Wien Bibliothek.

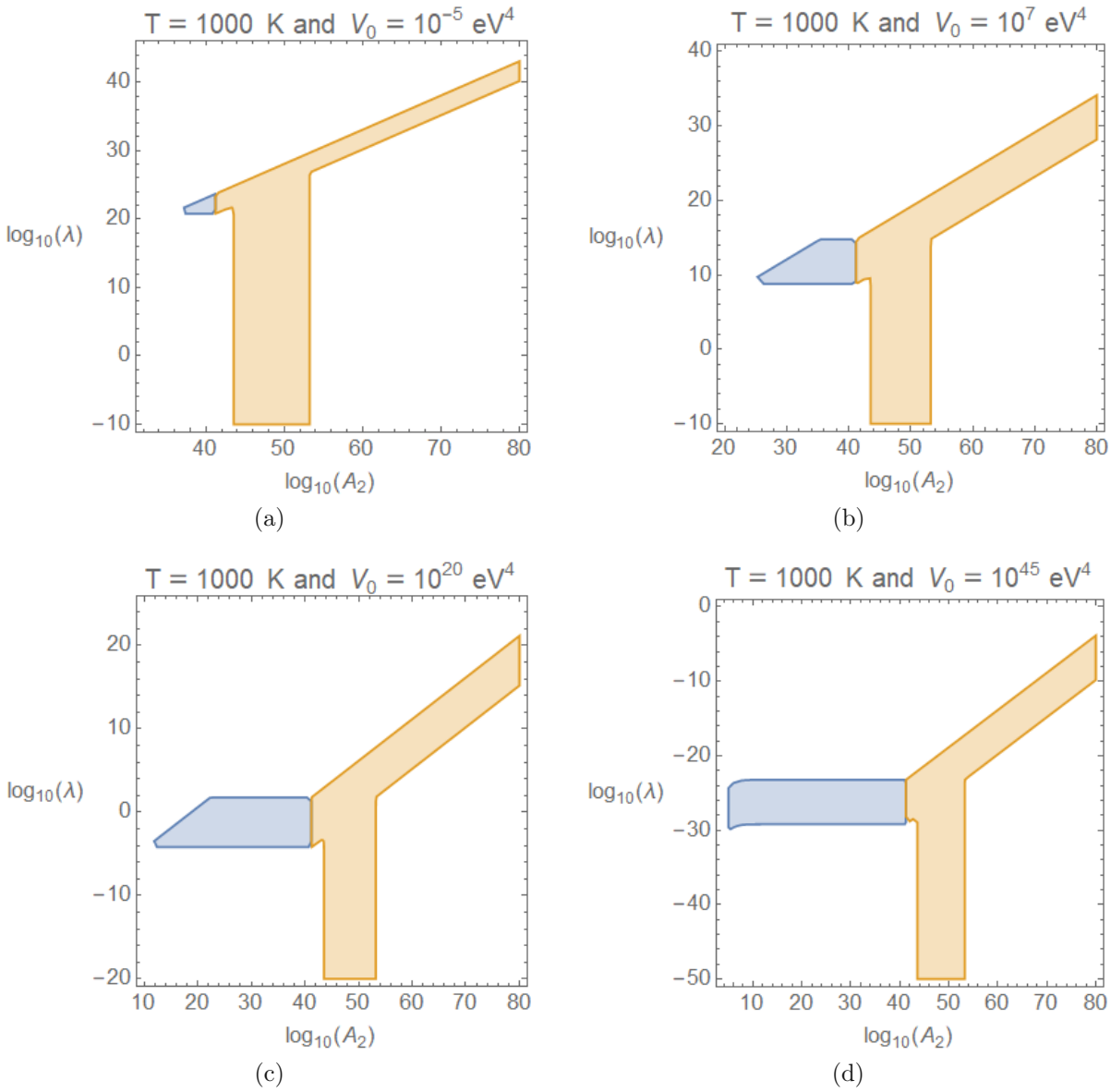

Figure 4.7.: Diagrammatic depiction of allowed parameter spaces for fixed T=1000 K and several values for V_0; the depicted domains show for which combination of λ and A_2 the dilaton-induced phase shift would be measurable. Blue areas correspond to the case $\lambda_C > L$ while orange areas correspond to $\lambda_C < L$.

Die approbierte gedruckte Originalversion dieser Diplomarbeit ist an der TU Wien Bibliothek verfügbar
The approved original version of this thesis is available in print at TU Wien Bibliothek.

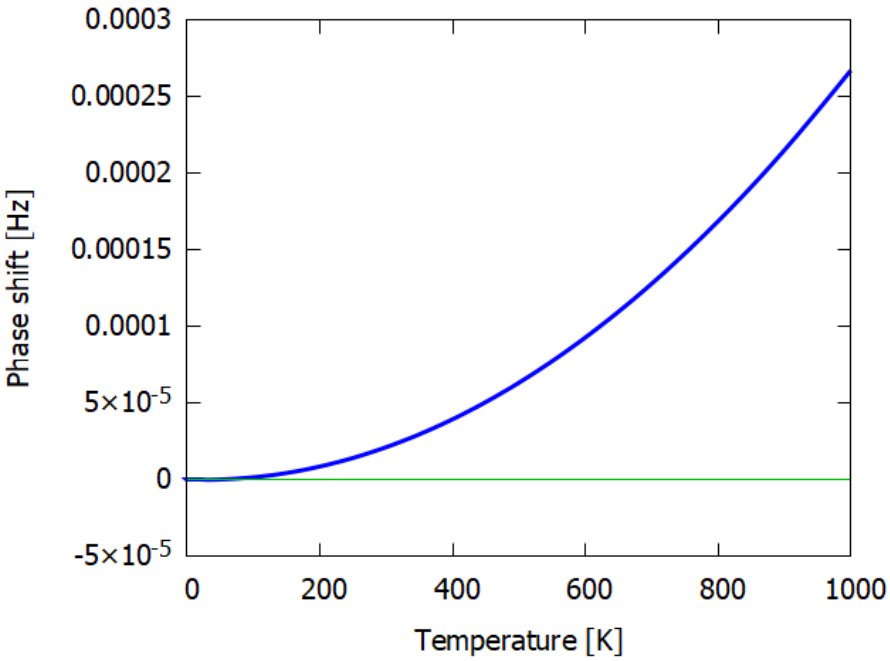

Figure 4.8.: Diagrammatic depiction of the temperature dependency of the dilaton-induced phase shift $|\Delta u|$ with $\lambda = 10^{-8}$, $V_0 = 10^7\,\mathrm{eV}^4$ and $A_2 = 10^{48}$ for $\mathrm{T} \in [0.5\,\mathrm{mK}, 1000\,\mathrm{K}]$ in blue with $\Delta u_{\min}$ being represented by the green line

excluded. However, even more parameter spaces could be covered by altering the experimental setup. For example, increasing the masses of the test masses (as long as they do not influence the screening mechanism) would be one possible alteration. For instance, [91] uses atom pairs (e.g. $^{85}\mathrm{Rb} - {}^{87}\mathrm{Rb}$) in an atom interferometry experiment, while [92] has used 10^{10} silica atoms in a Bell test. Another possibility would be to adjust the experimental setup in such a way that the two paths of the superposed states are traveling through areas of different background values $\langle X \rangle$. For this case, Eq. (4.27) has to be modified to also include a spatially inhomogeneous screened scalar field. In the present work these and other alterations will not be discussed further.

As already mentioned, the current discussion of experimental implications only focuses on phase shifts induced by a dilaton field and does not take into account other effects like momentum diffusion and decoherence. This was done because these effects are expected to be even less noticeable than the phase shift, which in itself is assumed to not be detectable similar to the effects of chameleons and symmetrons which have already been studied experimentally [76–82]. However, not detecting a phase shift puts constraints on the possible parameter spaces of these models.

Lastly, it should be mentioned again that assuming a scalar field to be a proxy for a non-relativistic and extended atom is a rough approximation. Therefore, all findings discussed here are expected to only be qualitative estimates of the true behavior. Applying this formalism to more realistic probe models, however, is not part of the present work and will be presented elsewhere.

Die approbierte gedruckte Originalversion dieser Diplomarbeit ist an der TU Wien Bibliothek verfügbar
The approved original version of this thesis is available in print at TU Wien Bibliothek.
TU Bibliothek Your knowledge hub WIEN

5. Conclusion

To this day, many phenomena of our universe are still a great mystery. A few of them are the natures of dark matter and dark energy. Some attempts to explain them include modifying Einstein's theory of general relativity by introducing new light scalar fields which couple to matter. However, such fields are expected to give rise to fifth forces similar to gravity which are tightly constrained by tests within our Solar System [10]. To circumvent these constraints, so-called screening mechanisms are introduced, which repress fifth forces in areas of high mass densities, while in less dense environments phenomenologically relevant effects are permitted. Scalar fields which show such screening mechanisms are called screen scalar fields and they are subjects of current theoretical and experimental research. While some screened scalar fields, like the chameleon and symmetron field, have already been investigated in numerous observations leading to their parameter spaces to have been constrained, other screend scalar fields, like the environmentally dependent dilaton field, still do not exhibit any meaningful limitations of their parameters.

Therefore, the aim of this master's thesis is to theoretically describe the interactions between the dilaton field and another scalar field as a proxy for a matter field using a new approach, which was first presented in [26]. This approach uses density matrices as a mean to describe the open quantum system of a matter field interacting with a dilaton field as its environment. By tracing out the environmental degrees of freedom, a reduced density operator can be obtained whose time evolution is given by a master equation. However, solving a master equation can be impossible, which is why this new approach to directly compute the reduced density matrix elements was established.

The calculation of the reduced density matrix elements is performed in a momentum basis in Fock space for weak coupling. Furthermore, it uses different techniques from non-equilibrium quantum theory, specifically the Feynman-Vernon influence functional, based on the Schwinger-Keldysh formalism, and thermo field dynamics (TFD). Additionally, it makes use of the fact that the quantum Liouville equation can be rewritten in a Schrödinger-like form in Schrödinger picture TFD, which then can be used to determine a general Hamiltonian. Afterwards, an LSZ-like reduction, first developed in [23], is applied to derive the equation for directly computing reduced density matrix elements.

This equation was then used to calculate the effects of a dilaton field on the system field for a single-particle state. Open quantum dynamical effects like phase shift, momentum diffusion and decoherence were found. All terms contributing to the phase shift, the

Die approbierte gedruckte Originalversion dieser Diplomarbeit ist an der TU Wien Bibliothek verfügbar
The approved original version of this thesis is available in print at TU Wien Bibliothek.
TU Bibliothek Your knowledge hub WIEN

effect assumed to be most prominent, were then also renormalized to avoid ultraviolet divergences. Finally, the found phase shift was used to qualitatively estimate parameter domains where effects induced by dilatons are expected to cause noticeable changes in an atom interferometry experiment by using common values for such an experiment.

However, approximating an atom by a scalar field is a rather rough estimate, since scalar fields allow for production and annihilation processes which are not permitted for structures as complex and stable as realistic atoms. Therefore, using a more realistic atomic model would be an interesting way to study this system more truthfully in the future. Additional improvements include the consideration of inhomogeneous scalar field backgrounds as well as the usage of more massive fields.

Die approbierte gedruckte Originalversion dieser Diplomarbeit ist an der TU Wien Bibliothek verfügbar
The approved original version of this thesis is available in print at TU Wien Bibliothek.
TU Bibliothek Your knowledge hub WIEN

A. Propagators of scalar fields

Propagators of scalar fields are significant in the derivation of this thesis. Therefore, they shall be looked at more closely here. Afterwards, two important properties of such propagators, which are also frequently used in this work, will be presented and proven, following the proof of [24].

The propagators without thermal corrections used here are given in terms of the doubled scalar degrees of freedom living on a closed time path contour by [15]

$$\langle \mathrm{T}\varphi_x^+\varphi_y^+\rangle = \Delta_{xy}^F = -i\int_k \frac{e^{ik\cdot(x-y)}}{k^2+m^2-i\epsilon}, \tag{A.1}$$

$$\langle \mathrm{T}\varphi_x^-\varphi_y^-\rangle = \Delta_{xy}^D = i\int_k \frac{e^{ik\cdot(x-y)}}{k^2+m^2+i\epsilon}, \tag{A.2}$$

$$\langle \varphi_y^+\varphi_x^-\rangle = \Delta_{xy}^< = \int_k e^{ik\cdot(x-y)} 2\pi\Theta(-k^0)\delta(k^2+m^2), \tag{A.3}$$

$$\langle \varphi_x^-\varphi_y^+\rangle = \Delta_{xy}^> = \Delta_{yx}^< = (\Delta_{xy}^<)^* \tag{A.4}$$

with T indicating time-ordering. These propagators are called Feynman propagator, Dyson propagator, negative frequency Wightman propagator and positive frequency Wightman propagator. In Figure A.1 the integration contours of these propagators in the complex plane can be found.

A.1. Coincidence in the equal time limit

In the following, an important property for the calculation presented in this thesis will be proven. It states that all four propagators of (A.1)-(A.4) coincide when taken in the equal time limit, more precisely:

$$\lim_{y^0\to x^0}\Delta_{xy}^F = \lim_{y^0\to x^0}\Delta_{xy}^D = \lim_{y^0\to x^0}\Delta_{xy}^< = \lim_{y^0\to x^0}\Delta_{xy}^>. \tag{A.5}$$

For this purpose a new notation for the equal time limit is defined, namely

$$\lim_{y^0\to x^0}\Delta_{xy} =: \Delta_{\mathbf{xy}}. \tag{A.6}$$

Die approbierte gedruckte Originalversion dieser Diplomarbeit ist an der TU Wien Bibliothek verfügbar
The approved original version of this thesis is available in print at TU Wien Bibliothek.

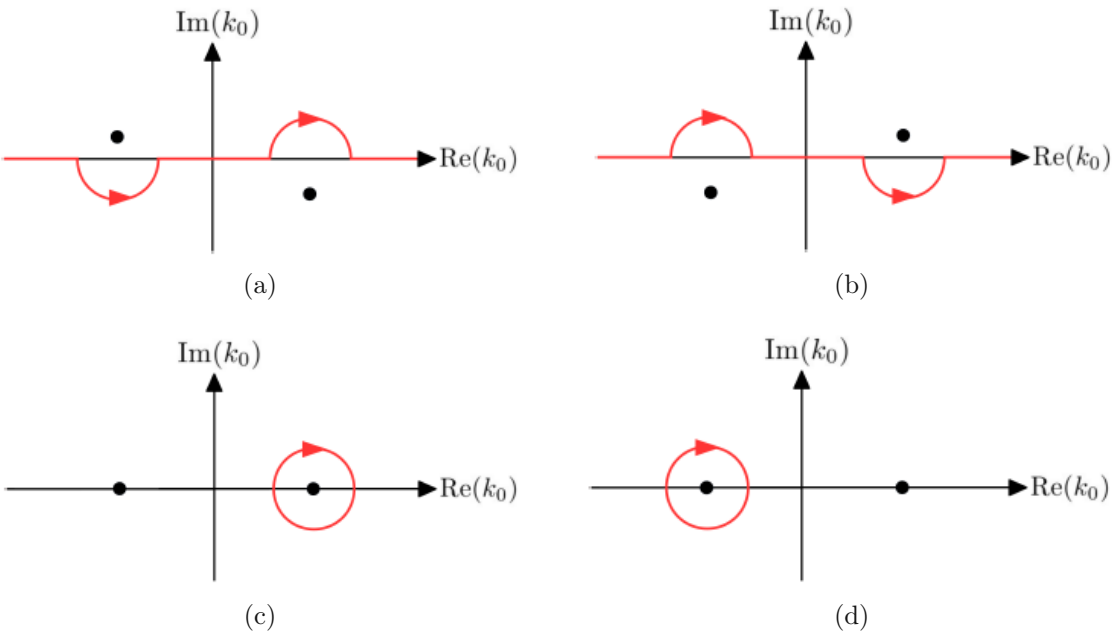

Figure A.1.: Integration contours in the complex plane of (a) the Feynman propagator, (b) the Dyson propagator, (c) the positive frequency Wightman propagator and (d) the negative frequency Wightman propagator; images taken from [24]

The last identity of Eq. (A.5) for both Wightman propagator can easily be shown to be true, when using the transformation $k^0 \to -k^0$ to switch between the propagators:

$$\begin{aligned} \Delta^{<}_{\mathbf{xy}} &= 2\pi \int_k e^{i\mathbf{k}\cdot(\mathbf{x}-\mathbf{y})} \Theta(-k^0)\delta(k^2+m^2) \\ &= 2\pi \int_k e^{i\mathbf{k}\cdot(\mathbf{x}-\mathbf{y})} \Theta(k^0)\delta(k^2+m^2) \\ &= \Delta^{>}_{\mathbf{xy}}. \end{aligned} \tag{A.7}$$

Proving the coincidence of (A.5) for the Feynman and Dyson propagator as well is more intricate. First, $\Delta^{F,D}_{\mathbf{xy}}$ have to be rewritten as

$$\begin{aligned} \Delta^{F,D}_{\mathbf{xy}} &= \mp i \int_k \frac{e^{i\mathbf{k}\cdot(\mathbf{x}-\mathbf{y})}}{k^2+m^2 \mp i\epsilon} \\ &= \mp i \int_k e^{i\mathbf{k}\cdot(\mathbf{x}-\mathbf{y})} \left[\frac{\mathcal{P}}{k^2+m^2} \pm i\pi\delta(k^2+m^2) \right], \end{aligned} \tag{A.8}$$

using the Sokhotskii-Plemelj theorem [93, 94]. Here, $\mathcal{P}$ stands for the principal value part [95, 96]. As can be seen, the second term already looks similar to the Wightman Propagators. Therefore, the first term with the principle value part has to vanish, which

Die approbierte gedruckte Originalversion dieser Diplomarbeit ist an der TU Wien Bibliothek verfügbar
The approved original version of this thesis is available in print at TU Wien Bibliothek.

is actually the case as can be seen by direct computation:

$$\begin{aligned}\int_{-\infty}^{\infty} dk^0 \frac{\mathcal{P}}{-(k^0)^2+E_{\mathbf{k}}^2} &= \lim_{\epsilon\to 0}\left(\int_{-\infty}^{-E_{\mathbf{k}}-\epsilon} + \int_{-E_{\mathbf{k}}+\epsilon}^{E_{\mathbf{k}}-\epsilon} + \int_{E_{\mathbf{k}}+\epsilon}^{\infty}\right)\frac{dk^0}{-(k^0)^2+E_{\mathbf{k}}^2} \\ &= \lim_{\epsilon\to 0}\left[\frac{1}{2E_{\mathbf{k}}}\log\left(\frac{E_{\mathbf{k}}+k^0}{E_{\mathbf{k}}-k^0}\right)\right]_{\{-\infty,-E_{\mathbf{k}}+\epsilon,E_{\mathbf{k}}+\epsilon\}}^{\{-E_{\mathbf{k}}-\epsilon,E_{\mathbf{k}}-\epsilon,\infty\}} \\ &= \lim_{\epsilon\to 0}\frac{1}{2E_{\mathbf{k}}}\left[\log\left(\frac{-\epsilon}{2E_{\mathbf{k}}}\right) - \log(-1) + \log\left(\frac{2E_{\mathbf{k}}}{\epsilon}\right)\right. \\ &\qquad \left. - \log\left(\frac{\epsilon}{2E_{\mathbf{k}}}\right) + \log(-1) - \log\left(\frac{2E_{\mathbf{k}}}{-\epsilon}\right)\right] \\ &= 0.\end{aligned} \tag{A.9}$$

Therefore, the Feynman and Dyson propagators become

$$\begin{aligned}\Delta_{\mathbf{xy}}^{F,D} &= \pi\int_k e^{i\mathbf{k}\cdot(\mathbf{x}-\mathbf{y})}\delta(k^2+m^2) \\ &= \pi\int_k e^{i\mathbf{k}\cdot(\mathbf{x}-\mathbf{y})}(\Theta(k^0)+\Theta(-k^0))\delta(k^2+m^2) \\ &= 2\pi\int_k e^{i\mathbf{k}\cdot(\mathbf{x}-\mathbf{y})}\Theta(k^0)\delta(k^2+m^2) \\ &= \Delta_{\mathbf{xy}}^{<,>}.\end{aligned} \tag{A.10}$$

A.2. Greatest time equation

Another important relation between the propagators of scalar fields is the so-called greatest time equation

$$\forall n\in\mathbb{N}: \sum_{a,b=\pm} ab\Delta_{ab}^n = 0, \tag{A.11}$$

where $++$ corresponds to the Feynman propagator, $+-$ and $-+$ to the negative and positive frequency Wightman propagator, respectively, and $--$ to the Dyson propagator.

In order to prove this identity, another connection between the propagators has to be derived first, namely the fact that Feynman and Dyson propagators can also be expressed in terms of the Wightman propagators:

$$\Delta_{xy}^{F,D} = \Theta[\pm(x^0-y^0)]\Delta_{xy}^{>} + \Theta[\pm(y^0-x^0)]\Delta_{xy}^{<}. \tag{A.12}$$

Starting with Eqs. (A.1) and (A.2) and using $X = x-y$ leads to

$$\begin{aligned}\Delta_X^{F,D} &= \mp i\int_k \frac{e^{ik\cdot X}}{k^2+m^2\mp i\epsilon} \\ &= \pm i\int\frac{d^3k}{(2\pi)^3}e^{i\mathbf{k}\cdot\mathbf{X}}\int\frac{dk^0}{2\pi}\frac{e^{-ik^0X^0}}{(k^0)^2-E_{\mathbf{k}}^2\pm i\epsilon}.\end{aligned} \tag{A.13}$$

Die approbierte gedruckte Originalversion dieser Diplomarbeit ist an der TU Wien Bibliothek verfügbar
The approved original version of this thesis is available in print at TU Wien Bibliothek.

Next, Cauchy's integral formula [97, 98]

$$\oint_\gamma \frac{f(z)}{z-a}dz = \omega 2\pi f(a) \tag{A.14}$$

is used, where γ is a closed curve in the complex plane and $\omega = \pm$ takes integrations in positive or negative directions into account. This leads to the propagators being rewritten as

$$\begin{aligned}
\Delta_X^{F,D} &= \int \frac{d^3k}{(2\pi)^3}\frac{e^{i\mathbf{k}\cdot\mathbf{X}}}{2E_\mathbf{k}}\left(\Theta(X^0)e^{\mp iE_\mathbf{k}X^0} + \Theta(-X^0)e^{\pm iE_\mathbf{k}X^0}\right) \\
&= \int \frac{d^4k}{(2\pi)^3}\frac{e^{ikX}}{2E_\mathbf{k}}\left(\Theta(X^0)\delta(k^0 \mp E_\mathbf{k}) + \Theta(-X^0)\delta(k^0 \pm E_\mathbf{k})\right) \\
&= \int \frac{d^4k}{(2\pi)^3}e^{ikX}\delta(k^2+m^2)\left(\Theta(X^0)\Theta(\pm k^0) + \Theta(-X^0)\Theta(\mp k^0)\right) \\
&= \Theta(X^0)\Delta_X^{\gtrless} + \Theta(-X^0)\Delta_X^{\lessgtr},
\end{aligned} \tag{A.15}$$

which is the identity needed for proving the greatest time equation (A.11).

For this proof, Eq. (A.12) is used in a simplified notation, namely

$$\Delta_X^{F,D} = \Delta_{++,--} = \Theta(\pm)\Delta_{-+} + \Theta(\mp)\Delta_{+-}. \tag{A.16}$$

Additionally, for the propagators considered here

$$\Theta(+)\Theta(-)\Delta(x,y) = \Theta(+)\Theta(-)\Delta(x_0 \equiv y_0, \mathbf{x}, \mathbf{y}) \tag{A.17}$$

holds. Using this, one can write

$$\begin{aligned}
\sum_{a,b=\pm} ab\Delta_{ab}^n &= \Delta_{--}^n + \Delta_{++}^n - \Delta_{-+}^n - \Delta_{+-}^n \\
&= [\Theta(-)\Delta_{-+} + \Theta(+)\Delta_{+-}]^n + [\Theta(+)\Delta_{-+} + \Theta(-)\Delta_{+-}]^n - \Delta_{-+}^n - \Delta_{+-}^n.
\end{aligned} \tag{A.18}$$

Using the binomial theorem, $(x+y)^n = \sum_{k=0}^n \binom{n}{k} x^{n-k}y^k$ [99], one can rewrite these first two terms as

$$[\Theta(-)\Delta_{-+} + \Theta(+)\Delta_{+-}]^n = \sum_{k=0}^n \binom{n}{k}\Theta^{n-k}(-)\Theta^k(+)\Delta_{-+}^{n-k}\Delta_{+-}^k, \tag{A.19}$$

$$[\Theta(+)\Delta_{-+} + \Theta(-)\Delta_{+-}]^n = \sum_{k=0}^n \binom{n}{k}\Theta^{n-k}(+)\Theta^k(-)\Delta_{-+}^{n-k}\Delta_{+-}^k \tag{A.20}$$

Die approbierte gedruckte Originalversion dieser Diplomarbeit ist an der TU Wien Bibliothek verfügbar
The approved original version of this thesis is available in print at TU Wien Bibliothek.

which leads to

$$\sum_{a,b=\pm} ab\Delta_{ab}^n = \sum_{k=0}^{n} \binom{n}{k} \left[\Theta^{n-k}(-)\Theta^k(+) + \Theta^{n-k}(+)\Theta^k(-)\right] \Delta_{-+}^{n-k}\Delta_{+-}^k - \Delta_{-+}^n - \Delta_{+-}^n. \tag{A.21}$$

Taking from this sum only the terms where $k = 0$ and $k = n$, one finds

$$\left[\Theta^n(+) + \Theta^n(-)\right](\Delta_{-+}^n + \Delta_{+-}^n). \tag{A.22}$$

Meanwhile, the remaining terms for which $1 \leq k \leq n-1$ are

$$\sum_{k=1}^{n-1} \binom{n}{k} \left[\Theta^{n-k}(-)\Theta^k(+) + \Theta^{n-k}(+)\Theta^k(-)\right] \Delta_{-+}^{n-k}\Delta_{+-}^k. \tag{A.23}$$

Next, Eq. (A.17) and the equal time limit Eq. (A.5) are made use of to find for the terms where $1 \leq k \leq n-1$

$$\sum_{k=1}^{n-1} \binom{n}{k} \left[\Theta^{n-k}(-)\Theta^k(+)\Delta_{-+}^n + \Theta^{n-k}(+)\Theta^k(-)\Delta_{+-}^n\right] \tag{A.24}$$

and making use of $\sum_{k=1}^{n-1} \Theta^{n-k}(-)\Theta^k(+) = \sum_{k=1}^{n-1} \Theta^{n-k}(+)\Theta^k(-)$ leads to

$$\sum_{k=1}^{n-1} \binom{n}{k} \Theta^{n-k}(+)\Theta^k(-)(\Delta_{-+}^n + \Delta_{+-}^n). \tag{A.25}$$

Recombining this with the terms for which $k = 0$ or $k = n$ (Eq. (A.22)) gives

$$\begin{aligned}(\Delta_{-+}^n + \Delta_{+-}^n) &\left[\sum_{k=1}^{n-1} \binom{n}{k} \Theta^{n-k}(+)\Theta^k(-) + \Theta^n(+) + \Theta^n(-)\right] \\ &= (\Delta_{-+}^n + \Delta_{+-}^n) \left[\sum_{k=0}^{n} \binom{n}{k} \Theta^{n-k}(+)\Theta^k(-)\right] \\ &= (\Delta_{-+}^n + \Delta_{+-}^n) \left[\Theta(+) + \Theta(-)\right]^n,\end{aligned} \tag{A.26}$$

where in the last line the binomial theorem was used again. Lastly, making use of the fact that $\Theta(+) + \Theta(-) = 1$, one finds for the greatest time equation (A.21)

$$\sum_{a,b=\pm} ab\Delta_{ab}^n = \left[\Theta(+) + \Theta(-)\right]^n (\Delta_{-+}^n + \Delta_{+-}^n) - \Delta_{-+}^n - \Delta_{+-}^n = 0. \tag{A.27}$$

Die approbierte gedruckte Originalversion dieser Diplomarbeit ist an der TU Wien Bibliothek verfügbar
The approved original version of this thesis is available in print at TU Wien Bibliothek.

B. Scalar field contractions

In order for the reader to better follow the calculations done to get from Eq. (4.15) to (4.16), one of the terms will be evaluated in more detail here. For these calculations the equations for ϕ-propagators ((4.2)-(4.3)) and χ-propagators without thermal corrections as given by (A.1)-(A.4) are used for simplicity. The term that is being presented is the first term in the fourth line of Eq. (4.15). It reads

$$\begin{aligned}
(*) &= -\alpha_1^2 M^2 \lim_{\substack{x^{0(\prime)}\to t^+ \\ y^{0(\prime)}\to 0^-}} \int d\Pi_{\mathbf{k}} d\Pi_{\mathbf{k}'} \rho_{1,1}(\mathbf{k},\mathbf{k}';0) \\
&\quad \times \int_{\mathbf{x}\mathbf{x}'\mathbf{y}\mathbf{y}'} e^{-i(\mathbf{p}\cdot\mathbf{x}-\mathbf{p}'\cdot\mathbf{x}')+i(\mathbf{k}\cdot\mathbf{y}-\mathbf{k}'\cdot\mathbf{y}')} \partial_{x^0,E^\phi_{\mathbf{p}}} \partial^*_{x^{0\prime},E^\phi_{\mathbf{p}'}} \partial^*_{y^0,E^\phi_{\mathbf{k}}} \partial_{y^{0\prime},E^\phi_{\mathbf{k}'}} \\
&\quad \times \int_{zz'} D^D_{x'y'} D^F_{xz} D^F_{zz'} D^F_{z'y} \Delta^F_{zz'} \\
&= -\alpha_1^2 M^2 \lim_{\substack{x^{0(\prime)}\to t^+ \\ y^{0(\prime)}\to 0^-}} \int d\Pi_{\mathbf{k}} d\Pi_{\mathbf{k}'} \rho_{1,1}(\mathbf{k},\mathbf{k}';0) \\
&\quad \times \int_{\mathbf{x}\mathbf{x}'\mathbf{y}\mathbf{y}'} e^{-i(\mathbf{p}\cdot\mathbf{x}-\mathbf{p}'\cdot\mathbf{x}')+i(\mathbf{k}\cdot\mathbf{y}-\mathbf{k}'\cdot\mathbf{y}')} \partial_{x^0,E^\phi_{\mathbf{p}}} \partial^*_{x^{0\prime},E^\phi_{\mathbf{p}'}} \partial^*_{y^0,E^\phi_{\mathbf{k}}} \partial_{y^{0\prime},E^\phi_{\mathbf{k}'}} \\
&\quad \times \int_{zz'} \int_{qlrns} \frac{ie^{iq\cdot(x'-y')}}{q^2+M^2+i\epsilon} \frac{-ie^{il\cdot(x-z)}}{l^2+M^2-i\epsilon} \frac{-ie^{ir\cdot(z-z')}}{r^2+M^2-i\epsilon} \frac{-ie^{in\cdot(z'-y)}}{n^2+M^2-i\epsilon} \frac{-ie^{is\cdot(z-z')}}{s^2+m^2-i\epsilon}.
\end{aligned} \tag{B.1}$$

Acting with the Klein-Gordon operators on the propagators in the last line gives

$$\partial_{x^0,E^\phi_{\mathbf{p}}} \partial^*_{x^{0\prime},E^\phi_{\mathbf{p}'}} \partial^*_{y^0,E^\phi_{\mathbf{k}}} \partial_{y^{0\prime},E^\phi_{\mathbf{k}'}} \to (-il^0 - iE^\phi_{\mathbf{p}})(-iq^0 + iE^\phi_{\mathbf{p}'})(in^0 + iE^\phi_{\mathbf{k}})(iq^0 - iE^\phi_{\mathbf{k}'}). \tag{B.2}$$

Next, the relation

$$\int_{\mathbf{x}} e^{i\mathbf{x}\cdot(\mathbf{p}-\mathbf{k})} = (2\pi)^3 \delta^{(3)}(\mathbf{p}-\mathbf{k}) \tag{B.3}$$

Die approbierte gedruckte Originalversion dieser Diplomarbeit ist an der TU Wien Bibliothek verfügbar
The approved original version of this thesis is available in print at TU Wien Bibliothek.

is used to determine the spatial integrals of Eq. (B.1). This leads to

$$\begin{aligned}(*) = &- i\alpha_1^2 M^2 \lim_{\substack{x^{0(\prime)}\to t^+\\ y^{0(\prime)}\to 0^-}} \int d\Pi_{\mathbf{k}} d\Pi_{\mathbf{k}'} \int \frac{d^4q\, d^4l\, d^4r\, d^4n\, d^4s}{(2\pi)^2} \rho_{1,1}(\mathbf{k},\mathbf{k}';0)\\ &\times \delta^{(3)}(\mathbf{l}-\mathbf{p})\delta^{(3)}(\mathbf{p}'+\mathbf{q})\delta^{(3)}(\mathbf{k}-\mathbf{n})\delta^{(3)}(\mathbf{k}'+\mathbf{q})\delta^{(3)}(\mathbf{r}+\mathbf{s}-\mathbf{l})\delta^{(3)}(\mathbf{n}-\mathbf{r}-\mathbf{s})\\ &\times (l^0+E^\phi_{\mathbf{p}})(q^0-E^\phi_{\mathbf{p}'})(n^0+E^\phi_{\mathbf{k}})(q^0-E^\phi_{\mathbf{k}'})\\ &\times \int_{z^0 z^{0\prime}} \frac{e^{-iq^0\cdot(x^{0\prime}-y^{0\prime})}}{q^2+M^2+i\epsilon}\frac{e^{-il^0\cdot(x^0-z^0)}}{l^2+M^2-i\epsilon}\frac{e^{-ir^0\cdot(z^0-z^{0\prime})}}{r^2+M^2-i\epsilon}\frac{e^{-in^0\cdot(z^{0\prime}-y^0)}}{n^2+M^2-i\epsilon}\frac{e^{-is^0\cdot(z^0-z^{0\prime})}}{s^2+m^2-i\epsilon}.\end{aligned} \tag{B.4}$$

After evaluating the 3-momentum integrations by using the δ-functions, this becomes

$$\begin{aligned}(*) = &- i\alpha_1^2 M^2 \lim_{\substack{x^{0(\prime)}\to t^+\\ y^{0(\prime)}\to 0^-}} \frac{1}{4E^\phi_{\mathbf{p}}E^\phi_{\mathbf{p}'}}\frac{1}{(2\pi)^8}\int dq^0\, dl^0\, d^4r\, dn^0\, ds^0 \rho_{1,1}(\mathbf{p},\mathbf{p}';0)\\ &\times (l^0+E^\phi_{\mathbf{p}})(q^0-E^\phi_{\mathbf{p}'})^2(n^0+E^\phi_{\mathbf{p}})\int_{z^0 z^{0\prime}} \frac{e^{-iq^0\cdot(x^{0\prime}-y^{0\prime})}}{-(q^0-E^\phi_{\mathbf{p}'})(q^0+E^\phi_{\mathbf{p}'})+i\epsilon}\\ &\times \frac{e^{-il^0\cdot(x^0-z^0)}}{-(l^0-E^\phi_{\mathbf{p}})(l^0+E^\phi_{\mathbf{p}})-i\epsilon}\frac{e^{-ir^0\cdot(z^0-z^{0\prime})}}{-(r^0-E^\phi_{\mathbf{r}})(r^0+E^\phi_{\mathbf{r}})-i\epsilon}\frac{e^{-in^0\cdot(z^{0\prime}-y^0)}}{-(n^0-E^\phi_{\mathbf{p}})(n^0+E^\phi_{\mathbf{p}})-i\epsilon}\\ &\times \frac{e^{-is^0\cdot(z^0-z^{0\prime})}}{-(s^0-E^\chi_{\mathbf{p}-\mathbf{r}})(s^0+E^\chi_{\mathbf{p}-\mathbf{r}})-i\epsilon}.\end{aligned} \tag{B.5}$$

The temporal momentum integrations can be evaluated by using Cauchy's integral formula, see Eq. A.14. Additionally, the directions from which $x^{0(\prime)}$ and $y^{0(\prime)}$ approach their limits are included. With this, the first of the remaining integrals, for example, is

$$\int dq^0 (q^0-E^\phi_{\mathbf{p}'})^2 \frac{e^{-iq^0\cdot(x^{0\prime}-y^{0\prime})}}{-(q^0-E^\phi_{\mathbf{p}'})(q^0+E^\phi_{\mathbf{p}'})+i\epsilon} = -2\pi i(2E^\phi_{\mathbf{p}'})e^{-E^\phi_{\mathbf{p}'}t}, \tag{B.6}$$

where the exponent on the left-hand side is always negative and thus the integration curve has to be closed in the lower half-plane for the auxiliary contour to vanish when going to $-i\infty$. All integrations with $z^{0(\prime)}$ in the exponent, however, have to consider the fact that both z^0 and $z^{0\prime}$ are not yet evaluated and can lie within the interval $[0;t]$. Solving all the remaining momentum integrations leads to

$$\begin{aligned}(*) = &- \alpha_1^2 M^2 \rho_{1,1}(\mathbf{p},\mathbf{p};0)\int_{\mathbf{r}} \frac{1}{8E^\phi_{\mathbf{p}}E^\phi_{\mathbf{r}}E^\chi_{\mathbf{p}-\mathbf{r}}} e^{-i(E^\phi_{\mathbf{p}}-E^\phi_{\mathbf{p}'})t}\\ &\times \int_{z^0 z^{0\prime}} \left[\Theta(z^0-z^{0\prime})e^{-i(E^\phi_{\mathbf{r}}+E^\chi_{\mathbf{p}-\mathbf{r}}-E^\phi_{\mathbf{p}})(z^0-z^{0\prime})} + \Theta(z^{0\prime}-z^0)e^{i(E^\phi_{\mathbf{r}}+E^\chi_{\mathbf{p}-\mathbf{r}}+E^\phi_{\mathbf{p}})(z^0-z^{0\prime})}\right].\end{aligned} \tag{B.7}$$

Die approbierte gedruckte Originalversion dieser Diplomarbeit ist an der TU Wien Bibliothek verfügbar
The approved original version of this thesis is available in print at TU Wien Bibliothek.

In a last step, the integrations over z^0 and $z^{0\prime}$ have to be performed:

$$\begin{aligned}
&\int_{z^0 z^{0\prime}} \Theta(z^0 - z^{0\prime}) e^{-i(E^\phi_{\mathbf{r}} + E^\chi_{\mathbf{p}-\mathbf{r}} - E^\phi_{\mathbf{p}})(z^0 - z^{0\prime})} + \int_{z^0 z^{0\prime}} \Theta(z^{0\prime} - z^0) e^{i(E^\phi_{\mathbf{r}} + E^\chi_{\mathbf{p}-\mathbf{r}} + E^\phi_{\mathbf{p}})(z^0 - z^{0\prime})} \\
&\quad = \frac{i}{E^\phi_{\mathbf{r}} + E^\chi_{\mathbf{p}-\mathbf{r}} - E^\phi_{\mathbf{p}}} \left[\frac{-i}{E^\phi_{\mathbf{r}} + E^\chi_{\mathbf{p}-\mathbf{r}} - E^\phi_{\mathbf{p}}} \left(1 - e^{-i(E^\phi_{\mathbf{r}} + E^\chi_{\mathbf{p}-\mathbf{r}} - E^\phi_{\mathbf{p}})t} \right) - t \right] \\
&\qquad + \frac{i}{E^\phi_{\mathbf{r}} + E^\chi_{\mathbf{p}-\mathbf{r}} + E^\phi_{\mathbf{p}}} \left[\frac{-i}{E^\phi_{\mathbf{r}} + E^\chi_{\mathbf{p}-\mathbf{r}} + E^\phi_{\mathbf{p}}} \left(1 - e^{-i(E^\phi_{\mathbf{r}} + E^\chi_{\mathbf{p}-\mathbf{r}} + E^\phi_{\mathbf{p}})t} \right) - t \right] \\
&\quad = \sum_{s=\pm} \frac{i}{s E^\phi_{\mathbf{p}} + E^\phi_{\mathbf{r}} + E^\chi_{\mathbf{p}-\mathbf{r}}} \left[\frac{-i}{s E^\phi_{\mathbf{p}} + E^\phi_{\mathbf{r}} + E^\chi_{\mathbf{p}-\mathbf{r}}} \left(1 - e^{-i(s E^\phi_{\mathbf{p}} + E^\phi_{\mathbf{r}} + E^\chi_{\mathbf{p}-\mathbf{r}})t} \right) - t \right].
\end{aligned} \tag{B.8}$$

Therefore, after renaming $\mathbf{r} \to \mathbf{q}$, the final solution for this term reads:

$$\begin{aligned}
(*) =& i\alpha_1^2 M^2 \rho_{1,1}(\mathbf{p}, \mathbf{p}; 0) e^{-i(E^\phi_{\mathbf{p}} - E^\phi_{\mathbf{p}'})t} \sum_{s=\pm} \int_{\mathbf{q}} \frac{1}{8 E^\phi_{\mathbf{p}} E^\phi_{\mathbf{q}} E^\chi_{\mathbf{p}-\mathbf{q}} (s E^\phi_{\mathbf{p}} + E^\phi_{\mathbf{q}} + E^\chi_{\mathbf{p}-\mathbf{q}})} \\
&\times \left[\frac{i}{s E^\phi_{\mathbf{p}} + E^\phi_{\mathbf{q}} + E^\chi_{\mathbf{p}-\mathbf{q}}} \left(1 - e^{-i(s E^\phi_{\mathbf{p}} + E^\phi_{\mathbf{q}} + E^\chi_{\mathbf{p}-\mathbf{q}})t} \right) + t \right],
\end{aligned} \tag{B.9}$$

which can be found in the seventh line of Eq. (4.16).

Die approbierte gedruckte Originalversion dieser Diplomarbeit ist an der TU Wien Bibliothek verfügbar
The approved original version of this thesis is available in print at TU Wien Bibliothek.

References

1. Clifton, T., Ferreira, P. G., Padilla, A. & Skordis, C. Modified gravity and cosmology. *Physics Reports* **513,** 1–189 (2012).
2. Joyce, A., Jain, B., Khoury, J. & Trodden, M. Beyond the cosmological standard model. *Physics Reports* **568,** 1–98 (2015).
3. Hu, W., Barkana, R. & Gruzinov, A. Fuzzy Cold Dark Matter: The Wave Properties of Ultralight Particles. *Phys. Rev. Lett.* **513,** 1158–1161 (2000).
4. Hui, L., Ostriker, J. P., Tremaine, S. & Witten, E. Ultralight scalars as cosmological dark matter. *Phys. Rev. D.* **95,** 043541 (2017).
5. Copeland, E. J., Sami, M. & Tsujikawa, S. Dynamics of dark energy. *International Journal of Modern Physics D* **15,** 1753–1935 (2006).
6. Perlmutter, S. *et al.* Measurements of Ω and Λ from 42 high-redshift supernovae. *The Astrophysical Journal* **517,** 565–586 (1999).
7. Bull, P. *et al.* Beyond ΛCDM: Problems, solutions, and the road ahead. *Physics of the Dark Universe* **12,** 56–99 (2016).
8. Fujii, Y. & Maeda, K. *The scalar-tensor theory of gravitation* (Cambridge University Press, 2004).
9. Ishak, M. Testing general relativity in cosmology. *Living Reviews in Relativity* **22,** 1 (2018).
10. Adelberger, E., Gundlach, J., Heckel, B., Hoedl, S. & Schlamminger, S. Torsion balance experiments: A low-energy frontier of particle physics. *Progress in Particle and Nuclear Physics* **62,** 102–134 (2009).
11. Zee, A. *Quantum field theory in a nutshell* (Princeton university press, 2010).
12. Koyama, K. Cosmological tests of modified gravity. *Reports on Progress in Physics* **79,** 046902 (2016).
13. Burrage, C. & Sakstein, J. Tests of chameleon gravity. *Living Reviews in Relativity* **21,** 1 (2018).
14. Breuer, H.-P. & Petruccione, F. *The theory of open quantum systems* (Oxford University Press, 2002).

Die approbierte gedruckte Originalversion dieser Diplomarbeit ist an der TU Wien Bibliothek verfügbar
The approved original version of this thesis is available in print at TU Wien Bibliothek.
TU Bibliothek Your knowledge hub WIEN

15. Calzetta, E. & Hu, B.-L. B. *Nonequilibrium Quantum Field Theory* (Cambridge University Press, 2009).

16. Schlosshauer, M. *Decoherence: and the quantum-to-classical transition* (Springer Science & Business Media, 2007).

17. Agarwal, G. I Master Equation Methods in Quantum Optics. *Elsevier* **11,** 1–76 (1973).

18. Carmichael, H. *An open systems approach to quantum optics: lectures presented at the Université Libre de Bruxelles, October 28 to November 4, 1991* (Springer, 1993).

19. Rivas, Á. & Huelga, S. F. *Open Quantum Systems. An Introduction* (Springer, 2012).

20. Diehl, S. *et al.* Quantum states and phases in driven open quantum systems with cold atoms. *Nature Physics* **4,** 878–883 (2008).

21. Müller, M., Diehl, S., Pupillo, G. & Zoller, P. Engineered Open Systems and Quantum Simulations with Atoms and Ions. *Advances In Atomic, Molecular, and Optical Physics* **61,** 1–80 (2012).

22. Sieberer, L. M., Buchhold, M. & Diehl, S. Keldysh field theory for driven open quantum systems. *Reports on Progress in Physics* **79,** 096001 (2016).

23. Burrage, C., Käding, C., Millington, P. & Minář, J. Open quantum dynamics induced by light scalar fields. *Phys. Rev. D* **100,** 076003 (2019).

24. Käding, C. *Astro- and Quantum Physical Tests of Screened Scalar Fields* Doctoral dissertation (University of Nottingham, 2019).

25. Burrage, C., Käding, C., Millington, P. & Minář, J. Influence functionals, decoherence and conformally coupled scalars. *Journal of Physics: Conference Series* **1275,** 012041 (2019).

26. Käding, C. & Pitschmann, M. New method for directly computing reduced density matrices. *Phys. Rev. D* **107,** 016005 (2023).

27. Käding, C. & Pitschmann, M. Density matrix formalism for interacting quantum fields. *Universe* **8** (2022).

28. Schwinger, J. Brownian motion of a quantum oscillator. *Journal of Mathematical Physics* **2** (1961).

29. Keldysh, L. Diagram technique for nonequilibrium processes. *Soviet Physics JETP* **20** (1965).

30. Feynman, R. & Vernon, F. The Theory of a General Quantum System Interacting with a Linear Dissipative System. *Annals of Physics* **281,** 547–607 (1963).

31. Arimitsu, T. & Umezawa, H. A General Formulation of Nonequilibrium Thermo Field Dynamics. *Progress of Theoretical Physics* **74,** 429–432 (1985).

Die approbierte gedruckte Originalversion dieser Diplomarbeit ist an der TU Wien Bibliothek verfügbar
The approved original version of this thesis is available in print at TU Wien Bibliothek.

32. Arimitsu, T. & Umezawa, H. Non-Equilibrium Thermo Field Dynamics. *Progress of Theoretical Physics* **77,** 32–52 (1987).

33. Wentzel, G. *Quantum theory of fields* (Dover Publications, 2003).

34. Srednicki, M. *Quantum field theory* (Cambridge University Press, 2007).

35. Feynman, R., Hibbs, A. & Styer, D. *Quantum Mechanics and Path Integrals* (Dover Publications, 2010).

36. Peskin, M. E. & Schroeder, D. V. *An Introduction to Quantum Field Theory* (Addison-Wesley, 1995).

37. Greiner, W. & Reinhardt, J. *Field Quantization* (Springer-Verlag Berlin Heidelberg, 1996).

38. Higggs, P. W. Broken Symmetries and the Masses of Gauge Bosons. *Phys. Rev. Lett.* **13,** 508–509 (1964).

39. Englert, F. & Brout, R. Broken Symmetry and the Mass of Gauge Vector Mesons. *Phys. Rev. Lett.* **13,** 321–323 (1964).

40. Aad, G. *et al.* Observation of a new particle in the search for the Standard Model Higgs boson with the ATLAS detector at the LHC. *Physics Letters B* **716,** 1–29 (2012).

41. Chatrchyan, S. *et al.* Observation of a new boson at a mass of 125 GeV with the CMS experiment at the LHC. *Physics Letters B* **716,** 30–61 (2012).

42. Polchinski, J. *String Theory. An Introduction to the Bosonic String* (Cambridge University Press, 1998).

43. Polchinski, J. *String Theory. Superstring Theory and Beyond* (Cambridge University Press, 1998).

44. Freedman, D. Z. & Proeyen, A. V. *Supergravity* (Cambridge University Press, 2012).

45. Sotiriou, T. P. & Faraoni, V. $f(R)$ Theories of Gravity. *Reviews of Modern Physics* **82,** 451–497 (2010).

46. Borodulin, V. I., Rogalyov, R. N. & Slabospitskii, S. R. CORE 3.1 (COmpendium of RElations, Version 3.1) (2017).

47. Patt, B. & Wilczek, F. Higgs-field portal into hidden sectors. arXiv: `0605188 [hep-ph]` (2006).

48. Battaglieri, M. *et al.* US Cosmic Visions: New Ideas in Dark Matter 2017: Community Report. arXiv: `1707.04591 [hep-ph]` (2017).

49. Jordan, P. *Schwerkraft und Weltall: Grundlagen der theoretischen Kosmologie* (Die Wissenschaft, 1952).

Die approbierte gedruckte Originalversion dieser Diplomarbeit ist an der TU Wien Bibliothek verfügbar
The approved original version of this thesis is available in print at TU Wien Bibliothek.
TU Bibliothek Your knowledge hub WIEN

50. Brans, C. & Dicke, R. H. Mach's Principle and a Relativistic Theory of Gravitation. *Phys. Rev.* **124,** 925–935 (1961).

51. Adelberger, E. G., Heckel, B. R. & Nelson, A. E. Tests of the gravitational inverse-square law. *Annual Review of Nuclear and Particle Science* **53,** 77–121 (2003).

52. Damour, T. & Polyakov, A. The string dilation and a least coupling principle. *Nuclear Physics B* **423,** 532–558 (1994).

53. Brax, P., van de Bruck, C., Davis, A.-C. & Shaw, D. Dilaton and modified gravity. *Physical Review D* **82,** 063519 (2010).

54. Gessner, E. A new scalar tensor theory for gravity and the flat rotation curves of spiral galaxies. *Astrophysics and Space Science* **196,** 29–43 (1992).

55. Hinterbichler, K. & Khoury, J. Screening Long-Range Forces through Local Symmetry Restoration. *Phys. Rev. Lett.* **104,** 231301 (2010).

56. Hinterbichler, K., Khoury, J., Levy, A. & Matas, A. Symmetron cosmology. *Phys. Rev. D* **84,** 103521 (2011).

57. O'Hare, C. A. J. & Burrage, C. Stellar kinematics from the symmetron fifth force in the Milky Way disk. *Phys. Rev. D* **98,** 064019 (2018).

58. Khoury, J. & Weltman, A. Chameleon Fields: Awaiting Surprises for Tests of Gravity in Space. *Phys. Rev. Lett.* **93,** 171104 (2004).

59. Khoury, J. & Weltman, A. Chameleon cosmology. *Phys. Rev. D* **69,** 044026 (2004).

60. Vainshtein, A. I. To the problem of nonvanishing gravitation mass. *Physics Letters B* **39,** 393–394 (1972).

61. Nicolis, A., Rattazzi, R. & Trincherini, E. Galileon as a local modification of gravity. *Phys. Rev. D* **79,** 064036 (2009).

62. Ali, A., Gannouji, R., Hossain, M. W. & Sami, M. Light mass galileons: Cosmological dynamics, mass screening and observational constraints. *Physics Letters B* **718,** 5–14 (2012).

63. Bloomfield, J. K., Burrage, C. & Davis, A.-C. Shape dependence of Vainshtein screening. *Phys. Rev. D* **91,** 083510 (2015).

64. Brax, P., van de Bruck, C., Davis, A.-C., Li, B. & Shaw, D. Nonlinear structure formation with the environmentally dependent dilaton. *Physical Review D* **83,** 104026 (2011).

65. Brax, P., Davis, A.-C. & Jha, R. Neutron stars in screened modified gravity: Chameleon versus dilaton. *Phys. Rev. D* **95,** 083514 (2017).

66. Damour, T., Piazza, F. & Veneziano, G. Runaway Dilaton and Equivalence Principle Violations. *Phys. Rev. Lett.* **89,** 081601 (2002).

Die approbierte gedruckte Originalversion dieser Diplomarbeit ist an der TU Wien Bibliothek verfügbar
The approved original version of this thesis is available in print at TU Wien Bibliothek.
TU Bibliothek Your knowledge hub WIEN

67. Damour, T., Piazza, F. & Veneziano, G. Violations of the equivalence principle in a dilaton-runaway scenario. *Physical Review D* **66,** 046007 (2002).

68. Gasperini, M., Piazza, F. & Veneziano, G. Quintessence as a runaway dilaton. *Physical Review D* **65,** 023508 (2002).

69. Brax, P., Burrage, C. & Davis, A.-C. Laboratory constraints. *International Journal of Modern Physics D* **27** (2018).

70. Brax, P., Fischer, H., Käding, C. & Pitschmann, M. The environment dependent dilaton in the laboratory and the solar system. *The European Physical Journal C* **82,** 934 (2022).

71. Millington, P. & Pilaftsis, A. Perturbative nonequilibrium thermal field theory. *Phys. Rev. D* **88,** 085009 (2013).

72. Lehmann, H., Symanzik, K. & Zimmermann, W. On the Formulation of Quantized Field Theories. *Il Nuovo Cimento (1955-1965)* **6,** 319–333 (1957).

73. Khanna, F., Malbouisson, A., Malbouisson, J. & Santana, A. Quantum field theory on toroidal topology: Algebraic structure and applications. *Physics Reports* **539,** 135–224 (2014).

74. Millington, P. & Pilaftsis, A. Perturbative non-equilibrium thermal field theory to all orders in gradient expansion. *Physics Letters B* **724,** 56–62 (2013).

75. Bellac, M. L. *Thermal field theory* (Le Bellac, Michel. Thermal field theory. Cambridge university press, 2000).

76. Jaffe, M. *et al.* Testing sub-gravitational forces on atoms from a miniature in-vacuum source mass. *Nature Physics* **13,** 983–942 (2017).

77. Elder, B. *et al.* Chameleon dark energy and atom interferometry. *Phys. Rev. D* **94,** 044051 (2016).

78. Burrage, C. & Copeland, E. J. Using atom interferometry to detect dark energy. *Contemporary Physics* **57,** 164–176 (2016).

79. Burrage, C., Kuribayashi-Coleman, A., Stevenson, J. & Thrussell, B. Constraining symmetron fields with atom interferometry. *Journal of Cosmology and Astroparticle Physics* **1612,** 041 (2016).

80. Hamilton, P. *et al.* Atom-interferometry constraints on dark energy. *Science* **349,** 849–851 (2015).

81. Burrage, C., Copeland, E. J. & Hinds, E. A. Probing dark energy with atom interferometry. *Journal of Cosmology and Astroparticle Physics* **1503,** 042 (2015).

82. Sabulsky, D. O. *et al.* Experiment to Detect Dark Energy Forces Using Atom Interferometry. *Phys. Rev. Lett.* **123,** 061102 (2019).

Die approbierte gedruckte Originalversion dieser Diplomarbeit ist an der TU Wien Bibliothek verfügbar
The approved original version of this thesis is available in print at TU Wien Bibliothek.
TU Bibliothek Your knowledge hub WIEN

83. Cronin, A. D., Schmiedmayer, J. & Pritchard, D. E. Optics and interferometry with atoms and molecules. *Reviews of Modern Physics* **81,** 1051–1129 (2009).

84. Narducci, F. A., Black, A. T. & Burke, J. H. Advances toward fieldable atom interferometers. *Advances in Physics: X* **7,** 1946426 (2022).

85. Martynov, D. V. *et al.* Sensitivity of the Advanced LIGO detectors at the beginning of gravitational wave astronomy. *Phys. Rev. D* **93,** 112004 (2016).

86. Paschotta, R. *Field guide to lasers* (SPIE Press, 2008).

87. *Stahl. Allgemeine physikalische Eigenschaften* `https://de.wikipedia.org/wiki/Stahl#Allgemeine_physikalische_Eigenschaften`. (last accessed: April 26, 2023).

88. Barrett, B. *et al.* Testing the universality of free fall using correlated 39K–87Rb atom interferometers. *AVS Quantum Science* **4,** 014401 (2022).

89. Estey, B., Yu, C., Müller, H., Kuan, P.-C. & Lan, S.-Y. High-Resolution Atom Interferometers with Suppressed Diffraction Phases. *Phys. Rev. Lett.* **115,** 083002 (2015).

90. Khoury, J. & Weltman, A. Chameleon cosmology. *Phys. Rev. D* **69,** 044026 (2004).

91. Zhou, L. *et al.* Joint mass-and-energy test of the equivalence principle at the 10^{-10} level using atoms with specified mass and internal energy. *Phys. Rev. A* **104,** 022822 (2021).

92. Marinković, I. *et al.* Optomechanical Bell Test. *Phys. Rev. Lett.* **121,** 220404 (2018).

93. Sokhotskii, Y. W. *On definite integrals and functions used in series expansions* Doctoral dissertation (St. Petersburg, 1873).

94. Plemelj, J. Riemannsche Funktionenscharen mit gegebener Monodromiegruppe. *Monatshefte für Mathematik und Physik* **19,** 211–245 (1908).

95. Guiggiani, M. The evaluation of cauchy principal value integrals in the boundary element method—a review. *Mathematical and Computer Modelling* **15,** 175–184 (1991).

96. Fox, C. A Generalization of the Cauchy Principal Value. *Canadian Journal of Mathematics* **9,** 110–117 (1957).

97. Stein, E. M. & Shakarchi, R. *Complex analysis* (Princeton University Press, 2010).

98. Gamelin, T. *Complex analysis* (Springer Science & Business Media, 2003).

99. Abramowitz, M. & Stegun, I. A. *Handbook of Mathematical Functions with Formulas, Graphs, and Mathematical Tables* 10th ed. (National Bureau of Standards Applied, 1972).

Die approbierte gedruckte Originalversion dieser Diplomarbeit ist an der TU Wien Bibliothek verfügbar
The approved original version of this thesis is available in print at TU Wien Bibliothek.

List of Figures

Die approbierte gedruckte Originalversion dieser Diplomarbeit ist an der TU Wien Bibliothek verfügbar
The approved original version of this thesis is available in print at TU Wien Bibliothek.